

UNIVERSITÄTSKLINIKUM HAMBURG-EPPENDORF

Zentrum für Molekulare Neurobiologie

Prof. Dr. rer. nat. Matthias Kneussel

Neuropeptidergic control of innate and adaptive behaviors

Dissertation

zur Erlangung des Doktorgrades PhD

an der Medizinischen Fakultät der Universität Hamburg.

vorgelegt von:

Bibi Nusreen Imambocus

aus Mauritius

Hamburg 2021

Für papa und mama

All that I am,
or hope to be, I owe to
my mother and father

Abraham Lincoln

wird von der Medizinischen Fakultät ausgefüllt

Angenommen von der

Medizinischen Fakultät der Universität Hamburg am: 17.05.2021

Datum der Disputation: 25.08.2021

Veröffentlicht mit Genehmigung der

Medizinischen Fakultät der Universität Hamburg.

Prüfungsausschuss, der/die Vorsitzende: Prof. Dr. Thomas G. Oertner

Prüfungsausschuss, zweite/r Gutachter/in: Prof. Dr. Manuel A. Friese

Prüfungsausschuss, dritte/r Gutachter/in: Prof. Dr. Christian Lohr

TABLE OF CONTENTS

1 Introduction	1
1.1 Innate and adaptive behaviors	1
1.1.1 Nociceptive behaviors.....	2
1.1.2 Feeding behaviors.....	3
1.1.3 Internal state and drive for feeding.....	4
1.2 Circuits, networks and motifs	5
1.3 Connectome and neuromodulation	8
1.3.1 Neuropeptide biosynthesis, release, and action through GPCR.....	9
1.3.2 Neuromodulatory control of innate behaviors.....	11
1.4 Context and state dependent adaptation of innate behavior	12
1.5 Integration and hierarchy in innate circuits and behavioral selection	13
1.6 <i>Drosophila melanogaster</i> as a model organism	13
1.6.1 Life cycle of <i>Drosophila melanogaster</i>	14
1.6.2 EM reconstruction of the first instar <i>Drosophila</i> larval brain.....	15
1.6.3 <i>Drosophila</i> larvae to study neuromodulation.....	15
1.7 The somatosensory system in <i>Drosophila</i> larvae	16
1.8 The gustatory system in <i>Drosophila melanogaster</i>	19
1.9 Neuromodulatory computation of adaptive and context-dependent behaviors in <i>Drosophila</i>	20
1.10 Objectives	21
Aim 1: How is noxious light input integrated and processed by Dp7 neurons and its neuropeptides?.....	22
Aim 2: How is gustatory fructose input integrated and processed by Dp7 neurons and its neuropeptides?.....	23
Aim 3: How is innate avoidance and foraging behavior adapting in a multisensory context and depending on the animal's state?.....	24
Aim 4: Do Dp7 neurons influence innate behavioral choice in a multisensory context in an internal state-dependent manner?.....	25
2 Materials and Methods	26
2.1 Chemicals and reagents	26
2.2 Consumable materials	28
2.3 Agar plates	29
2.3.1 Grape agar plates.....	29
2.3.2 For light avoidance assay.....	29
2.3.3 For fructose preference assay.....	29
2.3.4 For context and state dependent behavior and tolerance assay.....	30

2.4 Fly food	30
2.5 Antibodies	31
2.6 <i>Drosophila</i> stocks	32
2.7 Primers	34
2.8 Technical equipment, Web based browser and softwares	34
2.9 <i>Drosophila melanogaster</i> stocks	36
2.10 Fly maintenance	36
2.11 Genetics	38
2.11.1 Gal4-UAS and LexA-LexAOP systems.....	38
2.11.2 Restriction of spatial expression pattern of Gal4 with Gal80 and Split-Gal4	39
2.11.3 Trojan Gal4 (T2A Gal4).....	39
2.12 Calcium imaging	40
2.13 Two choice behavior assays	41
2.13.1 Light avoidance assays.....	42
2.13.2 Fructose preference assay	42
2.13.3 Context and state-dependent behavior assay	43
2.13.4 Tolerance assay.....	43
2.14 Starvation protocol	44
2.15 Mechanonociception assay	44
2.16 Dissection and Immunohistochemistry	44
2.17 Neuronal reconstruction and circuit mapping	45
2.18 Generation of transgenes	46
2.19 Statistics	46
3 Results	47
3.1. Dp7 neurons are necessary for light avoidance in <i>Drosophila</i> larvae	47
3.2. Dp7 neurons connect the VNC to the higher brain regions	49
3.3. Dp7 neurons have somatosensory and gustatory presynaptic partners	51
3.4. A subset of tracheal neurons is highly connected to Dp7 neurons	54
3.5 Dp7 neurons integrate noxious light from multiple somatosensory circuits	56
3.6 A08n neurons respond to acute UV stimulation but are not necessary for light avoidance behavior	57
3.7. V^{td2} neurons are light sensing neurons and required for light avoidance behavior	58

3.8. Vtd2 neurons are functionally connected to Dp7 neurons mediating light avoidance, but not mechanonociceptive behavior	60
3.9. Circuit mapping for identifying neurons downstream of Dp7 in the light avoidance circuit	61
3.10 Domain-specific compartments for processing of noxious light and noxious touch information	63
3.11 Putative peptide release events occur on the lateral dendritic branch of Dp7 neurons adjacent to ABLK neurons	65
3.12 ABLK neurons are involved in light avoidance responses.....	66
3.13 ABLK neurons are functionally downstream of Dp7 neurons in the light avoidance circuit	68
3.14 Generation of a neuropeptide release reporter for Ilp7	69
3.15 UV light induces acute Ilp7 neuropeptide release from Dp7 neurons	71
3.16 ABLK expresses the Relaxin-family receptor Lgr4.....	73
3.17 Lgr4 receptor is required for light avoidance responses.....	74
3.18 ABLK neurons are selectively required for light avoidance	75
3.19 Fructose foraging behavior in <i>Drosophila</i> larvae is modulated by Ilp7 and sNPF neuropeptides	77
3.20 Dp7 neurons and its Ilp7 neuropeptide limits foraging behavior in <i>Drosophila</i> larvae	79
3.21 Candidate neurons from the Dp7 connectome that may be involved in foraging behaviors	80
3.22 <i>Drosophila</i> larvae integrate context and internal state to select for the most imminent behavior	83
3.23 <i>Drosophila</i> larvae adaptively tune down light avoidance when starved to forage on fructose.....	86
3.24 Dp7 neurons mediate a context and internal state-dependent behavioral switch	87
3.25 Ilp7 regulates context and internal state-dependent innate behavior.....	90
3.26 sNPF neuropeptide modulates integration of light and fructose	92
3.27 Potential circuit elements linked to integration of contextual sensory input.....	93
4. Discussion	95
4.1 Network computation relies on modality- and circuit-specific neuromodulation to generate discrete escape behaviors.....	95
4.1.1 Sensory neurons coding for different nociceptive modalities converge on peptidergic Dp7 hub neurons.....	96

4.1.2 Dp7 neuron derived Ilp7 and the Lgr4 receptor are involved in light avoidance behavior in the larvae.	97
4.1.3 Dp7 neurons gate the generation of modality-specific behaviors through distinct neuropeptide actions	98
4.1.4 Modality-specific circuits converge on distinct domains of Dp7 neurons .	101
4.1.5 Ilp7 mediated co-transmission occurs during light avoidance behavior ...	102
4.1.6 Ilp7 neuropeptide is acutely released upon light exposure	102
4.1.7 Ilp7-Lgr4 signaling mediating escape behaviors might be a conserved across species	104
4.2 Neuropeptidergic control of fructose foraging behavior in <i>Drosophila melanogaster</i> larvae.....	105
4.2.1 Dp7 neurons limit fructose-foraging behavior in the larvae.....	105
4.2.2 Dp7-derived Ilp7 neuropeptide limits fructose foraging behavior in the larva	106
4.2.3 Dp7 neurons connect to several feeding-related neurons	108
4.2.4 Dp7 neurons and Ilp7 possibly regulate local feeding networks in the SEZ region	109
4.2.5 sNPF neuropeptide promotes fructose foraging behavior in the larvae ...	110
4.3 Context and state-dependent adaptation of innate behavior.....	111
4.3.1 Internal state does not influence uni-sensory light avoidance or foraging behaviors	111
4.3.2 A behavioral paradigm integrating contextual cues with the larval internal state	113
4.3.3 <i>Drosophila</i> larvae integrate contextual cues with internal state to generate innate adaptive behaviors	113
4.3.4 Dp7 neurons mediate a context and state-dependent behavioral switch	115
4.3.5 Neuromodulatory control of internal state-dependent innate behaviors ..	117
4.3.6 Neuronal and peptidergic framework for achieving innate behavioral plasticity	120
5 Summary	124
5.1 Zusammenfassung	125
6 Abbreviations.....	127
7 Appendix	130
Appendix 1: Reconstructed synaptic partners of Dp7 neurons	130
Appendix 2: EM reconstructed MIP neurons	131
8 References	132
9 Acknowledgements.....	149
10 Curriculum vitae	150
11 Publication	151
12 Affidavit	152

LIST OF FIGURES

Figure 1: The structural and functional motifs.	7
Figure 2: Motifs from <i>C.elegans</i> includes the feedforward loop, bifan and bi-parallel.	8
Figure 3: <i>Drosophila</i> larvae with sensory neurons td, C1da to C4da neurons along its body wall.	16
Figure 4: Rolling requires sensory integration and neuromodulatory feedback from Dp7 derived sNPF.	18
Figure 5: Illustration of Aim 1.	23
Figure 6: Illustration of Aim 2.	23
Figure 7: Illustration of Aim 3.	24
Figure 8: Illustration of aim 4.	25
Figure 9: Dp7 neurons and its neuropeptide <i>Ilp7</i> are required for light avoidance behavior.	48
Figure 10: EM reconstruction of Dp7 neurons derived from pCC pioneering neurons	51
Figure 11: Dp7 connectome includes different classes of somatosensory and gustatory neurons.	53
Figure 12: EM reconstruction of upstream v`td neurons synapsing onto Dp7 neurons and circuit analysis.	55
Figure 13: Analysis of the somatosensory wiring diagram of Dp7 neurons.	57
Figure 14: A08n neurons downstream of C4da neurons are responding to UV light, but not required for light avoidance.	58
Figure 15: V`td2, but not v`td1 neurons respond to noxious light.	59
Figure 16: V`td2 neurons are upstream of Dp7 neurons in the light avoidance circuit.	60
Figure 17: Analysis of the Dp7 synaptic wiring diagram and motifs deduced from it.	63
Figure 18: Light avoidance and mechanonociceptive circuits converge on discrete compartments of Dp7 neurons.	64
Figure 19: <i>Ilp7</i> localization and peptide release in the lateral dendritic region of Dp7 neurons.	65
Figure 20: ABLK neurons are part of the light avoidance circuit.	67
Figure 21: ABLK neurons are functionally downstream of Dp7 neurons and <i>Ilp7</i> in the light avoidance circuit.	69
Figure 22: Generation of an <i>Ilp7</i> neuropeptide release reporter (<i>NPRR^{ilp7}</i>).	70
Figure 23: <i>Ilp7</i> neuropeptide is acutely released upon UV stimulation.	72
Figure 24: <i>Lgr4</i> is expressed in ABLK neurons and is localized next to <i>Ilp7</i> puncta.	73
Figure 25: <i>Lgr4</i> is needed for UV light responses of ABLK neuron and light avoidance behavior.	75
Figure 26: Divergence of mechanonociceptive and light avoidance circuits occurs at ABLK neurons level.	76
Figure 27: Sugar preference in the larva and its modulatory elements.	78
Figure 28: Dp7 neurons and its neuropeptide <i>Ilp7</i> modulate fructose preference in <i>Drosophila</i> larvae.	80
Figure 29: Potential circuit elements linked to Dp7 neurons.	82

Figure 30: <i>Drosophila</i> larvae integrate context and hunger state to switch from avoidance of light to foraging for fructose under light exposure.	85
Figure 31: Adaptability of light avoidance on fructose under starvation.	87
Figure 32: Modulatory Dp7 neurons mediate the behavioral switch from light avoidance to light tolerance in presence of fructose and hunger drive.	89
Figure 33: Ilp7 peptide derived from Dp7 neurons is involved in context and state-dependent behavior.	91
Figure 34: sNPF promotes integration of light and fructose to enable state dependent responses.	92
Figure 35: Bamas neurons possibly integrate noxious light and gustatory inputs.	94
Figure 36: Schematic showing convergence of mechano and light avoidance circuit onto Dp7 neurons which are facilitating rolling and light avoidance behaviors by discrete peptide actions on specific circuit components.	96
Figure 37: The larvae integrate contextual cues and internal state to decide for an appropriate behavioral response.	115
Figure 38: Neural framework for the context and state dependent behavioral switch	123

LIST OF TABLES

Table 1: Chemical and reagents.....	26
Table 2: Ingredients for 1L of 10x PBS solution	27
Table 3: Ingredients for GRASP buffer.....	27
Table 4: List of consumable materials	28
Table 5: Ingredients for preparation of 1L grape agar	29
Table 6: Ingredients for 1L of standard fly food	30
Table 7: Primary antibodies.....	31
Table 8: Fly stocks.....	32
Table 9: Primers	34
Table 10: List of technical equipment.....	34
Table 11: List of Web based browser and softwares used.....	35

1 INTRODUCTION

1.1 Innate and adaptive behaviors

Animals are born with a huge repertoire of innate behaviors, which they inherited genetically from their parents (Scheller and Axel, 1984). Innate behaviors support vital life sustaining actions of feeding, escaping from danger, sleep, mating and aggression. These behaviors are generally devoid of learning experiences and persist throughout an animal's lifespan, although innate behaviors can also be modified by experience (Grunwald Kadow, 2019).

Animals reside in multisensory environments, thus context, the sensory perception of odor, taste, smell, hearing, vision from the immediate environment is also implemented into innate behavioral decisions (Lee and Lee, 2013; Liu and Kanoski, 2018; Sayin et al., 2018). Aside from context, innate behaviors are also influenced by internal states, which refer to central forces of arousal, motivation, drive and emotion pertaining to behavioral states like feeding, escape, mating and sleep (Anderson, 2016). Context and internal states are not mutually exclusive and uncorrelated factors but are synergistically encoded by neural circuits to give rise to a specific behavior.

At times, an animal may also need to prioritize and choose an innate behavior over another. Such a hierarchy in innate behavior was proposed by Tinbergen as early as 1951. One example is that of foraging animals fleeing from a predator attack, a common phenomenon in the wild. In this example, the animals exhibit a contextual - item selection (Lee and Lee, 2013), whereby they choose the item predator attack over food to engage in an escape response. By fleeing from the predator, animals also show adaptive behavioral response towards a foraging need. Though the behavior is adaptive in the presence of the predator, without the latter, the same act would be perceived as maladaptive.

In other contexts, adaptive behavior is also consistent with an exploration-exploitation axis or cost-benefit decision, which is tuned by context and internal state to enforce the main goal, that of surviving. An example is that *Drosophila melanogaster* larvae are feeding on noxious food when starved (Wu et al., 2005).

1 Introduction

In this case, the animal exhibits a contextual response selection (Lee and Lee, 2013), where it produces a different response towards the noxious food source. However, the adaptive behavior is based not only on context, but also on the internal state of the animal.

Feeding and escape behaviors, though both critical for survival, have antagonistic drives and the selection of one behavior likely suppresses the other. For my thesis, I focused on understanding the neural and molecular mechanisms of innate escape and feeding-related behaviors at the circuit level and how internal state acts together with contextual cues to coordinate and prioritize the most imminent innate behavior.

1.1.1 Nociceptive behaviors

Nociception describes the universally conserved detection, processing and escape reaction of an animal towards a noxious sensory stimulus (Basbaum et al., 2009). Nociception precedes nociceptive pain in vertebrates (reviewed in (Yam et al., 2018)). Thus, understanding the circuit mechanism of nociception is the basis for understanding pain.

Noxious cues sensed by animals are often species-specific and can generally include harsh touch, high heat, high intensity light, intense cold, chemicals, high osmotic strength, heavy metals, pH and certain odorants (Im and Galko, 2012; Tracey, 2017; Basbaum et al., 2009). The primary sensors of noxious cues are sensory cells called nociceptors (Smith et al., 2009; Woolf and Ma, 2007). In vertebrates, nociceptors comprise unmyelinated C-fibres and the myelinated A δ , and the A β fibres (Kandel et al., 2000). In invertebrates, nociceptors tile the body walls of the animals and include the Class IV dendritic arborisation neurons (C4da) in flies and the PVD and the ASH neurons in *C. elegans* (Tobin and Bargmann, 2004; Tracey, 2017).

Across species nociceptors are either unimodal, that is they respond to a single noxious cue, or polymodal, in which case they are activated by several noxious stimuli (Basbaum et al., 2009; Tobin et al., 2004). In mammals, for example, the polymodal C fibers can detect heat, chemicals and harsh touch and connect to second order projection neurons in the dorsal horn of the spinal cord (Kandel et al., 2000).

1 Introduction

Submodality-specific activation of 12 different low-threshold mechanoreceptor neuron types encodes different touch sensations and participate in noxious touch responses (Li et al., 2011; Zimmerman et al., 2014).

Nociceptive escape responses are diverse and can range from acute reflex actions to hide or flight responses with a general aim of avoiding or reducing bodily harm (Branco and Redgrave, 2020). Defective noxious information processing can under-activate or over-activate the “danger alarm” in an organism: a maladaptive behavior, which can have life threatening consequences. In very rare cases, animals are incapable of detecting noxious stimuli and engaging in defensive responses. For example, mutations of the SCN9A gene, which encodes for the alpha subunit of the voltage gated sodium channel (Nav.1.7), in nociceptors leads to incapability of humans to sense pain (Cox et al., 2006). Sensitisation of the nociceptive pathways in humans is also associated with conditions like allodynia and hyperalgesia. Allodynia is the condition whereby nociceptors become sensitised by pro-inflammatory substances like substance P and bradykinin which make them react to innocuous stimuli (reviewed (Dubin and Patapoutian, 2010)). Hyperalgesia is a condition where the response of nociceptors towards painful stimuli is enhanced. Hyperalgesia may ultimately give rise to chronic pain that is a common condition with so far unmet medical needs (Basbaum et al., 2009; Sandkühler, 2009).

1.1.2 Feeding behaviors

Feeding is a critical behavior, which is present in all forms of life whereby an organism acquires energy to sustain life. Feeding behavior can be broken up into two behavioral layers starting with an appetitive phase also known as the exploratory or gustatory phase, which leads to the consummatory phase (Craig, 1918). The two feeding stages are quite independent of each other and involve discrete circuits as well as modulatory elements (reviewed in (Schneider et al., 2013)). In vertebrates, once the consummatory phase is reached, the appetitive phase is put to rest. The appetitive phase is also a decisive phase, where the neural circuits balance context (for example, nutritive content of food, imminent danger from predation) with internal state (drive, arousal, and motivation).

1 Introduction

To maximise the chances of proceeding to the consummatory phase, animals have also evolved foraging strategies to optimise their success of feeding. The Carpenter bee is normally a diurnal animal. However, when seasonal night blooming plants blossom, they extend their foraging period to night time (reviewed in (Somanathan et al., 2019)). *C.elegans* alternate their foraging behaviors between roaming and dwelling to meet metabolic needs, avoid predation and to explore their environment (Ben Arous et al., 2009).

Foraging also has genetic links whereby different allelic combinations are maintained in populations with different foraging strategies (Fitzpatrick et al., 2007; Kaun et al., 2007). In *Drosophila* natural variations in the *foraging* (*for*) gene encode for either the rover (*for^R*) or sitter (*for^S*) configuration. Compared to sitters, rovers typically forage more and move between food patches, which gives rovers a survival advantage in scarce food conditions (Kaun et al., 2007). Similarly in *C.elegans*, heritable variation of the receptor for Ascaroside pheromones generates alternative foraging strategies (Greene et al., 2016).

1.1.3 Internal state and drive for feeding

The internal state reflects an animal's status, such as motivation, drive, arousal or emotion, which can affect the behavioral outcome. For example, hunger state normally generates a homeostatic drive, which is driven by interoceptive cues like nutrient availability in the bloodstream. A homeostat normally functions at a given set point. Drives including that for hunger are generated when the equilibrium differs from the set point. The purpose of the drive for hunger is to bring back the system to a set point that is to return to the sated state to meet metabolic demands (Kandel et al., 2000). The drive for hunger has moreover been proposed to be under very strong selection and it can dominate over other needs or behaviors (reviewed in (Grunwald Kadow, 2019)).

1 Introduction

In mammals, the hypothalamus is the main region responsible for maintaining feeding homeostasis (Sternson, 2013). In *Drosophila melanogaster* a functionally homologous region known as the sub-oesophageal zone (SEZ) is involved in processing feeding-related behaviors (Miroschnikow et al., 2020).

Aside from the homeostatic drive, feeding also involves a non-homeostatic process which is driven by environmental and cognitive factors (Liu and Kanoski, 2018). Defects in non-homeostatic processes of feeding have been linked to conditions like obesity and anorexia. As reviewed in (Liu and Kanoski, 2018), the neural pathways for homeostatic and non-homeostatic feeding are not totally dissociable. Homeostatic feeding mostly involves lower-level neural processing, while the latter involves more of higher brain processing. Thus, knowledge learned about factors which drive the homeostatic feeding pathway can potentially also be applied to the non-homeostatic pathways.

1.2 Circuits, networks and motifs

Innate behaviors are resulting from the flow of sensory information and processing by circuits in the nervous system to produce a specific motor output. The simplest innate behavior is that of the defensive reflex action, like the gill withdrawal reflex in *Aplysia* and the knee jerk reflex in humans (Kandel et al., 2000). The simple reflex action involves the passage of information along three-unit circuits made up of sensory, relay and motor neurons. More sophisticated innate behaviors like feeding, however, rely on more complex neuronal networks, which can be composed of several sub-circuits (Miroschnikow et al., 2018). Understanding how neural networks are organised to compute information effectively is of paramount importance for understanding innate, adaptive and maladaptive behaviors.

Over the past decades, several approaches such as dye filling methods (Kandel et al., 2000), viral (Callaway and Luo, 2015) and genetic tracing (Talay et al., 2017), diffusion tensor imaging (Gigandet et al., 2013) and electron microscopy (EM) reconstruction (white J.G, southGate E, Thomson J.N, 1986) have made it possible to trace neurons and track their connecting partners.

1 Introduction

A unique feature of EM reconstruction is that it also provides precise information at synaptic levels about how strong the connections between two neurons are. It also provides the opportunity to find parallel pathways, which are connected indirectly by 2-hop connections. EM reconstruction has allowed mapping out the whole nervous system of *C. elegans* with 300 neurons, while the *Drosophila* first instar larval brain with approx. 10000 neurons has been reconstructed to about 70% (Eichler et al., 2017; Ohyama et al., 2015). EM reconstruction has also been done in smaller regions in the brain of larger animals like mice and zebrafish (Helmstaedter et al., 2013; Wanner et al., 2016).

Information about synaptic connection between neurons can also be analyzed mathematically to define so called motifs (Alon, 2007; Milo et al., 2011). Network motifs are recurring small patterns, which are typically composed of nodes representing neurons and vertices, which relate to interconnection between nodes based on synaptic numbers. Motifs can also be viewed as building blocks, which make up complex network architectures in the brain (Alon, 2007). Circuit motifs in the brain have been proposed to be of two types, namely the structural motif and the functional motif. The structural motif refers to all the motifs that can be deduced from a neuron (Fig. 1A). The functional motif refers to those motifs among others (found in the structural motif) (Fig.1B), which are activated in response to a specific stimulus (Sporns and Kötter, 2004).

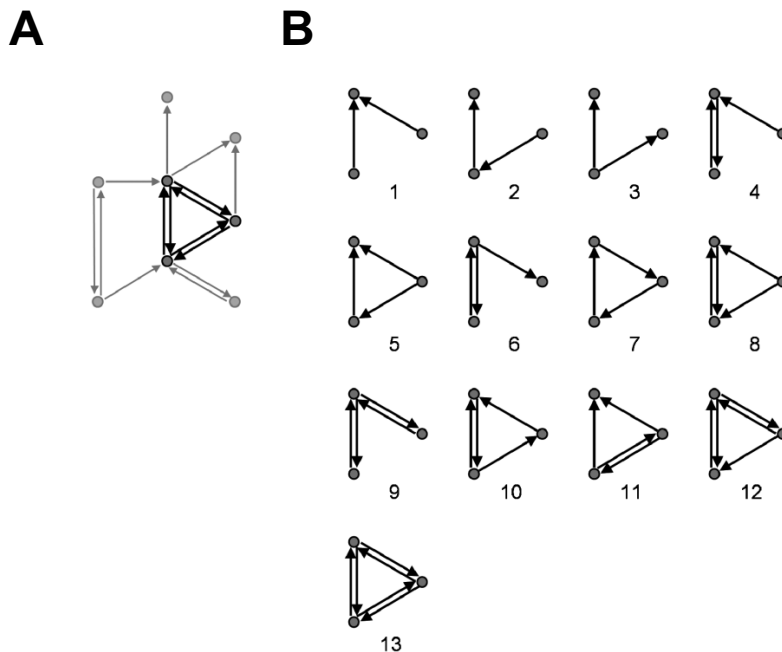


Figure 1: The structural and functional motifs. **A.** the structural motif includes all the connections, which can be deduced from a neuron. **B.** the functional motif refers to selective motifs from a given neuron which may be active at a given time. Taken from (Sporns and Kötter, 2004).

Motifs can serve as a platform to assess information-processing capabilities of the subset of neurons. As motifs are found across biological as well as non-biological systems, the functional role of a motif can be predicted from other systems. For example, a four-node feedforward loop motif can be found in neural networks as well as in transcription systems and electronic circuits. From the connectome of *C.elegans*, three types of motifs were deduced, namely the feedforward, bifan and biparallel motifs (Milo et al., 2011) (Fig. 2).

1 Introduction

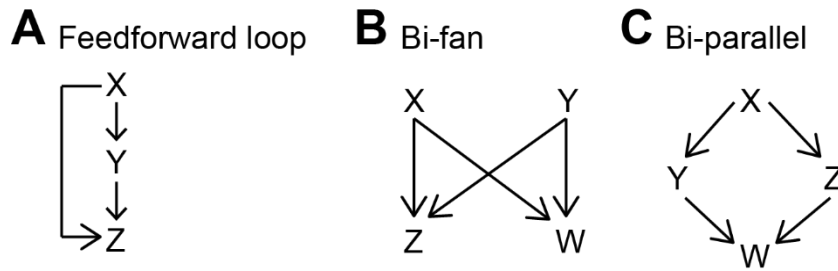


Figure 2: Motifs from *C.elegans* includes the feedforward loop, bifan and bi-parallel. The letters X, Y, Z, W refers to neurons and the arrows indicate synaptic connections. Adapted from (Milo et al., 2011).

Network motifs undoubtedly offer a platform to understand how groups of neurons represent discrete information, how they can combine multisensory information and how circuit elements may be integrated and used to make behavioral decisions (Kandel et al., 2000). Indeed, information which can be obtained about the computational efficiency of motifs are diverse and can range from the ability to filter noise and to enhance the processing power of neural architectures (Burgos et al., 2018; Ohyama et al., 2015). Hunching and bending are two different locomotive behaviors, which are generated by *Drosophila* larvae in response to mechanical cues. The neural elements mediating these behaviors were shown to occur through shared motifs, which consist of several inhibitory nodes. Activation of inhibitory nodes in the bending motif was shown to inhibit hunching behavior and vice versa, while disinhibition as a result of reciprocally connected feedforward inhibition promoted both hunching and bending (Jovanic et al., 2016).

1.3 Connectome and neuromodulation

Behaviors are the result of extensive processing of information by various neural elements in a circuit. While knowledge of the connectome is fundamental for getting insights into the anatomical synaptic wiring diagram of a circuit, interpreting behavior solely on connectomes can be challenging. This is because of a number of factors such as uncertainty about which synapses are potentially active during a specific behavior, the presence of parallel pathways where two neurons may be connected by direct or indirect synaptic routes, and uncertainty about the excitatory/inhibitory nature of the connections (reviewed in (Bargmann and Marder, 2013)).

1 Introduction

Thus, bringing in additional elements that enable neuron to neuron communication on top of the connectome are essential for understanding behaviors. One such other form of neuron-to-neuron communication are neuromodulators, which are widespread across the nervous system of animals (Li and Kim, 2008; Nässel, 2002; Taghert and Nitabach, 2012).

Neuromodulation is in fact the process by which the function and output of a synaptic circuit and network is changed through modulatory signalling via monoamines (e.g. Dopamine, Serotonin) or peptides and their corresponding G-protein coupled receptors (GPCRs) (Bargmann, 2012; Taghert and Nitabach, 2012). Neuromodulators have broad functions in the brain ranging from the synaptic to the circuit and network level. They are altering the strength of synapses, conductance or the properties of intrinsic membrane channels (Marder and Thirumalai, 2002). In contrast to small molecules neurotransmitters, neuropeptides can also function asynchronously and act on neurons which are at considerable distances from their site of production (van den Pol, 2012). In this respect, neuromodulation can bring another layer to circuit function which cannot be gleaned from connectome data. Thus, while the connectome with a given number of potential circuits can be regarded as a road map, neuromodulators can be seen as traffic signs. Neuromodulators can direct context and internal state-dependent information flow through the network to select for an appropriate behavior (Bargmann, 2012).

1.3.1 Neuropeptide biosynthesis, release, and action through GPCR

Neuropeptides are mostly composed of 5-50 amino acids long polypeptide gene products which are produced by most neurons. They are primarily synthesized as large neuropeptide precursors and then transported to the Golgi apparatus where they are packaged into secretory vesicles after several sorting sessions (Jung and Scheller, 1991; Kelly, 1985).

The secretory vesicles bud off the trans-Golgi and condense into mature opaque large dense core vesicles (LDCVs), which are subsequently targeted to their site of release (Sossin and Scheller, 1991). The firing mode of peptidergic neurons may range from normal stimulation frequencies to higher frequencies including burst and tonic firing (Marder and Thirumalai, 2002).

1 Introduction

The high frequency firing mode of peptidergic neurons is beneficial to induce consistent circuit activity to extend a behavioral state, for example the sleep state (reviewed in (Oishi and Lazarus, 2017)).

Following neuronal stimulation, LDCVs are released by two modes of exocytosis, the so called kiss-and run or full release (Breckenridge and Almers, 1987; Ding et al., 2019; He et al., 2006; Wong et al., 2015). Kiss and run release refer to partial release, in which the vesicle content exits through a fusion pore. Full release means complete release of the vesicle contents and completes fusion of the vesicle with the plasma membrane. Release can be parasynaptic, which refers to release close to active synaptic zones or asynaptic via volume transmission (Leng and Ludwig, 2008). Parasynaptically released neuropeptides can act either directly on opposite cells or on distantly located cells. Volume transmission can be of paracrine mode, whereby a neuropeptide produced by one cell acts on several cells which may be located far away. A limitation with paracrine signalling, however, is that it may be difficult to trace the neuron receptive to the neuropeptide, especially so if the receptor for the neuropeptide is unknown (Nässel and Winther, 2010). Neuropeptides have also been reported to act in an autocrine manner. Galanin produced by the magnocellular neurons in the hypothalamus exerts an autocrine effect through Galanin receptor 1 present in its dendritic zone (Landry et al., 1998, 2003).

Neuropeptides signal to cells expressing their cognate receptor, which are typically members of GPCRs family. GPCRs are classified based on their sequence and structural similarities. In vertebrates, five families are distinguished, with most neuropeptide receptors belonging to the largest class of rhodopsin or class A GPCRs. Once a neuropeptide binds to its receptor, a specific intracellular signalling cascade is triggered, which may signal through cyclic adenosine monophosphate (cAMP), inositoltriphosphate (IP3), calcium or mitogen activated protein kinase (MAPK) among others. Knowledge of GPCRs has proven to be very valuable, not only in understanding physiology, but also serving as major drug targets (Hauser et al., 2017).

Peptidergic neurons are not only activated synaptically by upstream neurons but may also be activated by the action of other neuropeptides. Peptide to peptide hierarchy is quite often observed in the nervous system and may act in feedback loops.

1 Introduction

For example during ecdysis, a positive feedback loop of Eclosion hormone (EH)/ Ecdysis triggering hormone (ETH) system ensures that ecdysis initiation is proceeding to its conclusion (Ewers, 2012).

1.3.2 Neuromodulatory control of innate behaviors

Neuromodulation is widespread in escape behaviors across the animal kingdom. In vertebrates, the C nociceptors release substance P, Calcitonin-gene related peptide (CGRP) and Tachykinin (Tk), which all modulate nociception (Basbaum et al., 2009). Feeding is also highly subjective to neuromodulation, which provides flexible, context and state-dependent control over feeding network dynamics (Atasoy et al., 2012; Flavell et al., 2013; Lewis et al., 2015; Shang et al., 2013).

Feeding is mediated through coordinated signals between several organs, which send peptidergic signals to the brain regulating feeding initiation or aversion (Murphy and Bloom, 2006; Yang et al., 2011). Positive regulators of feeding in vertebrates include among others Ghrelin, Agouti related peptide (AgRP) and Neuropeptide Y (NPY) (reviewed in (Morton et al., 2006)). In rodents, intracerebroventricular administration of Ghrelin stimulates food intake within 5 mins in the animals (Nakazato et al., 2001). This increased intake of food is due to the action of Ghrelin that is produced by the hypothalamic cells acting on NPY and AgRP neurons. In addition, the NPY and AgRP neurons also release the neurotransmitter Gamma-aminobutyric acid (GABA), which promotes feeding by inhibiting satiety neurons in other hypothalamic regions (reviewed in (Morton et al., 2006)).

Leptin on the other hand acts on the hypothalamic neurons, the pro-opiomelanocortin (POMC) neurons to suppress feeding (Cowley et al., 2001). Other suppressing signals of feeding include insulin which is produced by pancreatic cells and which enters the brain in relation to its plasma levels (reviewed in (Baskin et al., 1988; Schwartz et al., 2000)). Insulin act by suppressing the activity of the NPY and AgRP in the hypothalamus (Morton et al., 2006)).

1 Introduction

1.4 Context and state dependent adaptation of innate behavior

Adaptability of behavioral action, brought about by flexible neural circuits, is very important to maximise chances of survival. Such flexible mechanisms are conferred to a great extent by peptide regulation of circuits, although local interneurons may as well have facilitating or inhibitory effects on circuit function mediating innate behaviors (Barik et al., 2018).

Context and internal state are crucial players pertaining to adaptive behaviors. Hunger, for example, influences the hedonic values of food by modulating the processing of sensory inputs to odor, vision and taste (Inagaki et al., 2015; Root et al., 2011; Stoeckel et al., 2007). The fruit fly feeds on rotten fruit, which contains both, innate attractive odors from acetic acid and repulsive carbon dioxide (CO₂). Flies learn to integrate the two conflicting odors at the mushroom body (MB) level and selectively implement it into their feeding behaviors. In the starved state, feeding is promoted at the expense of the repulsive cue by the action of the protocerebral anterior medial cluster (PAM) dopaminergic cells, which promote attractive odor preference and feeding by inhibiting the mushroom body output neuron (MBON) responsive to aversive CO₂ (Lewis et al., 2015).

While adaptive behaviors can be advantageous to animals, at the same time they can also be challenging when the choice between the contextual cues involves an exploration-exploitation axis. Zebrafish for example, shift their behavior from avoidance to approach towards predators when starved, with the intention of exploring resources to meet metabolic demands, while at the same time increasing their chances to become a prey themselves. This behavioral transition is processed by the optic tectum in response to signals from the hypothalamic-pituitary-interrenal axis and the serotonergic systems (Filosa et al., 2016). Mice show a similar adaptive behavior by foraging in challenging areas under starved state, which in that case is driven by the action of the hypothalamic AgRP neurons (Padilla et al., 2016). Balancing cost versus benefits for survival thus requires flexibility at the circuit level to appropriately adapt behaviors.

1 Introduction

1.5 Integration and hierarchy in innate circuits and behavioral selection

One of the most important functions of the brain is to appropriately encode, decode and interpret information, which relies extensively on neuromodulatory computation at the network level (Kandel et al., 2000). Behaviors, whether innate, learned, or adaptive, are not mutually exclusive from each other at the circuit level. In fact, it has been proposed that there is interaction and overlap among the circuits mediating different behavioral states, such that the most critical one to meet survival demands at a given point determines the behavioral act (Grunwald Kadow, 2019).

Mice experience pain from inflammation mediated by central mechanisms and acute pain by the activation of nociceptors. During hunger state, the perception of pain in mice decreases to promote feeding. This behavioral transition depends on starvation, a state sensed by hypothalamic AgRP, which respond by secreting NPY that in turn acts on the NPY receptor 1 (NPYR1) in the parabrachial nucleus to subsequently desensitize inflammatory pain. Feeding is thus hierarchically above inflammatory pain during hunger (Alhadeff et al., 2018).

Hunger pangs also inhibit sleep, while a sated state induces sleep, a phenomenon which is seen in humans and in flies. In this example, hunger drive dominates over sleep need, which is modulated by NPY and Hypocretin/Orexin in rodents (Shang et al., 2013; Szentirmai and Krueger, 2006). In flies, sleep reduction due to hunger is mediated through the circadian clock genes independent of the sleep circuit (Keene et al., 2010).

1.6 *Drosophila melanogaster* as a model organism

Drosophila melanogaster is an organism with a simple yet complex enough brain to be capable of executing an array of complex innate, learned as well as adaptive behaviors, which in most cases can be quantitatively assayed (reviewed in (Diegelmann et al., 2013))(Hückesfeld et al., 2016; Ko et al., 2015; Ohyama et al., 2015). Other favourable features of *Drosophila* include its fast generation time, its huge genetic toolkit, as well as available connectome data for the first instar larvae, which makes it feasible to understand circuit motifs and their role in mediating behavioral selection.

1 Introduction

1.6.1 Life cycle of *Drosophila melanogaster*

Drosophila melanogaster is a holometabolous animal with a short developmental phase of 10 days when reared at 25°C. Its life cycle consists of the embryo, larval, pupal and adult stages. The life cycle starts with egg laying: females can lay 100 eggs per day, however, only in ideal food environments. Unfavourable conditions cause premature development of the eggs before oviposition.

The embryo develops into a 1st instar larva (L1) after 20 to 22h at 25°C. This is followed by a molt at 48 hrs to the 2nd instar larval stage (L2) and finally a 3rd molt at 72h to the 3rd instar larval stage (L3). Due to the presence of its thin cuticle lining the larva they are subjective to dehydration and show a light avoidance behavior (Sawin-McCormack et al., 1995). The third instar larvae is further classified into the foraging stage 3rd instar larvae (between 72 to 98h) and the wandering stage 3rd instar larvae (98h to 120h), at which time point the larva stops feeding. During this transition from feeding to wandering stage several behavioral changes occur in addition to food aversion: a switch from positive to negative geotaxis occurs, thermal preference shifts to a lower set point, and negative phototaxis turns into to neutral phototaxis (Keene and Sprecher, 2012; Sawin-McCormack et al., 1995; Sokabe et al., 2016; Wu et al., 2003). At day 5, the wandering larvae ecdyse to prepupae and remain in this immobile, starved state for 3 more days. Ecdysis involves the action of several neuropeptides including the Eclosion hormone, the crustacean cardioactive peptide and Bursicon (Krüger et al., 2015; McNabb et al., 1997). Coordination of growth with developmental timing during the larval to pupal stage is achieved by the insulin like peptide 8 and its cognate receptor Leucine rich G protein coupled receptor 3 (Lgr3) (Garelli et al., 2015). At day nine or ten an adult fly emerges from the pupae.

1 Introduction

1.6.2 EM reconstruction of the first instar *Drosophila* larval brain

The *Drosophila* larva has approximately 10,000 neurons (Nassif et al., 2003) as compared to 10^7 in rats (reviewed in (Lowell, 2019)), which made EM reconstruction of the whole first instar larval brain more feasible and less challenging than in rodents. To date, approximately 70 percent of the neurons have been reconstructed (Eichler et al., 2017; Gerhard et al., 2017; Ohyama et al., 2015; Schneider-Mizell et al., 2016) with several completed regions including the optic nerve, the mushroom body and the pharyngeal nerves (Eichler et al., 2017; Larderet et al., 2017; Miroshnikow et al., 2018). Connectome reconstruction in the larva has greatly promoted understanding of behaviors at the circuit level (Burgos et al., 2018; Fushiki et al., 2016; Jovanic et al., 2019; Ohyama et al., 2015). Quite complex motifs have also been dissected from *Drosophila* connectome reconstruction, which have aided to explain the hierarchy of specific behavioral sequences (Jovanic et al., 2016). Moreover, the *Drosophila* connectome data has helped in understanding of multimodal sensory integration at the behavioral level (Ohyama et al., 2015). EM larval reconstruction has to some extent also been done to topologically map large dense core vesicles on neuronal arbors (Schlegel et al., 2016).

1.6.3 *Drosophila* larvae to study neuromodulation

Drosophila melanogaster is also an ideal system to study the functions of neuropeptides in innate circuits as it contains a good ratio of neurons to neuropeptides and GPCRs (reviewed in (Nässel, 2002)), quite similar to vertebrates yet acting on fewer neurons. These features thus make the larva a feasible organism to map behavioral outcomes at the circuit and neuromodulatory levels.

1 Introduction

1.7 The somatosensory system in *Drosophila* larvae

The somatosensory neurons in *Drosophila* larvae consist of five major classes of neurons which includes the external sensory (es) neurons, the chordotonal neurons, the bipolar dendrites neurons, the tracheal neurons (td), and the dendritic arborisation neurons (Bodmer and Jan, 1987; Ghysen et al., 1986) (Fig. 3). The dendritic arborisation neurons are classified according to their increasing dendritic complexity from Class 1 (C1da), Class 2 (C2da), Class 3 (C3da) to the highly arborized C4da neurons (Grueber et al., 2002)(Fig. 3). The tracheal neurons (td) innervate the tracheal system and are further subcategorised into ν td1 and ν td2 neurons based on their morphological location (Qian et al., 2018).

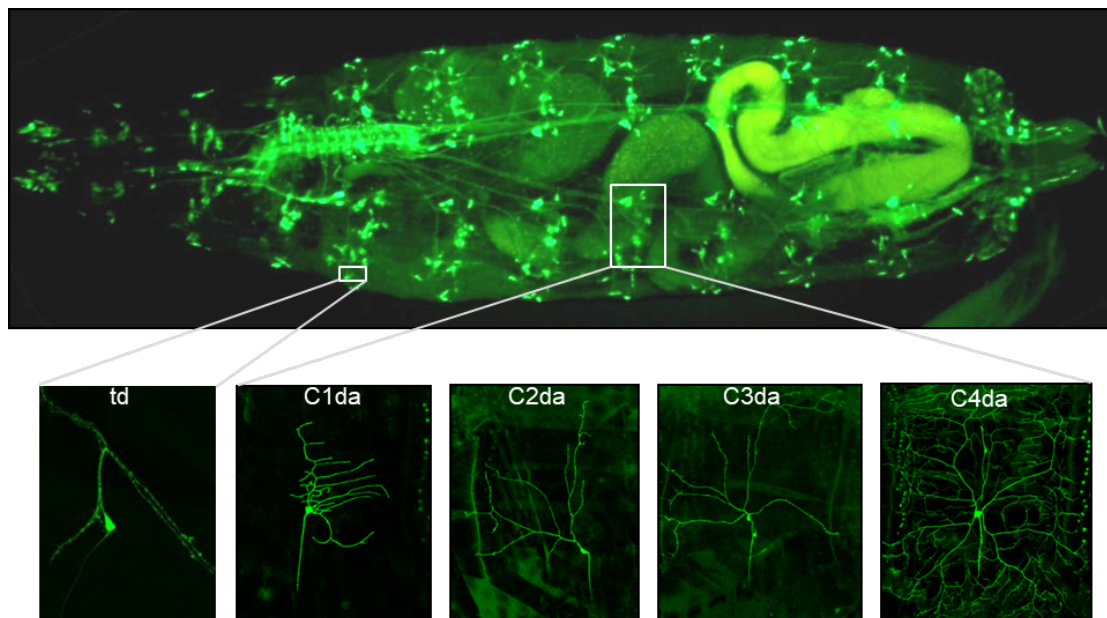


Figure 3: *Drosophila* larvae with sensory neurons td, C1da to C4da neurons along its body wall. Picture taken from Dr. Peter Soba and adapted from (Grueber et al., 2007; Qian et al., 2018).

C1da neurons are associated with proprioception (Cheng et al., 2010), while C2da and C3da neurons are involved in gentle touch sensations. Touch responses are mediated by specifically expressed mechanosensory ion channels including no mechanoreceptor potential channel (*nompC*), which is a member of the Transient receptor potential (Trp) family of ion channels, Ripped pocket (*rpk*) and NMDA receptors 1 and 2 (Tsubouchi et al., 2017; Yan et al., 2013).

1 Introduction

C2da and C3da are also involved together with C4da neurons in promoting nociceptive rolling responses in the larvae (Hu et al., 2017). C4da neurons tile the whole body wall of the larvae (Grueber et al., 2002). They are polymodal neurons that are capable of sensing and triggering modality-specific escape responses towards an array of noxious cues including noxious heat, light and touch (Tracey et al., 2003; Tsubouchi et al., 2017; Xiang et al., 2010; Yamanaka et al., 2013).

Mechanical stimulation and as well as predator attack from parasitoid wasps specifically trigger corkscrew-like rolling behavior, during which the larvae rotates around its anterior-posterior body axis (Robertson et al., 2013; Tracey et al., 2003). Noxious blue and UV light triggers on the other hand triggers stop and turn avoidance responses in the larvae (Xiang et al., 2010). Cell type-specific ablation of C4da neurons leads to loss of nocifensive responses in the larvae. C4da neurons rely on specific isoforms of the rhodopsin-like Gustatory Receptor 28b_c (Gr 28b_c) and TrpA1_c channels for phototransduction while pressure sensitive channels sense noxious mechanical stimuli (Kim et al., 2012). Noxious heat is sensed through the activation of another alternative spliced variant of the TrpA1 channel, TrpA1_D (Gu et al., 2019). Specificity in nociceptive signal reception in C4da neurons might be conferred by the nature of the currents evoked through the Trp channels: noxious heat currents are typically of higher magnitude than those for blue light (Terada et al., 2016). In contrast to glutamatergic nociceptors in vertebrates, insects nociceptors are generally cholinergic by nature (Lumpkin and Caterina, 2007).

Several mechanonociceptive circuit neurons and neuromodulatory elements have been elucidated downstream of C4da neurons. They include the C4da to A08n neuron connection (Hu et al., 2017; Kaneko et al., 2017) and the dorsal pair insulin-like peptide 7 (Dp7) neurons in the ventral nerve chord neuron, which also receive input from C2da and C3da neurons (Fig. 4A). C4da-A08n and Dp7 neurons function in a neuromodulatory feedback loop (Fig. 4B). Mechanonociceptive stimuli activate both A08n and Dp7, with Dp7 neurons providing sNPF neuropeptide-mediated feedback on the mechanosensory neurons, which express the cognate sNPF receptor (sNPFR). sNPF signalling in turn increases C4da to A08n output and facilitates mechanonociceptive responses (Hu et al., 2017) (Fig. 4).

1 Introduction

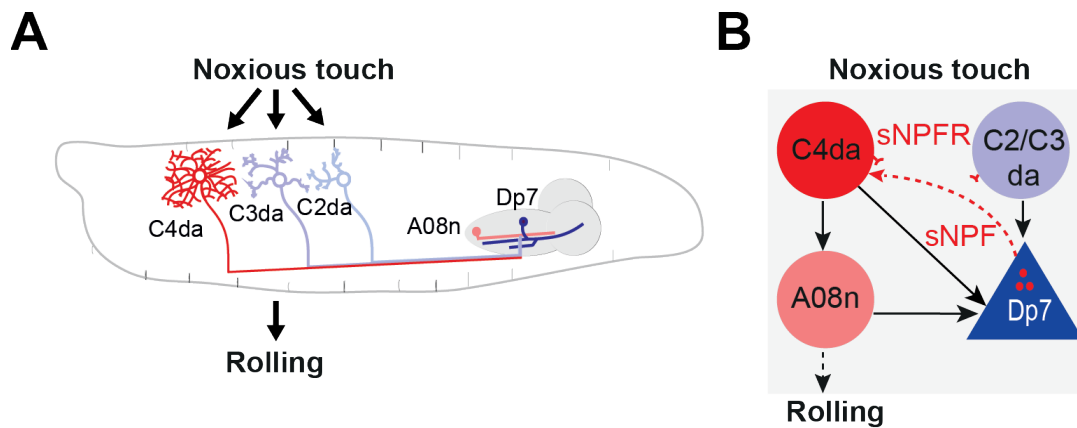


Figure 4: Rolling requires sensory integration and neuromodulatory feedback from Dp7 derived sNPF. **A.** Noxious touch is sensed by C4da neurons and synergistic action of C3da and C2da neurons. C4da neuron sends its axonal projection to the brain, where it synapses with both A08n and Dp7 neurons. **B.** Upon noxious touch C4da neurons are activated together with C2da and C3da neurons, which activate Dp7 neurons that release sNPF neuropeptide. sNPF acts in a feedback loop back on C4da as well as C3da and C2da neuron, which facilitates A08n output and rolling behavior (Hu et al., 2017).

Extensive mapping studies from EM connectome have also identified neurons downstream of the C4da neurons including the Down and Back neurons (DnB) and Basin-4, which also mediate rolling behavior (Burgos et al., 2018; Ohyama et al., 2015). However rolling behavior executed through the C4da-Basin 4 pathway has been proposed to be synergistically enhanced by inputs from mechanosensory chordotonal neurons, which converge onto Basin neurons (Ohyama et al., 2015).

The somatosensory light avoidance circuit however has not received as much attention as the mechanosensory circuit. Aside from C4da neurons, noxious light is also sensed by blue and UV light sensing rhodopsin 5 photoreceptors in Bolwig's organ, the larval eye (Sprecher et al., 2011). Ablation of Bolwig's organ by expressing the apoptotic gene *hid* abolishes light avoidance behavior in the larvae (Xiang et al., 2010). Downstream of the photoreceptors are the pigment dispersing factor (pdf) neurons (Gong et al., 2010). The circuits involved in light avoidance behavior, though from anatomically distinct regions, are linked asynchronously by neuromodulatory communication.

1 Introduction

The prothoracic hormone (PTTH) producing neurons release PTTH that acts through its cognate receptor Torso in both Bolwig's organ and the somatosensory C4da neurons to regulate light avoidance (Yamanaka et al., 2013).

1.8 The gustatory system in *Drosophila melanogaster*

Like higher vertebrates, the *Drosophila* larva is capable of sensing both attractive and aversive cues to either stimulate or inhibit food intake. The sensory taste systems in the *Drosophila* larvae are located at the anterior tip of the larval head and include the tarsal organ (TO) and the dorsal organ (DO), which can sense the three taste modalities sweet, salty and bitter. Sensory neurons located in the TO project their dendrites towards the external sensilla and their axons to the SEZ of the brain via the maxillary nerve bundle (Rist and Thum, 2017). Sensory neurons of the DO project their axons to the SEZ via the antennal nerve bundle (Apostolopoulou et al., 2015).

The TO residing sensory neurons encode aversive gustatory cues including bitter substances (Apostolopoulou et al., 2014). Specificity in gustatory cues detection by the sensory neurons is achieved by receptors specific to detecting substances. The existence of a large number of sensory gustatory neurons likely evolved with the capability of the larvae to sense diverse soluble compounds like salt, sugars, water, amino acids, fats, ribonucleosides, acids and bitter substances (Apostolopoulou et al., 2014; Mishra et al., 2018). Like nociceptors, some gustatory neurons are also multimodal and capable of sensing diverse gustatory cues through expression of multiple receptors. Receptors which have been found to be involved in gustation in *Drosophila* are from 4 major families including: (1) the seven transmembrane gustatory receptor (GRs) family, the ionotropic receptors (IRs), the *pickpocket* gene family (*ppk*) and *Trp* channels (Dahanukar et al., 2007; Kwon et al., 2011). *Drosophila melanogaster* larvae in the wild are often found foraging on decaying fruits, where the main sugar is fructose, which makes it an innately preferred sugar source. Fructose is detected by the Gustatory receptor 43a (Gr43a) in both adult flies and in the larvae (Mishra et al., 2013; Miyamoto et al., 2012). Aside from being a palatable sugar, fructose also acts as an interoceptive signal for the metabolic state of the larva (Mishra et al., 2013). In adult flies, Diuretic hormone 44 (DH44) neurons in the fly brain also act as an interoceptive sensor for hunger state through sugar sensing via a putative hexokinase transporter (Dus et al., 2016).

1 Introduction

Drosophila larvae, in contrast to the adult, have restricted locomotive capacities and the appetitive stage is mostly rooted in the palatability and nutritive value of the food in its local environment. Adults also need to assess the suitability of the environment for egg laying and mate availabilities.

Similarly to vertebrates, feeding is also a very complex behavior in *Drosophila* involving different factors such as motivation, assessment of the quality of food and involves several feeding command neurons (Gordon and Scott, 2009; Liman et al., 2014). These factors are integrated into feeding decisions through several insect neuropeptides, which in most cases share orthologous modulatory pathways with vertebrates. The fly tachykinin homologue Leucokinin is involved in regulating meal frequency in flies via the action of Leucokinin receptor (Al-Anzi et al., 2010). NPF, a mammalian NPY homologue, promotes food consumption (Beshel and Zhong, 2013). The glucagon-like peptide, Adipokinetic hormone (AKH) is elevated upon starvation to signal hunger (reviewed in (Pool and Scott, 2014)). The Insulin-like peptides (Ilps), Allatostatin A (AstA), the mammalian homologue for Galanin and Hugin neuropeptide, the mammalian homologue for Neuromedin U signal foraging and feeding aversion (Reviewed in (Pool and Scott, 2014)) (Melcher and Pankratz, 2005).

1.9 Neuromodulatory computation of adaptive and context-dependent behaviors in *Drosophila*

Drosophila melanogaster is equipped with a large repertoire of innate behaviors, which display adaptability as well as selectivity for executing the most urgent behavior. Studies have addressed adaptable behaviors by targeting particular neuronal and neuromodulatory elements, which can mediate behavioral transitions (Grunwald Kadow, 2019; Umezaki et al., 2018). For example, NPF-receptor positive neurons in the larval brain mediate adaptive behavior towards consuming noxious food under starvation conditions, aided by the concurrent action of insulin like peptide 2 (Ilp2) (Wu et al., 2005).

1 Introduction

Flies need both water and nutrients to survive. Selectivity for either is based the needs of the animal and regulated by a population of Interoceptive SEZ neurons (ISN). The ISN neurons are activated in response to AKH, which signals low nutrient levels and promotes food intake. At the same time water intake is restricted, likely due to high extracellular osmolarity, which is also sensed by the ISN neurons (Jourjine et al., 2016).

1.10 Objectives

Context and state, as well as neuromodulation, are undoubtedly critical players in the regulation of innate behaviors in *Drosophila melanogaster*. However, most studies so far lack connectome-based insight and cellular resolution of peptidergic actions on innate circuits. It is also unclear how context and state work together towards processing and selecting an innate behavior over another. To gain a better understanding of the underlying circuit mechanisms, I was focusing my thesis work on the innate escape and feeding circuits of *Drosophila melanogaster* larvae.

The Dp7 neurons are key modulators of escape responses. They receive multisensory input from mechanosensory C2da and C3da neurons as well as the polymodal C4da neurons, which are capable of sensing noxious light and noxious touch (Hu et al., 2017). In addition, Dp7 neuron axons project to known feeding centres in the larvae, the SEZ and the protocerebrum (PC) (Hu et al., 2017). The SEZ is the primary taste centre where gustatory neurons projections converge and where feeding decisions are made (Miroschnikow et al., 2020), while the PC region contains neurons which are involved in feeding and foraging responses (Hückesfeld et al., 2016; Rulifson, 2002).

Dp7 neurons are peptidergic and secrete two neuropeptides, sNPF and Ilp7. sNPF derived from Dp7 neurons facilitates mechanonociception by acting in a feedback loop on the sensory neurons to facilitate rolling behavior (Hu et al., 2017) (Fig. 4). Ilp7 and sNPF neuropeptides derived from other neurons have both also been implicated in regulating feeding responses in the larvae (Cognigni et al., 2011; Wu et al., 2003). Ilp7 is produced, aside from Dp7 neurons, in 16 other neurons in the larval brain, 8 of which are found in the ventral-posterior region of the VNC (Miguel-Aliaga et al., 2008).

1 Introduction

Ilp7 neurons were shown to modulate feeding depending on nutritional conditions (Cognigni et al., 2011). However, which Ilp7-expressing neurons mediate this effect is not clear. sNPF is widely expressed in the larval brain (Carlsson et al., 2013) and sNPF producing larval brain lobe neurons promote foraging responses towards glucose (Wu et al., 2003).

Feeding and avoidance behaviors are two conflicting drives that likely coincide in natural environments, such that context and hunger may select for the more demanding behavioral action. In their natural habitat, foraging in bright sunlight can very likely be a daily scenario for larvae. To corroborate this point, a study found that adult flies refrain from feeding under bright sunlight, due to the activation of a TrpA1 isoform sensitive to hydrogen peroxide generated by UV light (Du et al., 2016). Thus, avoidance and foraging behavior may be adaptively regulated depending on the sensory context and the internal state of the animal. Dp7 are among the few interneurons in larvae, which connect the VNC to higher brain regions including the sub-oesophageal zone (SEZ) and the brain lobes (Fig. 8). This distinct anatomical feature likely reflects on their ability to connect somatosensory input with SEZ or brain lobe-resident circuits regulating feeding. Dp7 neurons are thus good candidates for investigating how innate behaviors are regulated in a multisensory context and by the animal's hunger state.

Aim 1: How is noxious light input integrated and processed by Dp7 neurons and its neuropeptides?

My first aim was to find out whether Dp7 neurons and its neuropeptides are involved in light avoidance (Fig. 5). I aimed to specifically map the light avoidance circuit at the EM level to identify circuits required for light avoidance behavior. I further aimed to understand how and where Dp7-derived neuropeptides act on the light avoidance circuit during light avoidance behavior.

1 Introduction

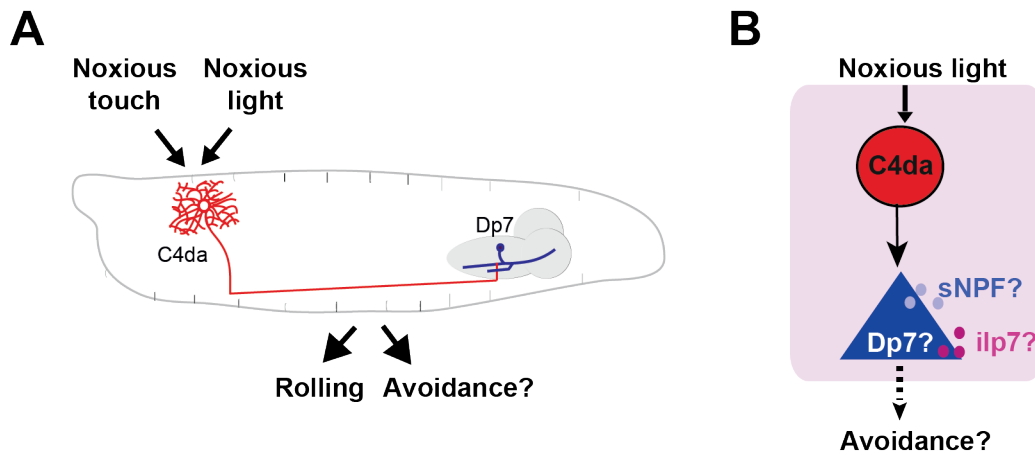


Figure 5: Illustration of aim 1. **A.** Schematic of *Drosophila* larvae with the C4da nociceptors on the body wall that can respond to noxious light and noxious touch. C4da neurons send axons to Dp7 neurons in the brain, and both C4da neurons and Dp7 neurons are involved in rolling escape behavior. Thus, Dp7 neurons might be involved in light avoidance responses as well. **B.** Are Dp7 neurons and its neuropeptides sNPF and Ilp7 involved in innate light avoidance, similarly as in mechanonociception (Hu et al., 2017)?

Aim 2: How is gustatory fructose input integrated and processed by Dp7 neurons and its neuropeptides?

The second aim of my thesis was to find out whether Dp7 neurons and its neuropeptides are involved in foraging responses towards fructose. I also aimed to identify the neuronal partners of Dp7 neurons, which may mediate foraging responses to fructose in the larvae (Fig. 6).

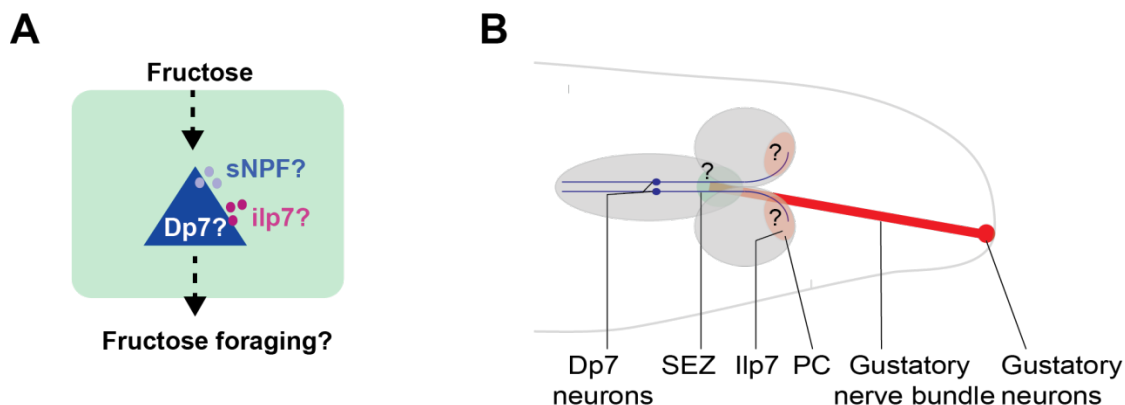


Figure 6: Illustration of aim 2. **A.** Are Dp7 neurons and the neuropeptides Ilp7 and sNPF involved in fructose foraging behavior?

1 Introduction

B. Dp7 neurons arborize in the PC and the SEZ regions (shaded green and orange region respectively). Neurons in those regions (indicated by a question mark) may potentially connect to Dp7 neurons to mediate fructose foraging behavior.

Aim 3: How is innate avoidance and foraging behavior adapting in a multisensory context and depending on the animal's state?

Taking advantage of two conflicting behaviors, feeding and light avoidance, I aimed to design a behavioral paradigm showing that *Drosophila larvae* display hunger-dependent adaptive behavior towards noxious light to promote feeding in the hunger state. The design should include a context of fructose as a food source paired with noxious light and no light. Depending on the state of the larvae, either light avoidance behavior or fructose foraging with adaptation to noxious light may prevail (Fig. 7).

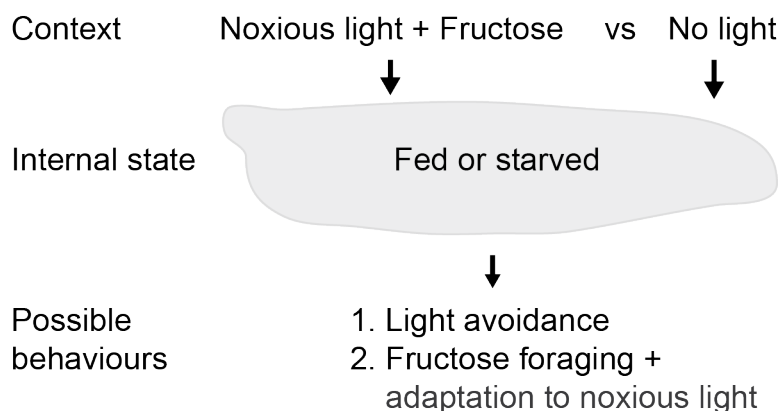


Figure 7: Illustration of aim 3. Larvae exposed to a sensory context of noxious light and fructose versus (vs) no light need to choose between light avoidance or fructose foraging with tolerance/adaptation to noxious light. Selectivity for a particular behavior may also be dependent on the internal state (fed or starved) of the animal.

1 Introduction

Aim 4: Do Dp7 neurons influence innate behavioral choice in a multisensory context in an internal state-dependent manner?

I aimed to ask if and how Dp7 neurons and its neuropeptides acutely coordinate feeding and avoidance at the circuit and behavioral level to prioritize for the most appropriate behavior depending on the hunger state.

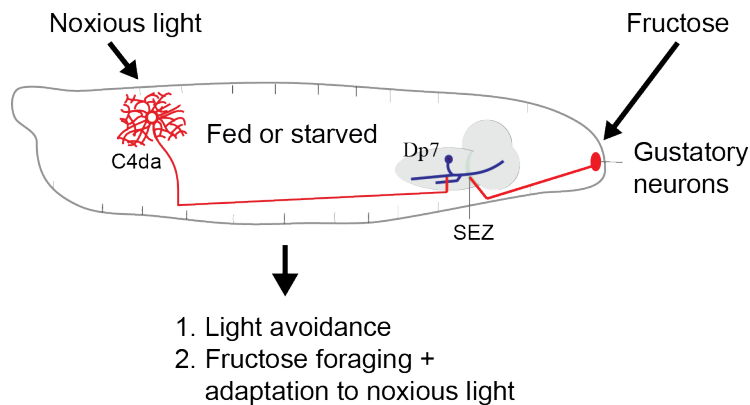


Figure 8: Illustration of aim 4. Dp7 neurons receive input from the VNC by noxious light sensing C4da neurons and arborize in the SEZ region innervated by gustatory neurons. The anatomy of Dp7 may relate to its functional role, which might involve integrating noxious light and foraging inputs to trigger an appropriate behavioral response.

2 MATERIALS AND METHODS

2.1 Chemicals and reagents

The chemicals and reagents which I used for my thesis are commercially available.

Table 1: Chemical and reagents

Material	Company
D-Fructose 99,5%	Carl Roth GmbH + co KG
Baysilone silicone grease (Medium viscous)	Bayer AG, Leverkusen, Germany
Formaldehyde solution 30% (methanol free)	Roth, Karlsruhe, Germany
Triton x-100	Roth, Karlsruhe, Germany
Poly-L-lysine	Sigma-Aldrich, USA
Slow fade Gold	Thermo Fisher, Carlsbad, CA, USA
Donkey serum	Dianova, Hamburg, Germany
Formaldehyde solution 30% (Methanol free)	Roth, Karlsruhe, Germany
Saf-Instant Red yeast	S.I Lesaffre, marcq-en-Baroeul, France
Baysilone® Silicone grease (medium viscous)	Bayer AG, Leverkusen, Germany
All-trans <i>Retinal</i>	Sigma-Aldrich, USA

2 Materials and Methods

1l of 10x phosphate buffer saline (PBS) solution is composed of the following ingredients

Table 2: Ingredients for 1L of 10x PBS solution

Quantity	Ingredient	Company
14.4 g	di-Sodium hydrogen phosphate dihydrate (141.96 g/mol)	Roth, Karlsruhe, Germany
80 g	Sodium Chloride (58.44 g/mol)	Roth, Karlsruhe, Germany
2.4 g	Potassium dihydrogen phosphate (136.09 g/mol)	Merck, Darmstadt, Germany
2 g	Potassium chloride (74.55 g/mol)	Roth, Karlsruhe, Germany

For a final volume of 50mL of dissection buffer the following ingredients were used:

Table 3: Ingredients for GRASP buffer

Quantity	Ingredient	Company
1.08 ml	Sodium Chloride (108 mM)	Roth, Karlsruhe, Germany
250 µl or 3.5 ml	Potassium Chloride (5 mM or 70 mM)	Roth, Karlsruhe, Germany
200 µl	Sodium Hydrogen Carbonate (4 mM)	Roth, Karlsruhe, Germany
100 µl	Sodium dihydrogen phosphate (1 mM)	Merck, Darmstadt, Germany

2 Materials and Methods

500 µl	Trehalose (5 mM)	Roth, Germany	Karlsruhe,
1388 µl	Sucrose (10mM)	Roth, Germany	Karlsruhe,
250 µl	HEPES (5 mM)	Roth, Germany	Karlsruhe,
2050 µl	Magnesium chloride (8.2 mM)	Roth, Germany	Karlsruhe,
100 µl	Calcium chloride (2 mM) pH 7.4	Roth, Germany	Karlsruhe,

2.2 Consumable materials

Table 4: List of consumable materials

Consummable materials	Company	
Cover slips (22 x 22 cm)	Roth, Karlsruhe, Germany	
Drosophila vials (wide, K-Resin)	Genesee Scientific, San Diego, USA	
Flugs® fly plugs for stock bottles	Genesee Scientific, San Diego, USA	
Flugs® fly plugs for plastic vials (wide)	Genesee Scientific, San Diego, USA	
Petri dishes (Ø 10cm or 6cm)	Sarstedt, Nümbrecht, Germany	
Petri dish with compartment	Sarstedt, Nümbrecht, Germany	
Stock bottles 80z round bottom	Genesee Scientific, San Diego, USA	
Superfrost Ultra Plus® microscope slides	Menzel-Gläser, Germany	Braunschweig,

2 Materials and Methods

Sterican® cannula, hypodermic-needle size 20 (0.40 x 20 mm), 27G B.Braun Melsungen AG, Melsungen, Germany

2.3 Agar plates

2.3.1 Grape agar plates

Grape agar plates were prepared by boiling water, agar, and grape juice. After the mixture had cooled down ethanol and propionic acid were added and a volume of 6ml was pipette into 6cm petri dishes.

Table 5: Ingredients for preparation of 1L grape agar

Volume	Ingredient	Company/Source
459 ml	Distilled water	Milli-Q®, Merck, Darmstadt, Germany
500 ml	Grape juice	Supermarket
20g	Agar-Agar, Kobe I powder	Roth, Karlsruhe, Germany
10.5 ml	Ethanol, 95%	Th. Geyer GmbH & Co. KG, Renningen, Germany
10 ml	Propionic acid	Roth, Karlsruhe, Germany

2.3.2 For light avoidance assay

2% of agar in distilled water was used. Agar was dissolved in distilled water, boiled and 12ml were poured in 10cm petri dishes.

2.3.3 For fructose preference assay

2M fructose was dissolved in 2% agar in distilled water by boiling. 28ml of the mixture was poured into one compartment of a 2-sided petri dish. 28ml of plain 2% agar dissolved in distilled water was poured into the other compartment of the petri dish.

2 Materials and Methods

2.3.4 For context and state dependent behavior and tolerance assay

For the context and state dependent behavior assay a two-compartment petri dish was used. 2% agar was dissolved in distilled water by boiling which was then poured in one compartment with a defined volume of 28ml. 2% agar with 2M of fructose was dissolved in distilled water by boiling and 28ml of the solution was poured in the other compartment of the petri dish. For the tolerance assay, 2% agar with 2M of fructose was dissolved in distilled water and 28ml of the solution was poured into each compartment of a two-sided petri dish.

2.4 Fly food

1l of fly standard fly food was prepared with the following ingredients that were dissolved in 1l of distilled water.

Table 6: Ingredients for 1L of standard fly food

Quantity	Ingredient	Company
8.75g	Agar strings	Probio GmbH, Eggenstein, Germany
0.08g	Corn flour	Spielberger-GmbH Brackenheim, Germany
10g	Soy flour	Spielberger-GmbH Brackenheim, Germany
25g	Brewer`s yeast (ground)	Gewürzmühle Brecht, Eggenstein, Germany
0.08g	Malt syrup	MeisterMarken -Ulmer Spatz, Bingen am Rhein, Germany
21.88g	Treacle (molasses)	Graschafter Krautfabrik, Meckenheim, Germany

2 Materials and Methods

1.88g	Nipagin (Methyl4-hydrobenzoate)	Merck, Darmstadt, Germany
9.38 ml	Propionic acid	Roth, Karlsruhe, Germany

2.5 Antibodies

The following primary and secondary antibodies were used:

Table 7: Primary antibodies

Primary antibody	Host	Dilution	Company/Source
Anti-Ilp7	Rabbit	1:5000	Dr. Miguele-Aliaga, MRC clinical Sciences Center, London, UK
Anti-Leucokinin	Rabbit	1:1000	Dr. Dick Nässel, Stockholm University, Sweden
Anti-GFP	Chicken	1:1000	Abcam number (#) ab13970
Anti-HA	Rat	1:200	Roche

Table 8: Secondary antibodies

Secondary antibody	Host	Dilution	Company/Source
Alexa 488	Anti-rat	1:800	Jackson Immunoresearch
Cy3	Anti-rabbit	1:500	Jackson Immunoresearch
Dylight 649	Anti-rabbit	1:250	Jackson Immunoresearch
Cy5	Anti-chicken	1:1000	Jackson Immunoresearch

2 Materials and Methods

2.6 *Drosophila* stocks

I used the following fly stocks for my thesis:

Table 8: Fly stocks

Line	Source
<i>w¹¹¹⁸</i>	Bloomington Stock Center, Indiana, USA, # 3605
<i>R35B01-Gal4</i>	Bloomington Stock Center, Indiana, USA, # 49898
<i>R73B01-Gal4</i>	Bloomington Stock Center, Indiana, USA, # 39809
<i>Gr28b.c-Gal4</i>	Bloomington Stock Center, Indiana, USA, # 57618
<i>UAS-GCaMP6s</i>	Bloomington Stock Center, Indiana, USA, # 91990
<i>UAS-GCaMP6m</i>	Bloomington Stock Center, Indiana, USA, # 91988
<i>UAS-GCaMP7s</i>	Bloomington Stock Center, Indiana, USA, # 80905
<i>ppk-Gal4</i>	Bloomington Stock Center, Indiana, USA, # 32078
<i>UAS-CsChrimson-Venus</i>	Bloomington Stock Center, Indiana, USA, # 55134
<i>UAS-CD4-tdGFP</i>	Bloomington Stock Center, Indiana, USA, # 35836
<i>Lgr4^{T2A}-Gal4</i>	Bloomington Stock Center, Indiana, USA, # 7775
<i>UAS-CD4-tdTomato</i>	Bloomington Stock Center, Indiana, USA, # 35837
<i>UAS-CD4-tdGFP</i>	Bloomington Stock Center, Indiana, USA, # 35836
<i>LexAop-spGFP₁₋₁₀-Syb, UAS-spGFP₁₁-CD4</i>	Bloomington Stock Center, Indiana, USA, # 64315
<i>Lgr4ko</i>	(Deng et al., 2019)
<i>LexAop-Kir2.1</i>	(Hu et al., 2017)

2 Materials and Methods

<i>UAS-spGFP₁₋₁₀-Syb</i>	obtained from M. Gallio, Northwestern University, Evanston, USA)
<i>LexAop-CD4-sp11-CD4-tdTomato</i>	(Hu et al., 2017)
<i>A08n-Gal4 (82E12-Gal4^{AD}, 6.14.3-Gal4^{DBD})</i>	(Hu et al., 2017)
<i>Dp7⁴⁻³-LexA</i>	(Hu et al., 2017)
<i>sNPF^{c000448}</i>	(Hu et al., 2017)
<i>sNPF^{MI01807}</i>	(Hu et al., 2017)
<i>Ilp7-Gal4</i>	(Yang et al., 2008)
<i>Ilp7-LexA</i>	(Yang et al., 2008)
<i>Ilp7^{ko}</i>	(Yang et al., 2008)
<i>Hugin^{VNC} Gal4</i>	(Schoofs et al., 2014)
<i>Lk-Gal4</i>	(de Haro et al., 2010)
<i>UAS-Kir2.1</i>	(Baines et al., 2001)
<i>Dp7-Gal4</i>	Dr. Soba lab
<i>UAS-NPRR^{ilp7}</i>	Generated for this study
<i>UAS-Ilp7</i>	Generated for this study
<i>UAS-Lgr4-HA-flag</i>	Dr. Gontijio, Portugal
<i>UAS-Cadps-RNAi</i>	Vienna Stock Center

2 Materials and Methods

2.7 Primers

The following primers were used:

Table 9: Primers

Primer name	Primer
Ilp7-NotI-c	aaGCGGCCGCATGACCAGAATGATAATAC
ILP7-Nde_nc	agaCATATGGTAGTGATTGCGTCGCTTG

2.8 Technical equipment, Web based browser and softwares

The following technical equipment, Web based browser and softwares were used:

Table 10: List of technical equipment

Equipment	Company
Basler ace 2040gm Camera	Basler, Switzerland
Forceps (Dumont)	Fine Science Tools Inc. Heidelberg, Germany
Light source	ZMNH, Hamburg, Germany
SZX12 stereo microscope	Carl Zeiss AG, Oberkochen, Germany
Olympus FV 1000 MP microscope	Olympus
Zeiss LSM 700 microscope	Carl Zeiss AG, Oberkochen, Germany
Zeiss LSM 900 microscope	Carl Zeiss AG, Oberkochen, Germany

2 Materials and Methods

Table 11: List of Web based browser and softwares used

Web based browser and softwares	Company
Collaborative annotation toolkit for massive amount of image data (CATMAID)	Janelia research campus, USA, (Saalfeld et al., 2009)
Ethovision XT-X2	Noldus Information Technology, Wageningen, Netherlands
Pylon	Basler, Switzerland
StreamPix 6	Norpix, Montreal, Quebec, Canada

2 Materials and Methods

2.9 *Drosophila melanogaster* stocks

Drosophila melanogaster flies were reared on standard fly food at 25°C and 70% humidity with a 12h light and dark cycle. *Drosophila* stocks were maintained at 18°C with a 12h light and dark cycle, which doubled the longevity of flies. The stocks were flipped to new food vials every 4 to 6 weeks. Transgenic flies were maintained in either white mutant (*w*) or yellow white (*y, w*) backgrounds.

2.10 Fly maintenance

Gender was selected based on specific morphological criteria, on flies which were locally anesthetized with carbon dioxide (Bouckaert and Bryant, 2014). New fly stocks were generated by following the standard *Drosophila* genetics (Bouckaert and Bryant, 2014). Balancer chromosomes were used to maintain flies in a heterozygous condition which is particularly well adapted for maintaining lethal stocks. Balancers are also used in setting up combination or recombination crosses as they are combined with phenotypic markers.

The following balancer chromosomes and Markers were used as described in (Chyb and Gompel, 2013):

Chromosome	Balancer chromosome/Marker gene	Abbreviation	Phenotypic description
x	<i>yellow</i>	<i>y</i>	Cuticle is less pigmented than WT, yellowish
x	<i>white</i>	<i>w</i>	Compound eye with ocelli ranging from orange color to completely white
x	<i>First Multiple 7a, Tubby</i>	<i>FM7a, Tb</i>	Marker, <i>Tb</i> : short, stout

2 Materials and Methods

			flies
2	<i>Sternopleural</i>	<i>Sp</i>	Extra bristles and hairs are present on the sternopleurite
2	<i>Curly</i>	<i>Cy</i>	Wings are curled upwards and outwards; degree of curliness vary 18°C to 25°C with more pronounced curliness at 25
2	<i>Curly of Oyster Wee-P</i>	<i>CyO_{WEE-P}</i>	Dominant Marker: <i>Cy</i> , ubiquitously expressed green, fluorescent marker
3	<i>Drop</i>	<i>Dr</i>	Looks like a drop with ventral pointed ends
3	<i>Third Multiple 3, Stubble</i>	<i>Tm3, Sb</i>	Dominant marker, <i>Sb</i> : Bristles stout and short, half the normal size
3	<i>Third Multiple 2, Ultrabithorax</i>	<i>Tm2, Ubx</i>	Dominant marker, <i>Ubx</i> : larger halteres with bristles
3	<i>Third Multiple 6B, Tubby, Humoral</i>	<i>TM6B, Hu, Tb</i>	Dominant Markers, <i>Tb</i> , tubby short stout larvae, hu, Additional 3-6 bristles, some are slightly shorter than normal
3	<i>Third Multiple 2,</i>	<i>Tm2, Ubx,</i>	Dominant markers,

2 Materials and Methods

	<i>Ultrabithorax</i>	<i>Third</i>	<i>Tm6B,</i>	<i>Tb,</i>	<i>ebony,</i>	Cuticle
	<i>Multiple 6B,</i>	<i>Humoral,</i>	<i>Hu, e</i>			pigmentation is darker
	<i>tubby, ebony</i>					than normal, <i>Tb, Ubx</i>

2.11 Genetics

Drosophila melanogaster is equipped with a powerful genetic toolkit in the form of the binary systems Gal4-UAS and LexA-LexAOP (Brand and Perrimon, 1993; Szüts and Bienz, 2000). Using these systems alone or in combination, one can easily report expression of a gene, downregulate or upregulate genes or neurons elements, monitor neuronal activity, overexpress genes of interest to specific subsets of neurons (Venken et al., 2011).

2.11.1 Gal4-UAS and LexA-LexAOP systems

The binary Gal4-UAS system derived from yeast is composed of two components, one component drives expression of the transcriptional activator Gal4 and the other component contains the upstream activator sequence (UAS) for Gal4 that in turn activates a responder (Brand and Perrimon, 1993; Pfeiffer et al., 2010). As Gal4 is not produced by flies, it requires an enhancer which specifically drives tissue or cell type specific expression of the Gal4. Wherever Gal4 protein is produced it binds to UAS which in turn drives expression of the downstream responder. In a forward genetic approach GAL4-UAS may drive expression of a reporter for expression like green fluorescent protein (GFP) or tomato or a reporter for activity like genetically encoded calcium indicator (GCaMP6s). Gal4-UAS system may also be used in reverse genetic approaches, where it enables one to determine the phenotypes associated with loss of a gene or neuronal function. This may be achieved through UAS-Kir2.1, the inward rectifying potassium channel that blocks neuronal activity (Baines et al., 2001).

The LexA-LexAOP system, which is of bacterial origin, works in a similar manner as the Gal4-UAS system. Both systems can also be used in combination like in Synaptobrevin- GFP reconstitution across synaptic partners (syb-GRASP) (Macpherson et al., 2015) or in reporting neuronal activity in silenced neurons (Hu et al., 2017).

2 Materials and Methods

2.11.2 Restriction of spatial expression pattern of Gal4 with Gal80 and Split-Gal4

In order to spatially restrict expression of Gal4, Gal80 the repressor of Gal4 can be used (Lee et al., 1999; Pfeiffer et al., 2010). Gal80 is also useful when combined with *teashirt* (*tsh*) enhancer, *tsh*-Gal80, which specifically blocks expression of Gal4 in the VNC of the larva (Bavelloni et al., 2015). In case driver lines label multiple neurons and one wants to specifically assess the function of neurons in the brain lobes or indirectly determine the function of neurons in the VNC, *tsh*-Gal80 can then be used.

Expression of Gal4 can also be spatially restricted to specific subsets of neurons or even to single neurons with the Split-Gal4 system. Gal4 consists of two functional domains namely a transcription activation domain (AD) and DNA binding domain (DBD). In Split-Gal4 the AD and the DBD of Gal4 are split and are driven by two independent regulatory elements. Thus, only in cells where there is overlap of the expression domains, the AD and DBD of Gal4 heterodimerize via Leucine zippers to reconstitute a functional Gal4 (Luan et al., 2006).

2.11.3 Trojan Gal4 (T2A Gal4)

Trojan Gal4 is used to determine the expression levels of genes in tissues as well in blocking gene functions. Trojan Gal4 consists of a T2A-Gal4-polyA exon carried on a transposon, which can be inserted in introns between coding exons of an endogenous gene. During translation, the T2A, a viral ribosomal skipping site, splice the 2 exons of the endogenous genes such that a truncated protein is produced (Diao and White, 2012; Lee et al., 2018), enabling the T2A to be used as a mutant for a specific gene. However, a fully functional Gal4 is produced in similar quantity as the endogenous gene which enables one to use it in combination with a UAS reporter line to assess the expression pattern of the endogenous gene (Diao and White, 2012; Lee et al., 2018).

2 Materials and Methods

2.12 Calcium imaging

Calcium imaging was recorded non-invasively in live larvae in the soma of specific neurons which was labelled with *UAS-GCaMP* (6s or 7s) that were under the control of specific neuronal Gal4-drivers. A third instar larva aged 94 ± 2 h was mounted on a microscope slide on 60% glycerol that was immobilized with a coverslip. Calcium imaging was done by using the Zeiss confocal microscopy (LSM700/900AS2) with a 40x/NA1.3 oil objective). 400 frame times series were acquired at a frame rate of 0.24 s or 0.34 s (240 x 240 pixels) and ultraviolet (UV) light was applied to the larva for 10 seconds (365nm, 60 μ W/mm² CoolLED).

At least 2 pulses of UV light were given to each larva during the 400 frame time series with an interval of 15 s between the pulses. 5-10 larvae were assayed for each genotype between the Zeitgeber (ZT) 3 to 6. Calcium imaging was performed with similar confocal microscope settings. The StackReg plugin (using translation function, Fiji, ImageJ) was used to correct for internal movement. A region of interest (ROI) was defined in the neuronal soma whereupon GCaMP signal intensity was quantified with the Time Series Analyzer V3 plugin (ImageJ).

Calcium response ($\Delta F/F_0$ (%)) was calculated by subtracting the amplitude of pre-stimulation baseline (average of 19 frames) from the stimulation evoked amplitude as shown below:

$$\Delta F/F_0 (\%) = (F - F_0)/F_0 \times 100.$$

The maximum fluorescence was calculated as

$$F_{max} - F_0 / F_0 \times 100$$

where F_{max} , is the maximum fluorescence observed during the stimulation and F_0 (average of 19 frames).

Graphs of mean \pm s.e.m were plotted using Prism. Comparison of maximum responses ($\Delta F_{max}/F_0$ (%)) were plotted and analyzed with one-way ANOVA and Tukey's *post-hoc* test.

2 Materials and Methods

Ilp7 neuropeptide release (NPPR^{ilp7}) was assayed either on Dp7 soma, its lateral dendritic arbor or on its proximal axonal arbor. Live larvae were subjected to UV stimulation 2 or 3 times with an interval of at least 100 frames in between during a time series during a times series of 500 frames, acquired at 0.24 s/frame with the Zeiss LSM 700 microscope. The baseline fluorescence was acquired on 19 frames followed by 40 frames of pulsed UV onset and offset delay of 40 frames. NPPR^{ilp7} release events were calculated for each puncta using the formula below:

$$\Delta F/F_0 (\%) = (F - F_0)/F_0 \times 100.$$

The n number refers to individual LDCV puncta release events from five different larvae.

Calcium imaging on semi-intact larvae was performed as described in (Hu et al., 2017). Optogenetic activation of v`td2 neurons and imaging of Dp7 soma responses were performed on mid third instar larvae as described in (Hu et al., 2017; Tenedini et al., 2019). Embryos were collected on grape agar plates which were supplied with yeast paste containing 5mM all *trans*-Retinal and kept in darkness at 25⁰C. Activation of sensory v`td2 neurons was induced by v`td2-specific CsChrimson activation using a 635nm light pulse. Comparison of maximum responses ($\Delta F_{\max}/F_0$ (%)) were plotted as box plots and analyzed with the Mann Whitney test.

2.13 Two choice behavior assays

All behavior assays were performed on mid-third stage larvae. Prior to egg collection, animals were pre-staged for half an hour on grape agar plates supplemented with fresh yeast paste to eliminate pre-mature deposited eggs. Following prestaging, embryos were staged on grape agar plates with yeast paste within a fixed time frame (Zeitgeber (ZT) 4-6) for 1 to 2 hours. The staging duration depended on the number of fertilized eggs to minimize the risk of overcrowding.

2 Materials and Methods

2.13.1 Light avoidance assays

Larvae aged 96 h \pm 2h AEL were subjected for 15 mins light avoidance assay originally described in (Mazzoni et al., 2005; Yamanaka et al., 2013) with modifications. The experimental setup was made up of a dark chamber with a white light source (365-580nm, intensity 6.9–3.3 $\mu\text{W}/\text{mm}^2$ and $<0.01 \mu\text{W}/\text{mm}^2$ on the light and dark side respectively) which illuminated one half of a 10cm agar plate. An infrared light emitting diode (LED) source surrounded the plates enabled visualization of the larval distribution in the dark compartment. Recording of larval distribution was done with a digital camera. For each genotype, at least 10 trials were performed with each trial containing 17-20 larvae. Prior to the experiments, 20 larvae were pre-incubated for 15 minutes in the dark. Light avoidance behavior was subsequently assayed by placing the animals in the middle of each petri dish at the light/dark junction. Each trial was run for 16-20 minutes recorded by the camera on top of the chamber using Ethovision, Pylon or StreamPix 6.

Performance index (PI) was calculated at 15 mins as:

(Number of larvae in the dark arena – number of larvae in the light arena) / total number of larvae.

PI data are shown as violin plots, with the middle line representing the median. If more than 3 animals escaped during the trial, the experiment was discarded and wherever possible only trials with all 20 larvae were considered.

2.13.2 Fructose preference assay

Prior to the experiments, 20 larvae were pre-incubated for 15 minutes in the dark. Fructose preference assay were performed using the above-described setup without light source and animals were assayed on plates which in one half contained 2% agar and the other half contained 2 Molar (M) fructose in 2% agar. 18-20 larvae were used for each trial and a total of 10 trials were performed for each genotype.

2 Materials and Methods

The PI was calculated at 15 mins as:

(Number of larvae in fructose compartment – number of larvae in compartment without fructose) / total number of larvae. PI was shown as violin plots.

2.13.3 Context and state-dependent behavior assay

Prior to the experiments, 20 larvae were pre-incubated for 15 minutes in the dark. The context and state-dependent behavior assay was designed such that half of a petri dish which was composed of 2% agar was in darkness while the other half with 2M fructose in 2% agar was lit with a white light source (365-580nm, intensity 6.9–3.3 $\mu\text{W}/\text{mm}^2$ and $<0,01 \mu\text{W}/\text{mm}^2$ on the light and dark side respectively). 18-20 larvae were used for each trial and a total of 10 trials were performed for each genotype.

The PI was calculated at 15 mins as:

(Number of larvae in dark compartment– number of larvae in lighted compartment with fructose) / total number of larvae. PI was shown as violin plots.

2.13.4 Tolerance assay

Prior to the experiments, 20 larvae were pre-incubated for 15 minutes in the dark. The tolerance assay was performed using 2M fructose in 2% agar plates with only one side being illuminated with a white light source and the other side in darkness (365-580nm, intensity 6.9–3.3 $\mu\text{W}/\text{mm}^2$ and $<0,01 \mu\text{W}/\text{mm}^2$ on the light and dark side respectively). 18-20 larvae were used for each trial and a total of 9 trials was performed.

The PI was calculated at 15 mins as:

(Number of larvae in dark compartment with fructose – number of larvae in lighted compartment with fructose) / total number of larvae.

PI was shown as violin plots. Heat maps were generated using Fiji as an average of all trials between the time frame of 10 to 15 minutes.

2 Materials and Methods

2.14 Starvation protocol

Larvae aged between 79 to 80hrs AEL that were reared on grape agar plates supplemented with yeast paste were subjected to food-deprived conditions. This was achieved by washing the larvae with distilled water until they were no longer coated in food particles or agar, the larvae were then carefully transferred to a dampened filter paper in a fly food vial that was then closed with a vial plug and kept in the fly incubator overnight for 16-20h. Behavioral experiments were performed on starved larvae aged 94-98h.

2.15 Mechanonociception assay

Mechanonociception assays were performed as in (Hu et al., 2017).

2.16 Dissection and Immunohistochemistry

Dissection of larval brains was performed in PBS and fixed in 4% paraformaldehyde/PBS solution for 15 min. The brains were then washed in PBST (0.3% Triton X-100 in 1xPBS) three times (10 min each) and either mounted directly or blocked for 30 min with PBST containing 10% Donkey serum and incubated overnight with a primary antibody in a blocking buffer at 4⁰C. After washing three times with PBST (10 min each), the brains were incubated with a secondary antibody in PBST for 1h at room temperature. Following the incubation, the brains were washed three times with PBST (10 min each) and mounted on either a poly-L-lysine coated coverslip or on Super frost coverslips in Slow Fade Gol images were collected using either the Zeiss confocal microscope LSM700 or LSM900 and processed with Fiji.

For Syb-GRASP (Macpherson et al., 2015), larval brains were dissected in 5 mM dissection buffer. Following dissection, brains were washed 3 times (5 seconds each) alternately in dissection buffer containing 5mM KCl and 70mM KCl. Finally, the brains were incubated for 10 min in 5 mM dissection buffer and fixed in 4% formaldehyde for 15 minutes, followed by immunohistochemistry and mounting as described above.

2 Materials and Methods

2.17 Neuronal reconstruction and circuit mapping

EM reconstruction was performed using the web-based CATMAID program, which contains compiled serial section Transmission Electron Microscopy (ssTEM) images of the first instar larvae (Saalfeld et al., 2009). Dp7 neurons were manually reconstructed as described in (Ohyama et al., 2015; Schneider-Mizell et al., 2016). I annotated the synapses by considering four key criteria: (1) Detection of a highly visibly T-bar, (2) numerous synaptic vesicles are docked near T-bars, (3) the pre and post synaptic membranes contact each other in at least two consecutive segments, (4) a synaptic cleft is visible.

By using this iterative method, pre- and post-synaptic neurons of Dp7 neurons were subsequently manually reconstructed. Validation of neuronal reconstruction was done as described in (Ohyama et al., 2015; Schneider-Mizell et al., 2016). Following reconstruction, the neuronal partners of Dp7 neurons were named based on comparison of their morphology with light microscopic data from the literature. The built-in CATMAID visualization 3D visualization tool was used to illustrate neuronal morphology as well as pre and postsynaptic sites. The customized graph tool in CATMAID was used to build network graphs. In the graph tool, the interaction between a pair of nodes referring to neurons was deduced based on the absolute number of synaptic counts with minimum of 2 synapses. Network graphs were made starting with the first processing layer, the sensory neurons that consisted of 3 nodes representing sensory neurons (C4da, v`td2 and v`td1), which connect to Dp7 neurons that makes up the second processing layer. 2-hop connections between sensory and Dp7 neurons were also extracted. The third layer was based on outputs of Dp7 neurons with (1) VNC projections and (2) being interconnected with sensory neurons (Hugin-VNC and ABLK). Arrow thickness was automatically determined on CATMAID as a function of synaptic counts. Analysis of synaptic counts between neurons present on the lateral arbor of Dp7 neurons was done with GraphPad Prism.

2 Materials and Methods

2.18 Generation of transgenes.

UAS-Ilp7 transgene was made by cloning Ilp7 cDNA via EcoRI into the pUAST vector and P-element mediated transformation. UAS-Ilp7 was inserted on the 3rd chromosome. The Ilp7 neuropeptide release reporter (NPRR^{ilp7}) was designed similarly to (Ding et al., 2019) whereby GCaMP6s was fused to the C-terminus of the Ilp7 neuropeptide. Ilp7 cDNA was amplified from clone F118537 by PCR with specific primers carrying NotI and NdeI restriction sites and fused in frame with GCaMP6s. Transgenes were generated by phiC31-mediated genomic integration into the AttP2 landing site. All constructs were verified by sequencing.

2.19 Statistics

Statistical analyses for the two choice behavioral assays were performed with one-way ANOVA with Tukey's *post-hoc* test for comparing more than 3 groups. Comparison of 2 groups was performed with the unpaired Student's *t*-test with Welch's correction or by using the Mann Whitney test. All tests were two-tailed, and the differences were considered significant for $p < 0.05$ (* $P < 0.05$, ** $P < 0.01$, *** $P < 0.001$, **** $P < 0.0001$). Statistical testing was done with Prism (GraphPad).

3 RESULTS

3.1. Dp7 neurons are necessary for light avoidance in *Drosophila* larvae

C4da neurons respond to noxious light (UV and blue light) and harsh touch that result in specific innate escape responses, light avoidance and rolling, respectively (Tracey et al., 2003; Xiang et al., 2011; Yamanaka et al., 2013). Dp7 neurons were previously shown to be downstream of C4da neurons in generating rolling behavior in response to noxious touch by providing modulatory feedback via the neuropeptide sNPF (Hu et al., 2017). As Dp7 neurons integrate input from various sensory neurons and have neuromodulatory functions, I reasoned that they might be potential candidates for computing discrete C4da neuron-dependent nociceptive behaviors.

To find out if Dp7 neurons are involved in light avoidance, I made use of a two choice avoidance assay (darkness versus white light) as described previously (Mazzoni et al., 2005; Yamanaka et al., 2013). Light is unattractive to the larva, which is defined here by a performance index with negative values indicating preference for light and positive values indicating preference for darkness. The inward rectifier potassium channel 2 (Kir2.1) (*LexAop-Kir2.1*) was expressed specifically in Dp7 neurons using a Dp7 neuron-specific line (*Dp7-LexA*). Kir-2.1 mediated Dp7 neuron silencing in larvae strongly reduced their light avoidance responses (Fig. 9A), suggesting that Dp7 neurons are needed for light avoidance, in addition to their role in mechanonociception (Hu et al., 2017).

As Dp7 neurons have modulatory roles in mechanonociception via sNPF (Hu et al., 2017), I tested whether sNPF or Ilp7 neuropeptides are involved in light avoidance behavior. I assayed light avoidance responses in *ilp7^{ko}* and *sNPF* mutants and found that Ilp7, but not sNPF is required (Fig. 9B). Ilp7 is expressed in 18 neurons in the larval brain including Dp7 (Miguel-Aliaga et al., 2008). Thus, to specifically test for the role of Ilp7 in Dp7 neurons, I used a specific line to express Ilp7 (*Dp7-Gal4>UAS-ilp7*) only in Dp7 neurons in an *ilp7^{ko}* background.

3 Results

Under these conditions, light avoidance responses were fully restored indicating that Dp7-derived Ilp7 is not only necessary, but also sufficient for driving light avoidance in *Drosophila* larvae (Fig. 9C). I next tested for a functional role of Dp7 neurons in response to noxious light. Live larvae expressing the calcium indicator GCaMP7s (Dana et al., 2019) in Dp7 neurons were stimulated with a 10s with UV-A light pulse (360 nm, 60 $\mu\text{W}/\text{mm}^2$). UV light stimulation elicited a robust calcium transient in the soma of Dp7 neuron (Fig. 9D), suggesting that Dp7 is part of the light avoidance circuit.

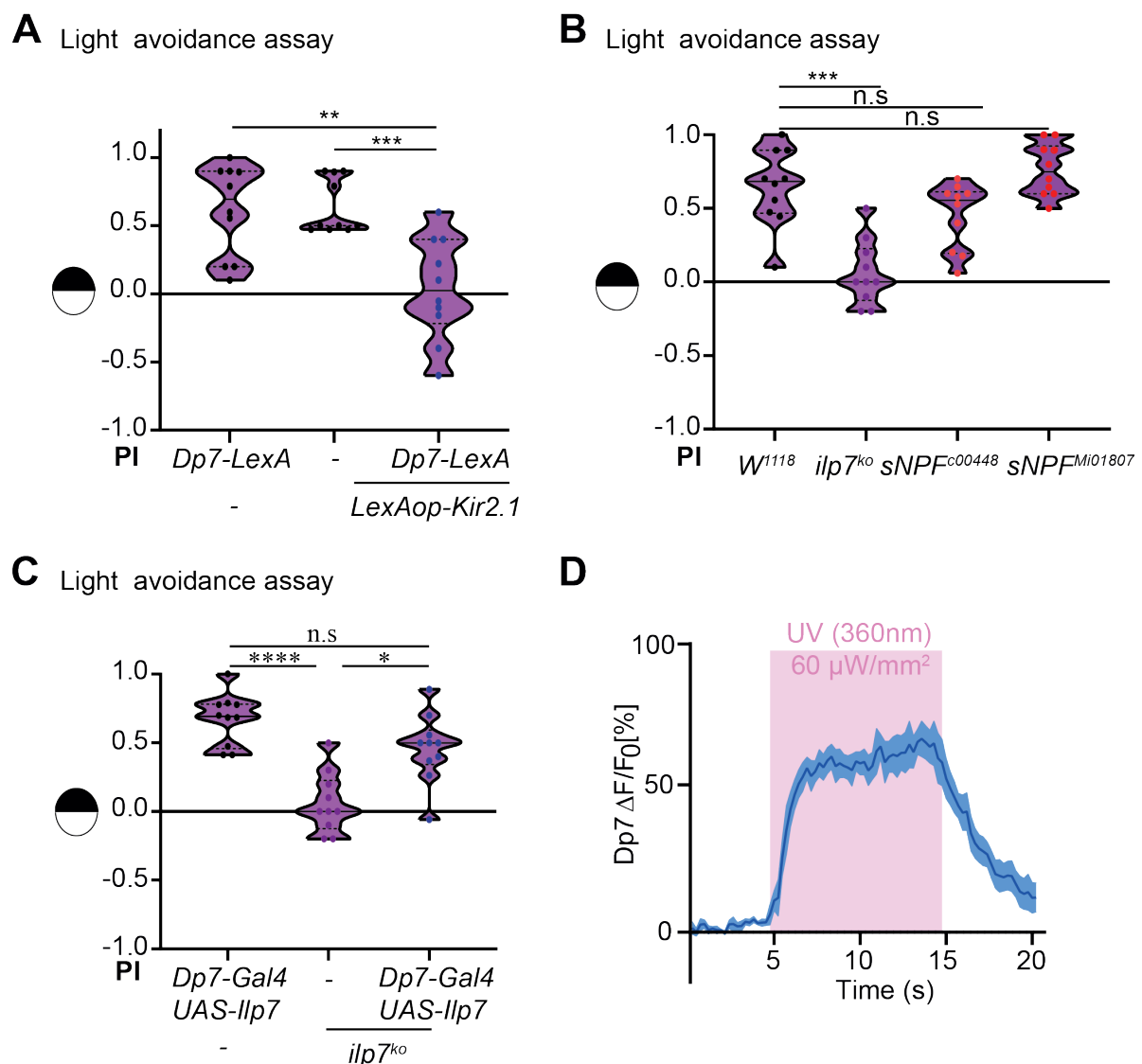


Figure 9: Dp7 neurons and its neuropeptide Ilp7 are required for light avoidance behavior.

3 Results

A. Kir2.1-mediated silencing of Dp7 neurons (*Dp7-LexA*) impaired larval light avoidance (n=10 trials, **P<0.01, ***P<0.001, one-way-ANOVA with Tukey's *post-hoc* test). **B.** *Ilp7^{ko}* but not *sNPF* mutant animals showed decreased light avoidance responses (n=10 trials, ***P<0.001, n.s., non-significant, one-way-ANOVA with Tukey's *post-hoc* test). **C.** Expression of *Ilp7* driving *UAS-Ilp7* exclusively in Dp7 neurons (*Dp7-Gal4*) in an *Ilp7* knockout (*ilp7^{ko}*) background restored light avoidance (n=10 trials, *ilp7* data set as in **B**, *P<0.05, ****P< 0.0001, n.s., non-significant, one-way-ANOVA with Tukey's *post-hoc* test). **D.** Dp7 neuron activity (*ilp7-Gal4>UAS-GCaMP7s*) in response to UV-A light (365 nm, 60 μ W/mm², mean \pm standard error of the mean (s.e.m.) indicated by shaded area, n=4)

3.2. Dp7 neurons connect the VNC to the higher brain regions

Knowing that Dp7 neurons are crucial elements of both light avoidance and mechanonociception, I was interested in understanding the underlying circuits generating discrete rolling and avoidance behaviors. To this end, EM reconstruction of Dp7 neurons and their synaptic partners was performed.

The web-based interface CATMAID was used for neuronal reconstruction of the compiled 7700 serial EM images of the first instar larval brain (Gerhard et al., 2017; Ohyama et al., 2015; Schneider-Mizell et al., 2016). I first used CATMAID to identify Dp7 neurons somata and their neural arbors were subsequently traced, and their synapses were annotated. From light microscopic studies, Dp7 neurons were known to be located in the A1 segment dorsally near the junction of the posterior commissure (Hu et al., 2017; Ito et al., 1995; Miguel-Aliaga et al., 2008). There are very few neurons in the dorsal region of the larvae except for the pioneering neurons, which set up axonal paths for follower neurons, notably the posterior commissural cells (pCC) and the anterior commissural derived cells (aCC) (Broadus et al., 1995; Hidalgo and Brand, 1997; Jacobs and Goodman, 1989). The pioneering pCC neurons are presumably present in each segments during the embryonic development and later on die after axogenesis is completed (Jacobs and Goodman, 1989). Since I detected only one soma in the dorsal hemisphere in the EM volume of the A1 segment that was not a motor or aCC neuron, I presumed that those cells corresponded to pCC-derived cell, which may be Dp7 neurons (Fig. 10A and A').

3 Results

To confirm that Dp7 neurons are located in between the motor neurons, a double labelling experiment with CD4-tdTomato expressed in motor neurons and CD4-tdGFP expressed in Dp7 neurons was performed. As shown in Fig. 10B, Dp7 somata are indeed localised in-between motor neurons, like the anatomical location of pCC and motor neuron somata in the EM volume (Fig. 10A and A'). Neuronal reconstruction of the pCC-derived cells indeed closely recapitulated the morphology of Dp7 neurons in the L1 larvae at the light microscopic level (Fig. 10C and D). These data suggest that Dp7 neurons are pCC-derived neurons, which are progenitors of the ganglionic mother cell (GMC) 1-1A (Bodmer and Jan, 1987), in contrast to the *llp7*-positive cells in the ventral region of the larvae, which are derived from the *dMP2* lineages (Miguel-Aliaga et al., 2008).

The morphology of Dp7 neurons is very interesting, as the axonal arbor extend from the T1 segment to the SEZ to the brain lobes, while its dendrites extend medially to the SEZ region and project medially and laterally into the ventral nerve cord (VNC) up to the abdominal segment 4 (A4) in the L1 larva (Fig. 10D and E). Based on the regions innervated by Dp7 neurons, they might be involved in other behaviors aside from escape responses. These include foraging and feeding behaviors, as feeding decisions are known to be made in the SEZ region of the larva (Miroschnikow et al., 2020).

3 Results

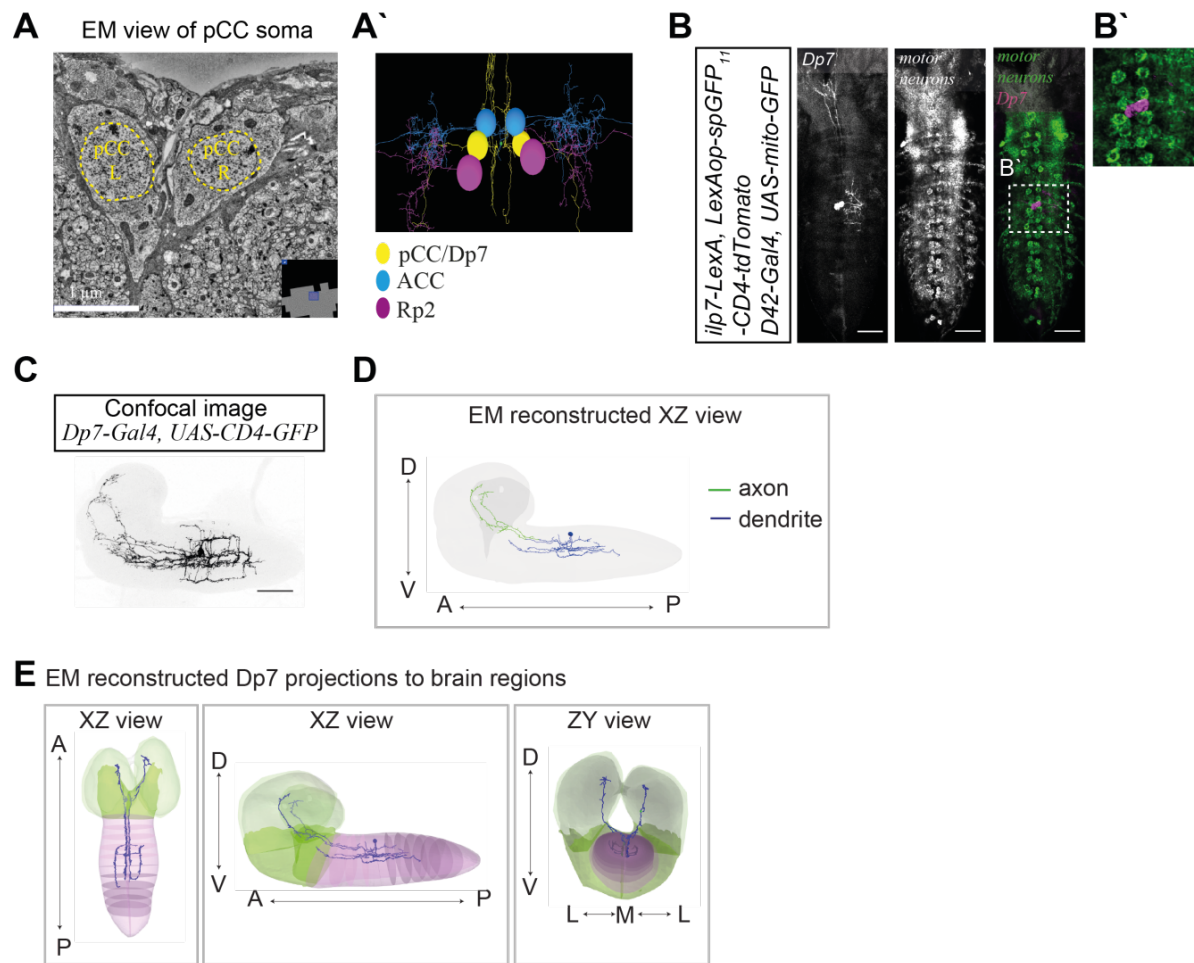


Figure 10: EM reconstruction of Dp7 neurons derived from pCC pioneering neurons **A.** Somatic location of Dp7 neurons corresponds to site of pCC neurons along the longitudinal connective in the dorsal region of the larval A1 segment. **A'.** Motor neurons aCC and Rp2 surround pCC neurons. **B and B'.** Light microscopic confocal image showing Dp7 neuron location in-between motor neurons. **C.** Confocal image of Dp7 neurons at L1 stage (*Dp7-Gal4>UAS-Cd4-GFP*) **D.** EM-reconstructed pCC/Dp7 images with axonal arbors projecting towards the brain lobes and lateral and medial dendritic arbors projecting to the VNC. **E.** Dp7 neurons shown from different angles projecting to the VNC (magenta), SEZ (green), and brain lobes (pale green), A: anterior, P: posterior, D: dorsal, V: ventral, L: lateral, M: medial.

3.3. Dp7 neurons have somatosensory and gustatory presynaptic partners

Having reconstructed Dp7 neurons, I traced all connected neurons starting from the synaptic sites on the Dp7 neuron. Dp7 neurons have approximately 45 presynaptic partners and approximately 60 postsynaptic partners (Fig. 11A and B, Appendix 1).

3 Results

Dp7 presynaptic partners are located mostly in the VNC region, while its postsynaptic partners are found mostly in the higher brain regions (Fig. 11A and B). The modulatory function of Dp7 neurons is supported by its connectome as it receives inputs from different subtypes of sensory neurons (Fig. 11C, D, E). The medio-lateral dendrites align topographically with somatosensory C2da, C3da and C4da neurons where they make synapses (Fig. 11C, C'), in line with light microscopic data (Hu et al., 2017). In addition to the dendritic arborisation neurons, Dp7 neurons are also connected to another class of sensory neurons, the tracheal neurons with yet unknown functions (Fig. 11D). Td neurons, unlike the dendritic arborisation neurons, project along the lateral dendritic branch and the proximal axonal region of Dp7 neurons, where they make synapses with the latter (Fig. 11D). Overall, this suggests that Dp7 neurons may be a hub for several sensory neuron classes and potentially act as a gate for distinct behavioral pathways.

Aside from the somatosensory cells, Dp7 neurons also receive weak synaptic input from subsets of the antennal nerve bundle (AN-B2) derived gustatory neurons in the SEZ region (Fig. 11E). Based on the synaptic inputs that Dp7 neurons receive from gustatory neurons, Dp7 neurons may also have functional relevance for feeding behaviors. As Dp7 neurons receive somatosensory input in the VNC and gustatory input in the SEZ region this might also suggest that different compartments of Dp7 neurons are involved in modulation of different kinds of innate behaviors.

3 Results

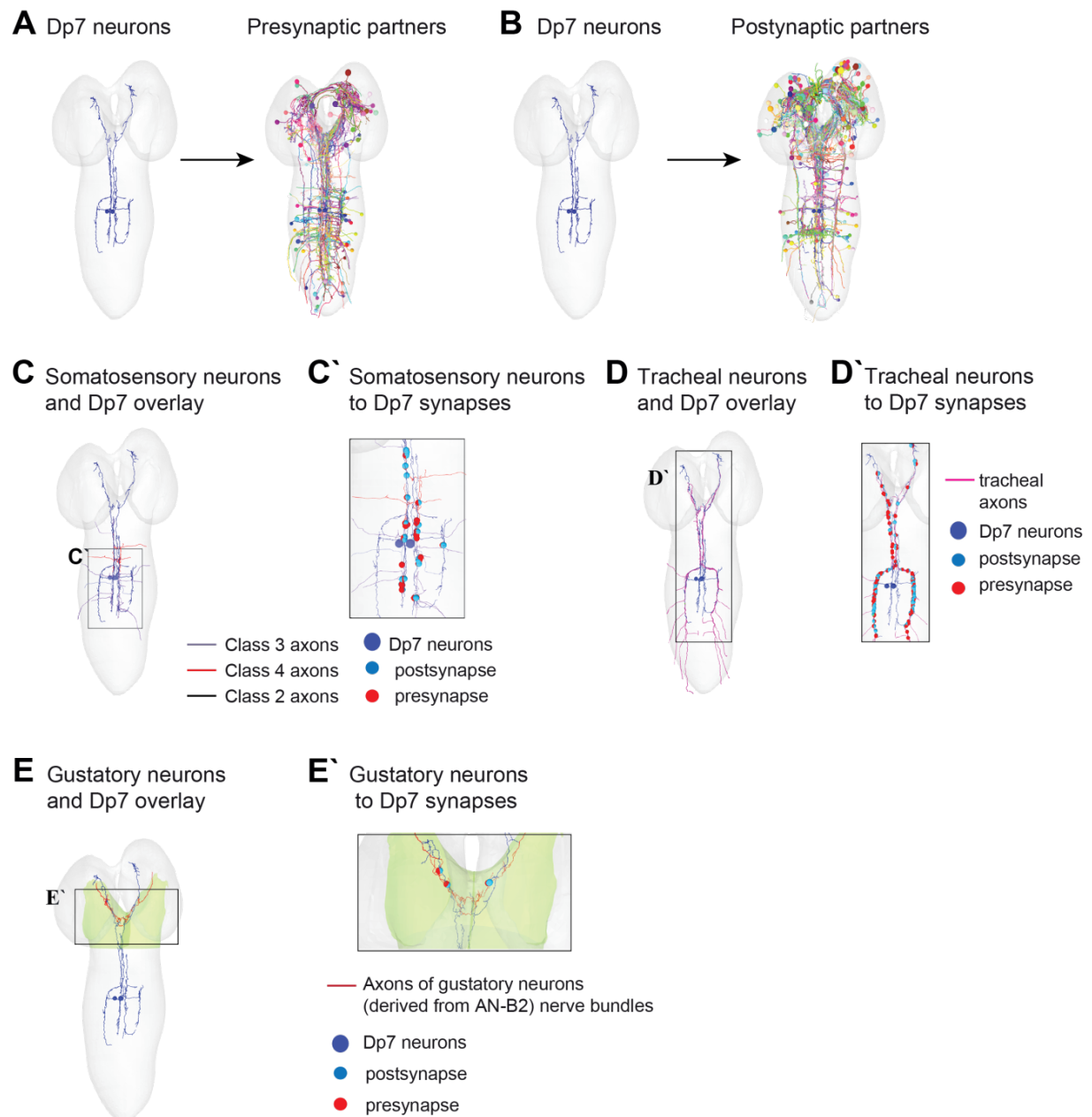


Figure 11: Dp7 connectome includes different classes of somatosensory and gustatory neurons. **A** and **B**. EM-reconstructed upstream and downstream partners of Dp7 neurons. **C** and **C'**. Somatosensory neurons align and make synapses with Dp7 neurons at its midline dendritic arbors **D** and **D'**. Tracheal neurons align and make synapses with Dp7 neurons along its lateral dendritic branch and proximal axonal arbors. **E** and **E'**. Gustatory neurons derived from the AN-B2 nerve bundle align and make synapses with Dp7 neurons along its axonal branch in the SEZ (green shaded area).

3.4. A subset of tracheal neurons is highly connected to Dp7 neurons

Based on their axonal morphology (Qian et al., 2018), I identified td neurons as a new upstream partner of Dp7 neurons (Fig. 12A). Two subsets of td neurons made synapses with Dp7 neurons. One subset had fairly weak synaptic connections, while the other subset had very high proportion of synaptic inputs (36%) onto Dp7 neurons (Fig. 12A). Based on their anatomical projections, I speculated that the strongly connected neurons with projection to the SEZ, VNC and midline are v`td2 neurons, and that the weakly connected neurons are v`td1 neurons, as the latter had projections to the SEZ region only, consistent with previous light microscopic analysis (Qian et al., 2018) (Fig. 12B, C, C`). Anatomically, the highly connected td neurons in the A1 to A3 segments had axonal projections which extended along the SEZ (td SEZ), while the highly connected td neurons in A4 to A6 segments projected their axons only to the VNC region (td VNC) (Fig. 12C'). The highly connected A7 td neuron had projections in the VNC, but also a projection towards the midline (td VNC MP) (Fig. 12C'). The subset of td neurons with less Dp7 connections had projections toward the SEZ region only (Fig. 12C'). V`td2 neurons moreover also express the putative light-sensitive receptor Gr28b_c (labelled by *Gr28b.c-Gal4*), which suggests that they might be potential light sensitive neurons on the larval body wall, in addition to the previously characterised C4da neurons (Qian et al., 2018; Xiang et al., 2011). Using a v`td2 Gal4 specific line (*73B01-Gal4*) (Qian et al., 2018), I confirmed synaptic connectivity with v`td2 and Dp7 neurons. Synapse-specific GFP reconstitution across synaptic partners (Syb-GRASP, (Macpherson et al., 2015) showed that v`td2 neurons make synapses at the lateral dendritic branch and proximal axon of Dp7 neurons (Fig. 12D).

3 Results

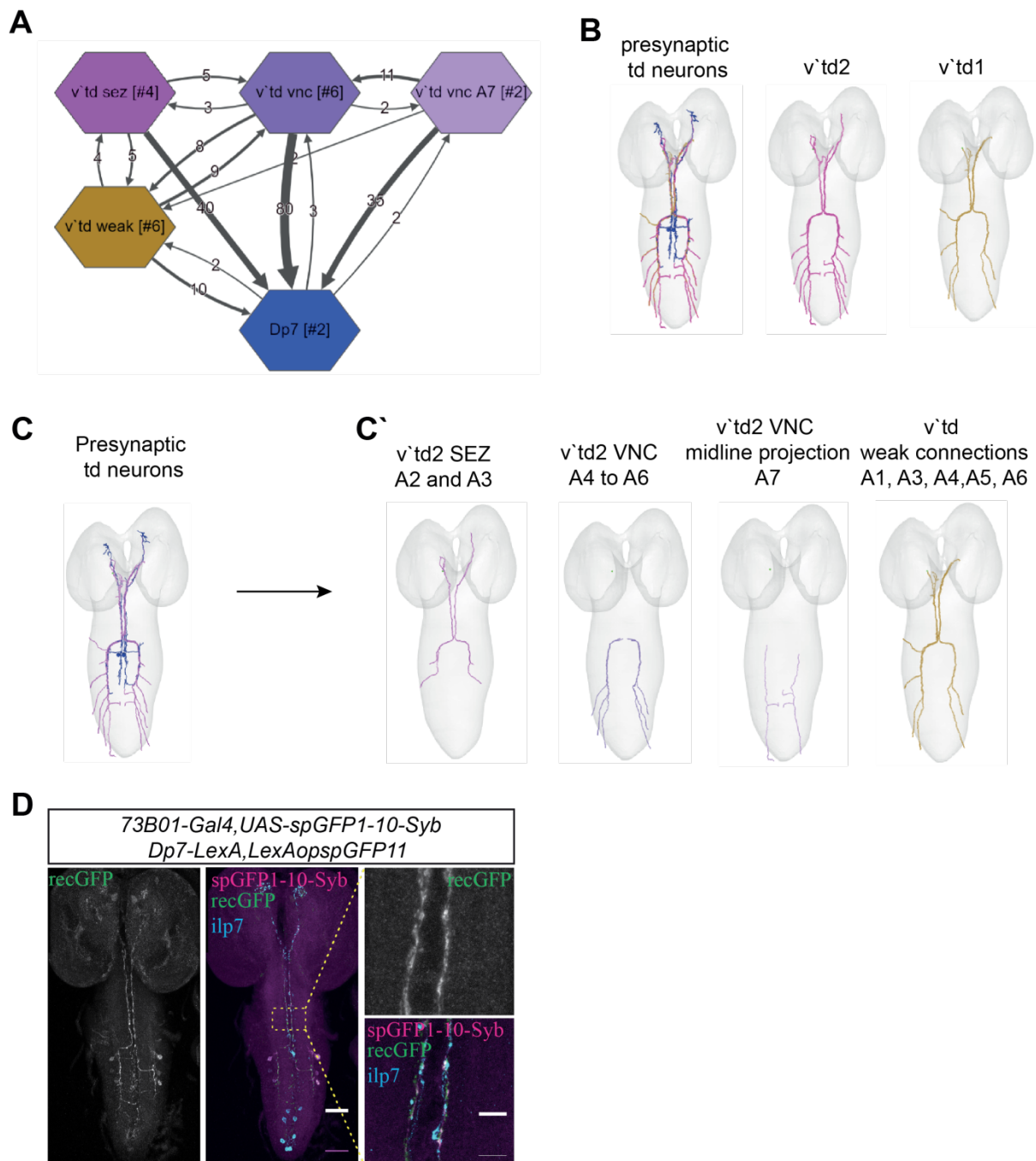


Figure 12: EM reconstruction of upstream v`td neurons synapsing onto Dp7 neurons and circuit analysis. A. Analysis of synaptic connections to Dp7 neurons shows that major inputs come from v`td SEZ, v`td vnc and v`td A7 with midline projections. **B.** the highly synaptically connected v`td neurons are likely v`td2 and lower connected ones v`td1 neurons. **C.** Dp7 neurons are shown in blue and v`td neurons in magenta. v`td neurons overlap with Dp7 neurons along its lateral dendritic arbor and the axon within the SEZ.

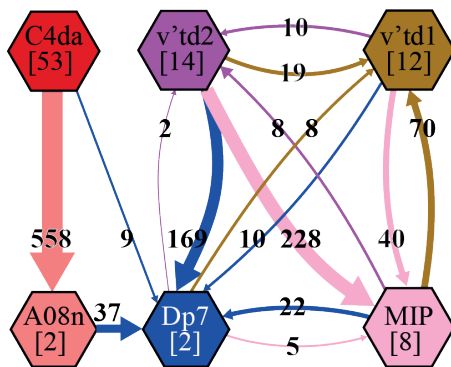
3 Results

C. Three morphologically different subsets of v^{td} neurons from different abdominal segments include: neurons in the A1-A3 segments projecting to the SEZ region (magenta), neurons in the A4-6 projecting to the VNC region (purple), and the neuron in the A7 segment projecting towards the midline (lilac); a synaptically weakly connected subset of v^{td} neurons (pale brown) projects exclusively to the SEZ region. **D**. Confocal images showing Syb-GRASP-labelled $v^{\text{td}2}$ to Dp7 neuron connections. Presynaptic spGFP1-10-Syb was expressed in $v^{\text{td}2}$ neurons (*73B01-Gal4*, magenta), postsynaptic spGFP11-CD4 was expressed in Dp7 neurons (*Dp7-LexA*). Reconstituted GFP (recGFP, green) signal labelling $v^{\text{td}2}$ -Dp7 synapses and Ilp7 neuropeptide immunostaining (cyan). Enlarged boxes showed proximity of $v^{\text{td}2}$ -Dp7 neuron synapses with ilp7 neuropeptide along the proximal axonal region of Dp7 neurons. Scale bars= 50 μ m, 10 μ m.

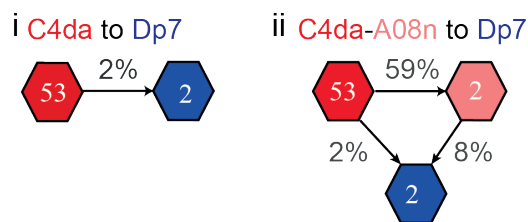
3.5 Dp7 neurons integrate noxious light from multiple somatosensory circuits

To uncover the interacting paths through which noxious light information flows, I performed detailed connectome analyses of the elucidated Dp7 network. The connectome data analysis revealed 2 major circuits which converge onto Dp7 neurons (Fig. 13A): one C4da-derived and the other $v^{\text{td}2}$ -derived. C4da and $v^{\text{td}2}$ converge directly onto Dp7 neurons, although the connection from $v^{\text{td}2}$ to Dp7 is much stronger than C4da to Dp7 (Fig. 13B and C). $V^{\text{td}2}$ neurons also connect indirectly to Dp7 neurons via so far uncharacterised midline projection (MIP) neurons (Fig. 13A, Appendix 2). Since the C4da to Dp7 link is quite weak (2%), I reasoned that it may potentially not be meaningful for light avoidance behavior. I therefore searched 2-hop polysynaptic pathways and identified an indirect yet strong link via the A08n neurons formerly shown to be strongly connected to C4da neurons (Fig. 13A, B) (Hu et al., 2017; Kaneko et al., 2018).

A Circuit analysis of Dp7 connectome



B C4da derived subcircuits onto Dp7



C v`td2 derived subcircuits onto Dp7

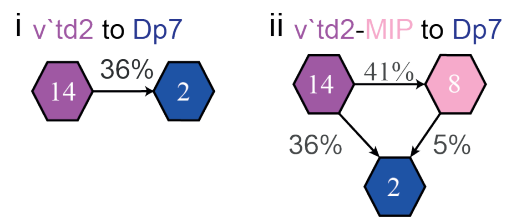


Figure 13: Analysis of the somatosensory wiring diagram of Dp7 neurons. A. Dp7 neuron presynaptic connectivity analysis showing the highest input from sensory v`td2 neurons. C4da to Dp7 connections are weak, but additional stronger indirect connections were found via A08n neurons. V`td2 are strongly connected to Dp7 neurons, both directly and indirectly, via MIP neurons. Numbers in brackets indicate number of neurons of the respective subtype; numbers on arrows indicate synapses from each additional subset forming direct connections. **B** and **C.** Inputs onto Dp7 neurons originating from either C4da neurons or v`td2 neurons from 2 direct and 2 indirect sub circuits. Percentages of overall synaptic input of the target cells are shown; numbers in the hexagons indicate the number of neurons involved.

3.6 A08n neurons respond to acute UV stimulation but are not necessary for light avoidance behavior

As C4da neurons respond to UV light (Xiang et al., 2011; Yamanaka et al., 2013), I tested the involvement of A08n neurons as a major downstream output connected to Dp7 neurons. However, Kir2.1 mediated silencing of A08n neurons didn't show a decrease in light avoidance responses (Fig. 14A), albeit strong calcium responses were detected in A08n neuron somata upon UV light stimulation (Fig. 14B). These data suggest that A08n neuron activity is dispensable for light avoidance behavior. As C4da neurons have been shown to be required for light avoidance (Xiang et al., 2011; Yamanaka et al., 2013), it is possible that other 2-hop neuron connections from C4da to Dp7 neurons are involved.

3 Results

These could include TepN5 or TepN19 neurons, which are also downstream of C4da neurons (Gerhard et al., 2017) and upstream of Dp7 neurons (Appendix 1).

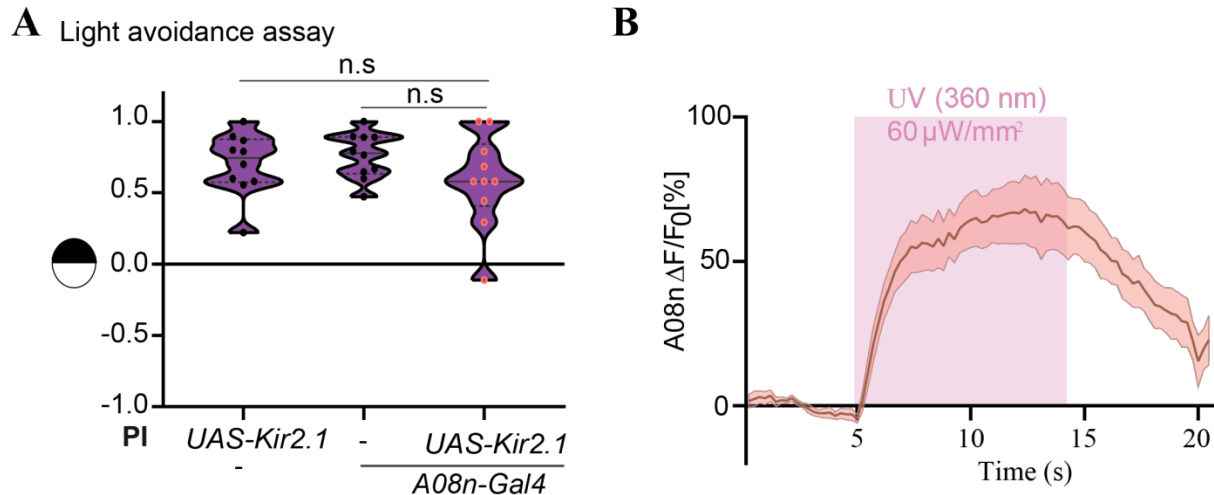


Figure 14: A08n neurons downstream of C4da neurons are responding to UV light, but not required for light avoidance. **A.** Light avoidance responses were not significantly impaired when A08n neurons were silenced with Kir2.1 (*82E12-Gal4>UAS-Kir2.1*) (n=10 trials, n.s. non-significant, one-way-ANOVA with Tukey's *post-hoc* test). **B.** UV light elicited calcium signals in the A08n soma (*82E12-Gal4>UAS-GCaMP6s*, mean \pm s.e.m., n=5).

3.7. v^{td2} neurons are light sensing neurons and required for light avoidance behavior

To test for a possible function of v^{td2} neurons as sensors of noxious light, I performed light avoidance behavior on animals with silenced v^{td2} neurons (*73B01-Gal4>UAS-Kir2.1*). v^{td2} neuron silencing resulted in significantly decreased light avoidance behavior (Fig. 15A). Furthermore, when calcium imaging was performed on v^{td2} neurons in live larvae, they responded acutely to UV light stimulation (Fig. 15B). Since the three subsets of v^{td2} were anatomically different from each other, I also tested the response of each subset to UV light. My data showed that all three subsets responded to UV light indicating that they are all required for sensing noxious light (Fig. 15C).

3 Results

V`td1 neurons on the other hand did not show any response to UV light stimulation (Fig. 15D), in line with its low connectivity with the Dp7 network (Fig. 13A). Thus, the highly connected v`td2 neurons upstream of Dp7 neurons, but not v`td1 are linked to UV light responses and light avoidance.

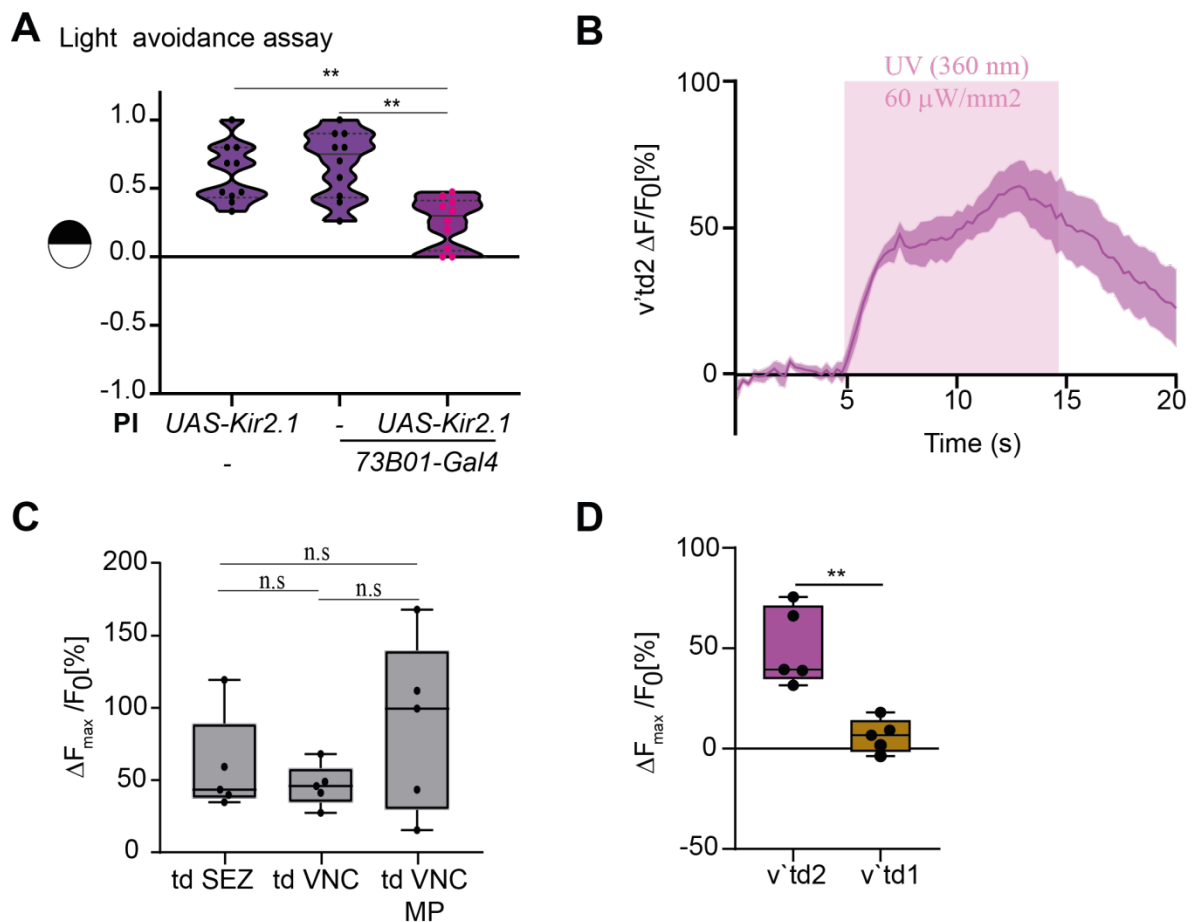


Figure 15: V`td2, but not v`td1 neurons respond to noxious light. **A.** Kir2.1 expression in v`td2 neurons reduced light avoidance responses (*73B01-Gal4>UAS-Kir2.1*, n=10 trials, **P<0.01, one-way-ANOVA with Tukey's *post-hoc* test). **B.** UV light triggered calcium transients in v`td2 neurons (*73B01-Gal4>GcaMP6s*, mean ± s.e.m., n=8). **C.** All 3 subset of v`td2 neurons (*73B01-Gal4>GcaMP6s*), imaged based on soma position in the larvae showed similar responses to UV light (ΔF_{max}/F₀ boxplot, n=5, n.s, one-way-ANOVA) **D.** Quantitative comparison of calcium responses (*GcaMP6s*) of v`td2 and v`td1 neurons to UV light using *R35B01-Gal4*, which labels both subtypes (ΔF_{max}/F₀ boxplot, n=5, **P<0.01, unpaired *t*-test with Welch's correction).

3 Results

3.8. v^{td2} neurons are functionally connected to Dp7 neurons mediating light avoidance, but not mechanonociceptive behavior

To find out whether v^{td2} neurons are functionally upstream of Dp7 in the light avoidance circuit, v^{td2} neurons were optogenetically activated and calcium signals were recorded in Dp7 neurons. Strong calcium transients in Dp7 neurons were detected upon optogenetic activation of v^{td2} neurons (Fig. 16A and B). Connectomic data indicated that two sensory circuits, v^{td2} and C4da derived converge onto Dp7 neurons and are involved in sensing UV light and in light avoidance behavior. Unlike C4da neurons however (Hu et al., 2017), v^{td2} neurons are not required for mechanonociceptive behavior (Fig. 16C).

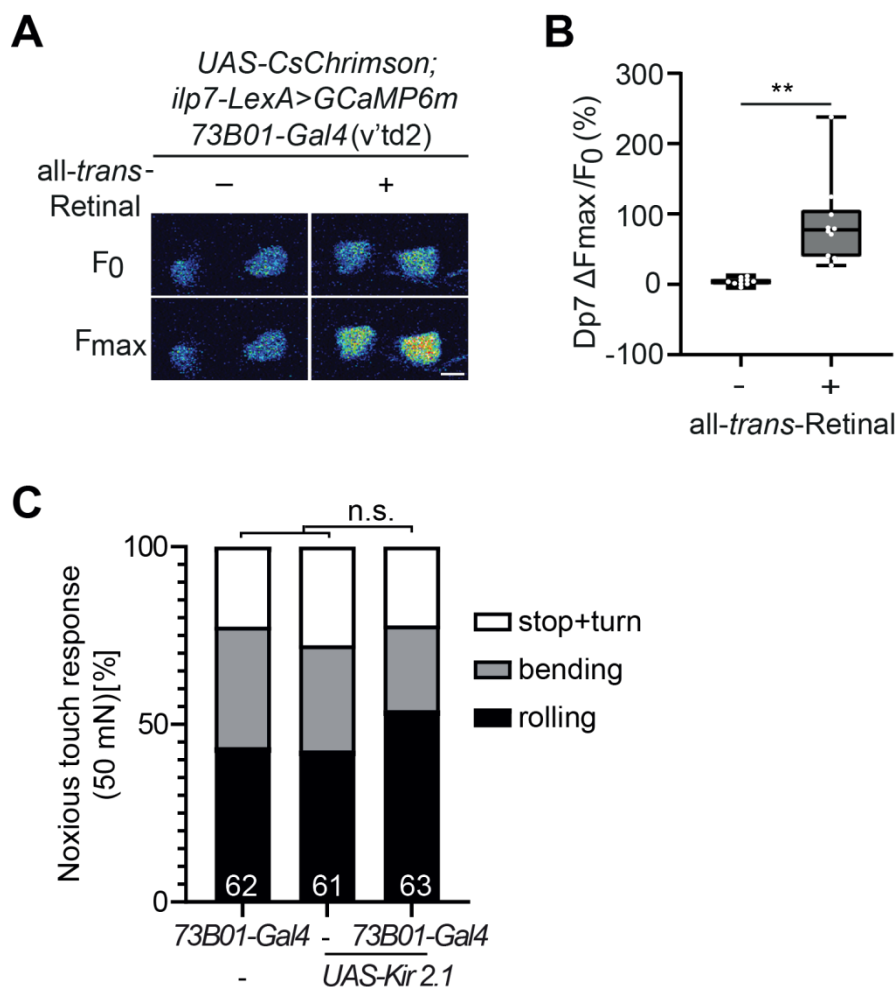


Figure 16: v^{td2} neurons are upstream of Dp7 neurons in the light avoidance circuit. **A.** Calcium signals in Dp7 neurons before (F_0) and after (F_{max}) CsChrimson-mediated optogenetic activation of v^{td2} neurons (*73B01-Gal4*, *UAS-Chrimson*; *ilp7-LexA*, *LexAop-GcaMP6m*, experiment performed by Chun Hu).

3 Results

B. Maximum responses ($\Delta F_{\max}/F_0$) in Dp7 neurons after CsChrimson activation with and without all-trans-Retinal (** $P < 0.01$, Mann-Whitney test). **C.** Mechanonociceptive behavior (rolling and bending) is unaffected by silencing of v^{td2} neurons (*73B01-Gal4>UAS-Kir2.1*, $n=62, 61, 63$ animals/genotype, n.s. = non-significant, χ^2 test, experiment performed by Federico Marcello Tenedini)

3.9. Circuit mapping for identifying neurons downstream of Dp7 in the light avoidance circuit

Dp7 neurons and its neuropeptide *llp7* are involved in light avoidance responses (Fig. 9). To identify the downstream synaptic partner of Dp7 neurons, which may also be involved in light avoidance behavior, I investigated 3rd order neurons in the synaptic wiring diagram. Out of the 60 downstream neurons (Appendix 1), I identified 2 neuronal subsets, Hugin-VNC and the abdominal leucokinin neurons (ABLK) (Fig. 17A and B), which could potentially be involved in light avoidance behavior based on their morphology and their previously known function in larval responses to noxious light. Hugin-VNC neurons receive synaptic inputs from Dp7 neurons in the SEZ region (Fig. 17A'), the zone for sensorimotor decisions (Tastekin et al., 2015) and send projections toward the VNC in the dorsal region where motor neurons reside. ABLK neurons have been implicated in rearing behavior in response to blue light through serotonergic input (Okusawa et al., 2014) and they are connected at the lateral dendritic region of Dp7 neurons (Fig. 17B').

Analysis of the synaptic wiring diagram revealed that Hugin-VNC neurons are however strongly connected to v^{td1} neurons, the UV-unresponsive sensory neurons (Fig. 17C). ABLK neurons receive direct input from Dp7 neurons and v^{td2} neurons, with strong 2-hop inputs via MIP neurons (Fig. 17C). Based on the connectivity graph, v^{td2} to Dp7 and v^{td2} to MIP are the strongest synaptic links that connect to ABLK and may relay noxious light sensed by v^{td2} via Dp7 neurons, or indirectly via the MIP neurons. Close inspection of the wiring diagram reveals seven potential motifs (Alon, 2007; Biswas and Banik, 2018; Milo et al., 2011), which may be potential paths along which noxious light information travels (Fig. 17D). Motif 1 is a direct monosynaptic connection from v^{td2} to ABLK which is quite weak and may not be functional on its own. Motifs 2 and 3 are feedforward circuits.

3 Results

In motif 2 information flow from v`td2 to MIP to ABLK while in motif 3 information flow from v`td2 to Dp7 to ABLK. Motif 4 is a feedforward loop which resembles the coherent type 1 motif present in transcription networks and quite common in sensory and motor networks (Shoval and Alon, 2010). Here, v`td2 would activate Dp7, which in turn activates ABLK while v`td2 also activates ABLK (Fig. 17D). This type of motif configuration may suggest the need for the system to filter out noise from the environment such that a behavioral output is dedicated to sensory stimuli perceived by v`td2 neurons. Furthermore, it may also suggest that information are encoded quickly and can be rapidly ended in case the sensory inputs ceases (Milo et al., 2011). Motif 5 resembles the diamond motif (Biswas and Banik, 2018), which bifurcates from v`td2 to MIP and Dp7, both of which converge on ABLK (Fig. 17D). Motif 6 includes unidirectional flow of information from MIP to Dp7 inside the diamond motif (Fig. 17D). Motif 7 is a combination of the feedforward loop with the diamond motif. The occurrence of several motifs suggests several possibly pathways that light information may pass through to reach ABLK neurons.

3 Results

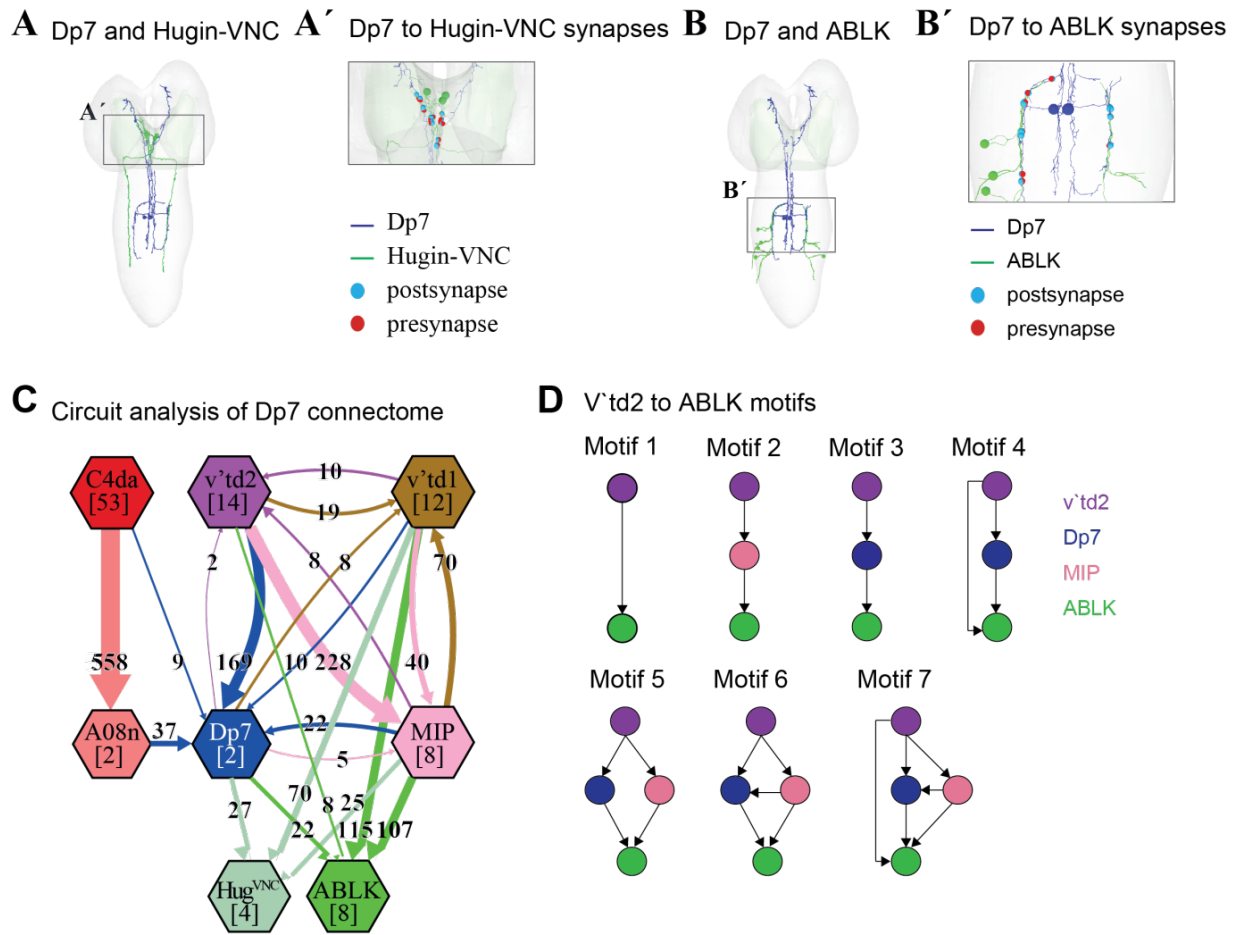


Figure 17: Analysis of the Dp7 synaptic wiring diagram and motifs deduced from it. **A.** Morphology of Dp7 neurons and Hugin-VNC. **A'.** Dp7 synapses with Hugin-VNC in the SEZ region. **B.** Morphology of Dp7 neurons and ABLK neurons. **B'.** Dp7 neurons synapse with ABLK neurons at its lateral dendritic arbor in the VNC region. **C.** Connectivity graph shows overlapping but distinct sub-circuits. The major outputs of v`td2 are to Dp7 and MIP neurons, while v`td1 neurons mainly connect to ABLK and Hugin-VNC neurons. Numbers in hexagons indicate the number of neurons named in the hexagon; numbers next to arrows indicate synapses from each neuronal subset forming direct connections. **D.** Motifs deduced from **C** from v`td2 neurons to ABLK neurons based on (Alon, 2007; Biswas and Banik, 2018; Milo et al., 2011).

3.10 Domain-specific compartments for processing of noxious light and noxious touch information

I further inspected the topographical relationship of the mapped neurons and found that v`td2, MIP and ABLK neurons anatomically converge on the lateral dendritic region of Dp7 neurons (Fig. 18A).

3 Results

Conversely, the overlapping mechanosensory circuit consisting of C2da, C3da and C4da neurons (Hu et al., 2017), of which C4da neurons also process noxious light information, primarily connects with the medial dendritic arbor of Dp7 neurons (Fig. 18C). MIP and v`td2 neurons also overlap with the axonal arbor of Dp7 neurons in the thoracic segments of the larval VNC and SEZ (Fig. 18A). However, most synapses of the respective postsynaptic partners reside on the Dp7 neuron lateral dendritic region (Fig. 18B), which suggests convergence of the light avoidance inputs and outputs. Within this region, Dp7 neurons receive extensive synaptic inputs from v`td2 neurons. These data indicate that processing of mechanonociceptive and noxious light information likely occurs in distinct compartments of Dp7 neurons.

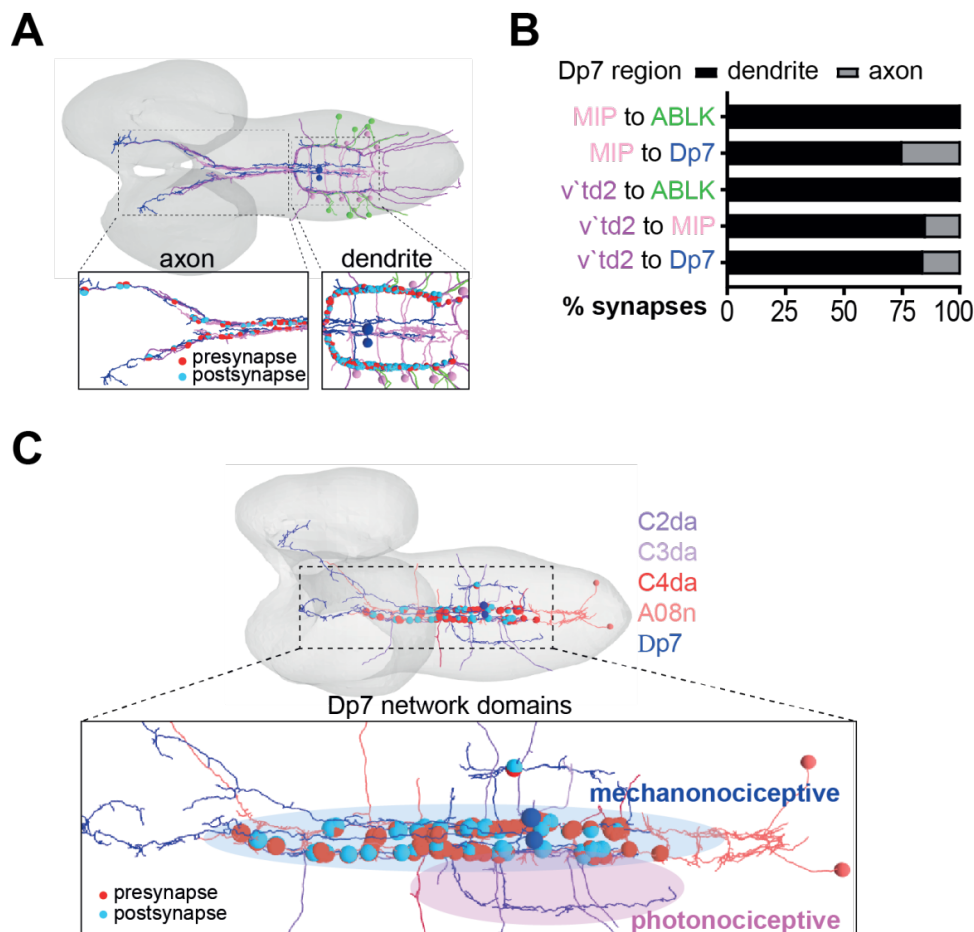


Figure 18: Light avoidance and mechanonociceptive circuits converge on discrete compartments of Dp7 neurons. **A.** Dp7 light avoidance network. Top view of the larval brain showing overlap of the reconstructed Dp7, v`td2, MIP and ABLK neuron at the lateral dendritic region of Dp7 neurons in the VNC region.

3 Results

Enlarged axon and dendrite regions of Dp7 neurons show local v`td2-Dp7, v`td2-MIP and MIP-ABLK synapse numbers on the lateral dendrites and the axons of Dp7 neurons. Scale bar = 200nm. **B.** Relative percentages of Dp7 inputs on its dendritic and axonal arbor regions are shown for each partner. **C.** Synaptic connectivity of mechanosensory (C2da, C3da, C4da) and A08n neurons with Dp7. Most synapses are located on Dp7 medial dendrites presumably providing mechanosensory inputs (shaded blue area).

3.11 Putative peptide release events occur on the lateral dendritic branch of Dp7 neurons adjacent to ABLK neurons

Interestingly, I noticed that the synaptic contact region of v`td2-MIP-ABLK neurons on the lateral dendritic arbor of Dp7 neuron also coincides with Ilp7 neuropeptide localisation (Fig. 19A), which suggest that this could be a site for local peptide release. Analysis of the lateral dendritic arbor of Dp7 neurons in the EM volume revealed putative events of large dense core vesicle release from Dp7 neurons to ABLK neurons (Fig. 19 B and C).

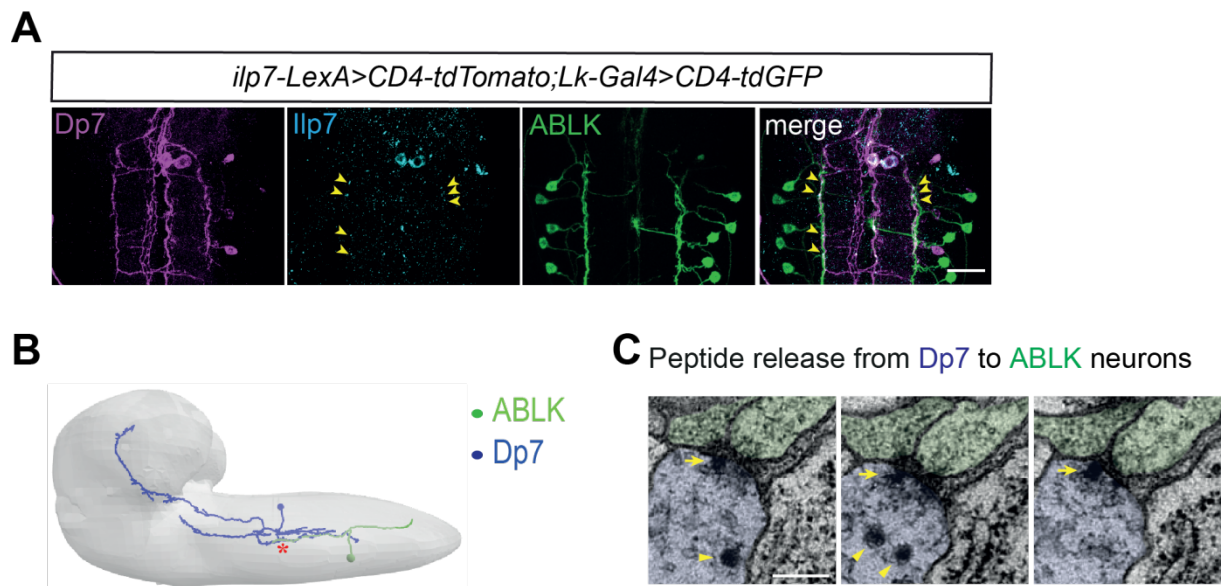


Figure 19: Ilp7 localization and peptide release in the lateral dendritic region of Dp7 neurons. **A.** Confocal image showing anatomical overlap of ABLK (*LK-Gal4>UAS-CD4-tdGFP*) and Ilp7 puncta (cyan) along the lateral dendritic region of Dp7 neurons (*ilp7-LexA>LexAop-CD4-td-Tomato*). **B.** Side view from the brain showing EM reconstructed ABLK and Dp7 neurons.

C. EM sections showing LDCVs (arrowheads) and putative release events (indicated by arrow) from Dp7 (blue) to ABLK neurons (green) occur at the region marked with a red asterisk in **B**.

3.12 ABLK neurons are involved in light avoidance responses

To find out whether ABLK neurons are needed for light avoidance, I performed behavioral experiments using Kir2.1-mediated silencing with a line that is expressed in Leucokinin (LK) neurons (*Lk-Gal4*) (de Haro et al., 2010), which resulted in significantly decreased light avoidance (Fig. 20A). In addition to the VNC-resident ABLK neurons, Leucokinin is also expressed in the brain including two pairs of SEZ LK neurons (SELK), two pairs of lateral horn LK neurons (LHLK) and a pair of anterior LK neurons (AHLK) (de Haro et al., 2010). Thus, to specifically attribute ABLK neuron functions to light avoidance, I genetically suppressed the expression of Kir2.1 only in ABLK neurons using *tsh-Gal80* (Fig. 20A). Silencing of the remaining LK-positive neurons did not impair light avoidance suggesting that it is specifically dependent on the function of ABLK neurons. I also tested for the function of Hugin-VNC neurons in light avoidance, which are strongly connected to Dp7 neurons, but receive major sensory input from non-UV responsive *v`td1* neurons (Fig. 17C). I did not detect significant defects in light avoidance behavior when silencing Hugin-VNC using a specific Gal4 line (Fig. 20A) (Schoofs et al., 2014) (*Hugin-VNC-Gal4>UAS-Kir2.1*), which is consistent with my connectome analysis (Fig. 17C). The data shows that ABLK, but not Hugin-VNC neurons are involved in light avoidance.

In addition, I assayed the functional response of ABLK neurons to UV light using GCaMP6s and found prominent calcium transients upon stimulation (Fig. 20B). My data thus shows that ABLK are involved both in light avoidance responses and behavior.

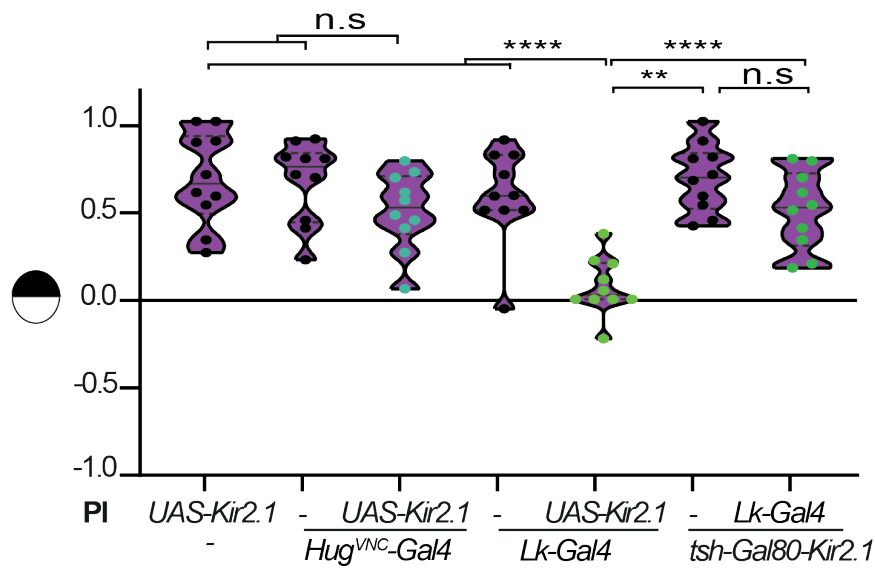
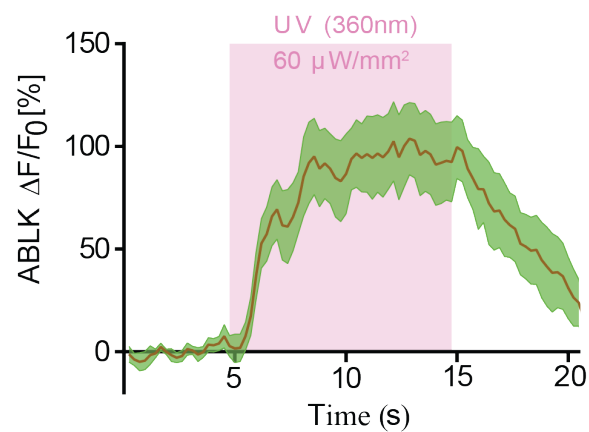
A Light avoidance assay**B**

Figure 20: ABLK neurons are part of the light avoidance circuit. A. Kir2.1 mediated silencing of LK neurons (*Lk-Gal4>UAS-Kir2.1*), but not when precluding ABLK expression (*tsh-Gal80, Lk-Gal4>UAS-Kir2.1*), abolishes light avoidance. Silencing of Hugin-VNC neurons (*Hug^{VNC}-Gal4>UAS-Kir2.1*), did not affect light avoidance (n=10 trials/genotype, ****P<0.0001, **P<0.01, n.s., non-significant, one-way ANOVA with Tukey's *post-hoc* test). **B.** Calcium transients recorded in ABLK neuron somata upon UV light stimulation (purple shaded area, mean \pm s.e.m., n=5).

3.13 ABLK neurons are functionally downstream of Dp7 neurons in the light avoidance circuit

Direct flow of information from Dp7 to ABLK neurons is plausible according to motifs 3, 4, 5, 6 and 7 (Fig. 17D). To determine whether the motifs are functional in the light avoidance circuit and the ABLK neuron response depends on Dp7, I silenced Dp7 using Kir2.1 expression. Under these conditions, ABLK-neuron calcium transients were completely abolished (Fig. 21A, B). Since Dp7 neuron derived Ilp7 neuropeptide is also crucial for regular light avoidance (Fig. 9C), I tested whether loss of Ilp7 neuropeptide impaired functional activity in ABLK neurons. To this end, I performed calcium imaging in *ilp7^{ko}* animals, where I detected a 70% decrease in ABLK neuron responses upon UV light stimulation (Fig. 21C, D). ABLK neurons still displayed approximately 30% of the normal responses to UV light in *ilp7^{ko}* animals (Fig. 21C), which may be due to the action of a small molecule neurotransmitter action from Dp7 neurons. However, this synaptic activity alone was not sufficient to trigger light avoidance behavior. Collectively, my data indicate that Ilp7 likely acts on top of the physical connectome to elicit light avoidance behavior.

3 Results

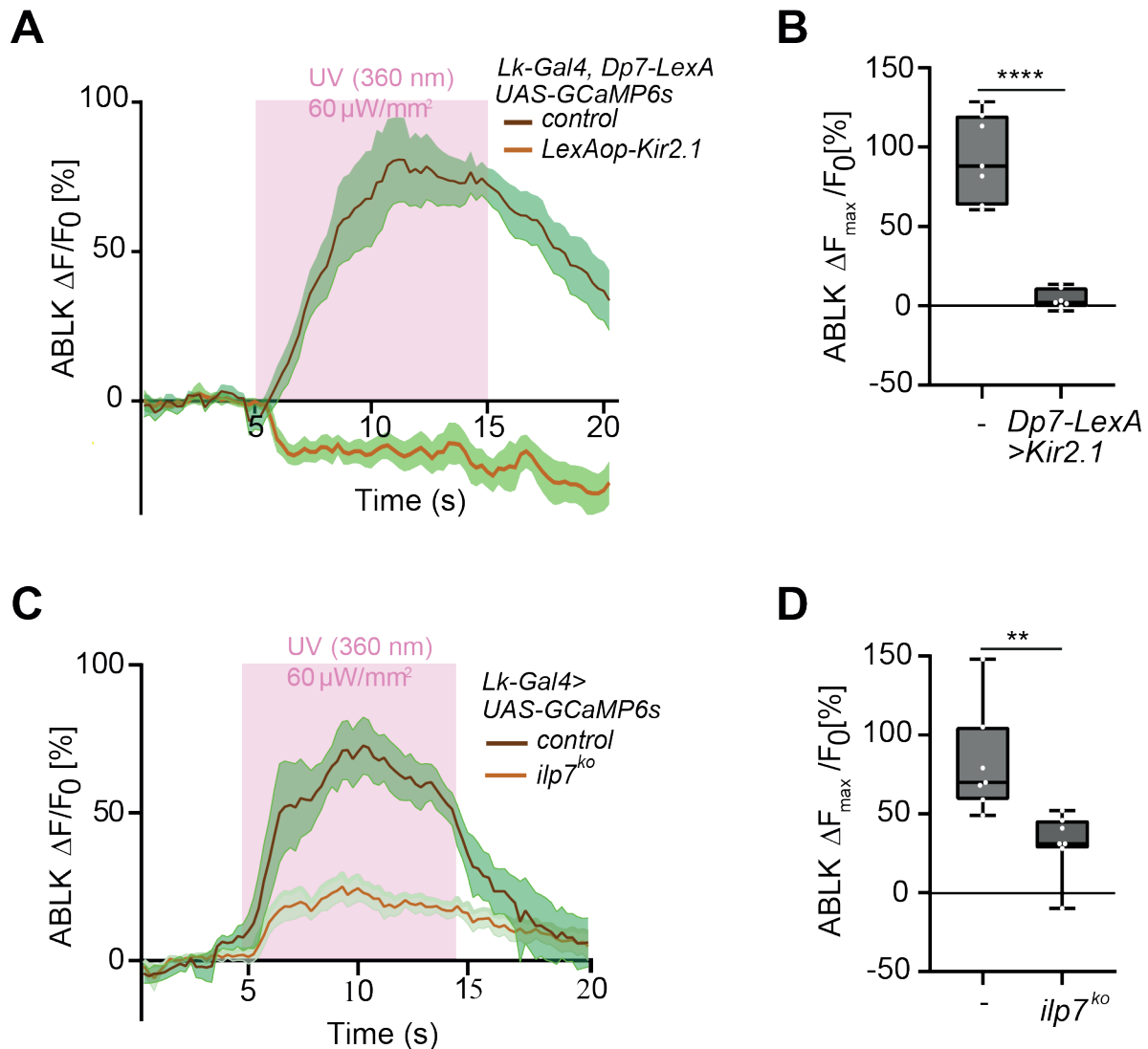


Figure 21: ABLK neurons are functionally downstream of Dp7 neurons and Ilp7 in the light avoidance circuit. **A.** Evoked calcium signals in ABLK neurons upon UV stimulation with silenced Dp7 neurons (*Dp7-LexA*, *LexAop-Kir2.1*, mean \pm s.e.m.) **B.** Boxplot quantification ($\% \Delta F_{\max}/F_0$) for **A** ($n=7$, **** $P<0.0001$ unpaired t-test with Welch's correction). **C.** ABLK neuron calcium transients evoked by UV light in control and *ilp7^{ko}* animals (mean \pm s.e.m.). **D.** $\% \Delta F_{\max}/F_0$ boxplots for **C** ($n=5$, ** $P<0.01$ unpaired t-test with Welch's correction).

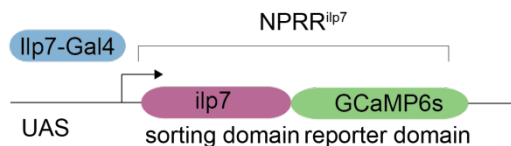
3.14 Generation of a neuropeptide release reporter for Ilp7

Neuropeptide release has been a challenge to visualize, partly because release can be tonic and may act on neurons which are located considerable distances from the site where they are produced (Nässel et al., 2019; van den Pol, 2012). I took advantage of the fact that I discovered peptide release event from Dp7 neurons in the EM volume and asked whether Ilp7 is acutely released upon UV stimulation.

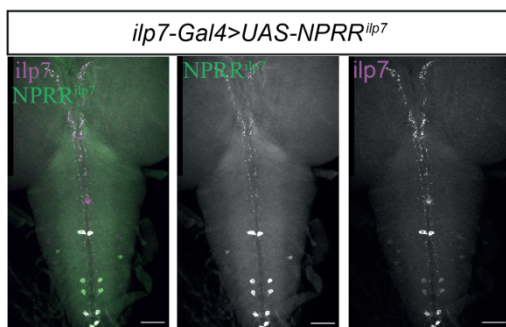
3 Results

In order to visualise *Ilp7* neuropeptide release, we developed a release reporter by fusing *Ilp7* to *GCaMP6s* (NPRR^{ilp7}) (Fig. 22A), analogously to previously characterised neuropeptide reporters (Ding et al., 2019). Release can be specifically monitored in *Dp7* neurons by using the binary *Gal4-UAS* system, whereby *Gal4* is produced in *Ilp7* neurons binds to *UAS* to drive expression of NPRR^{ilp7} (Fig. 22A). Fluorescence of the LDCV-targeted *Ilp7-GCaMP6s* is low in LDCVs due to low calcium, and should increase upon plasma membrane fusion and peptide release into the extracellular space, due to higher pH and high calcium (Ding et al., 2019). NPRR^{ilp7} is expressed in *Dp7* neurons in a punctate pattern on its lateral dendritic and axonal branches in a similar manner to endogenous *Ilp7* (Fig. 22B). To confirm correct reporter targeting, I co-expressed the LDCV marker *Synaptotagmin- α* (*Syt α*) (Park et al., 2014) with NPRR^{ilp7} in *Ilp7* neurons. My data shows that *Syt α* colocalized completely with NPRR^{ilp7} , therefore implying correct reporter targeting (Fig. 22C).

A Design of *ilp7* neuropeptide release reporter



B



C

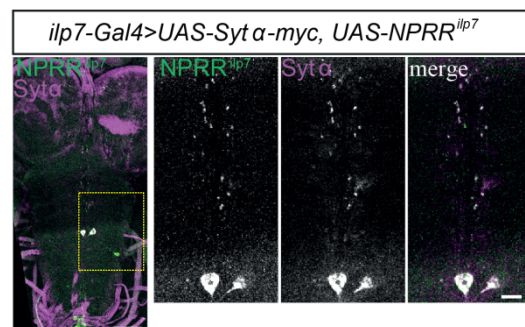


Figure 22: Generation of an *Ilp7* neuropeptide release reporter (NPRR^{ilp7}). **A.** Schematic illustration of NPRR^{ilp7} design. **B.** Immunohistochemical analysis of *Ilp7* neuropeptide reporter in *Ilp7* expressing neurons (*ilp7-Gal4>UAS-NPRR^{ilp7}*, anti-*Ilp7* and anti-GFP). Scale bar=50 μm . **C.** Immunohistochemical analysis of *Ilp7* neuropeptide reporter (NPRR^{ilp7} , anti-GFP, green) and *Syt α -myc* (anti-myc, magenta) localization in *ilp7* neurons (*ilp7-Gal4>UAS-Syt α -myc, UAS-NPRR^{ilp7}*). Dashed boxed area in overview image indicates *Dp7* neuron proximal dendrite and axon region shown in enlarged projections. Scale bar=50 μm , 10 μm .

3 Results

3.15 UV light induces acute *Ilp7* neuropeptide release from Dp7 neurons

To visualize *Ilp7* peptide release from Dp7 neurons, I imaged NPRR^{*ilp7*} responses to UV light in Dp7 neurons in live larvae. Baseline fluorescence of NPRR^{*ilp7*} was low in LDCVs due to low calcium levels. However, upon UV stimulation NPRR^{*ilp7*} fluorescence intensity peaked rapidly, stabilized (plateau phase) and decayed following stimulation offset. (Fig. 23A, B). Repeated UV-light stimulation resulted in consistent NPRR^{*ilp7*} responses in LDCV puncta (Fig. 23C, D).

The data is compatible with acute and rapid peptide release in the (milli) second range, similarly to described kiss and run-type peptide release upon electrical stimulation of the neuromuscular junction (NMJ) (Ding et al., 2019; Wong et al., 2015). Imaging of NPRR^{*ilp7*} in the Dp7 soma gave similar results, which suggests that release can also occur from the soma (Fig. 23E).

In contrast, the posterior *Ilp7*-positive neurons, which innervate the gut, did not show UV-light induced somatic NPRR^{*ilp7*} responses (Fig. 23E). To further confirm that NPRR^{*ilp7*} reports LDCVs fusion with the plasma membrane, I used RNAi to knock down Calcium- dependent secretion activator (Cadps), which is a conserved protein that is required for LDCV release but not biogenesis (Farina et al., 2015; Renden et al., 2001). UV-light-induced NPRR^{*ilp7*} responses in the Dp7 soma were strongly diminished upon Cadps-RNA interference (RNAi) showing that the observed responses are LDCV release-dependent (Fig. 23F). These data indicate that LDCVs containing *Ilp7* are acutely released from Dp7 neurons in response to UV light, possibly acting directly on neighboring ABLK neurons and reminiscent of small molecule neurotransmitter action.

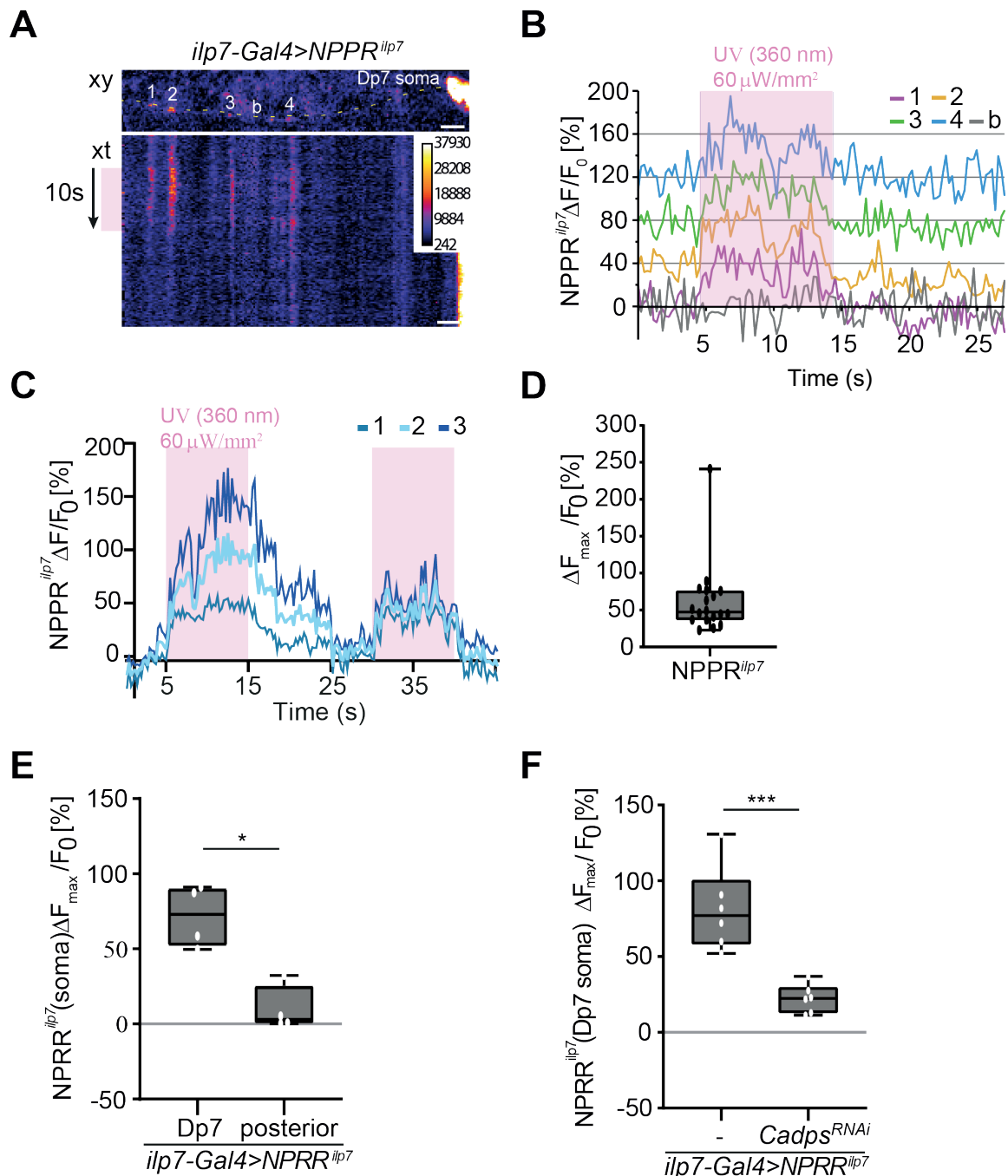


Figure 23: Ilp7 neuropeptide is acutely released upon UV stimulation. **A.** Time series (xt) along the dotted line which correspond to the proximal axonal arbor of Dp7 neurons showing acute NPPR^{ilp7} fluorescence increase in response to 10s UV-light exposure (360nm, 60 μ W/mm²). Scale bars= 10 μ m. **B.** Stacked individual traces of NPPR^{ilp7}-labelled LDCVs (numbered 1-4) and background (b) shown in **A.** **C.** Repeated UV light-induced responses of individual NPPR^{ilp7} puncta located along the proximal axon or lateral dendrite of Dp7 neurons (3 representative experiments). **D.** $\Delta F_{\max}/F_0$ boxplot of Dp7 NPPR^{ilp7} responses to UV light (n=18 punctae for 6 larvae). **E.** Boxplot quantification (% $\Delta F_{\max}/F_0$) shows that NPPR^{ilp7} somatic release occurs exclusively in Dp7 neurons and not in the posterior Ilp7 expressing neurons upon UV light stimulation, (n=4, *P<0.05, unpaired t-test with Welch`s correction). **F.**

3 Results

F. Boxplot quantification ($\% \Delta F_{\max}/F_0$) of maximum NPRR^{llp7} fluorescence in Dp7 somata upon UV light stimulation with or without Cadps-RNAi. Cadps knock-down significantly decreases NPRR^{llp7} responses (n=6 larvae/genotype, ***P<0.001, unpaired *t*-test with Welch's correction).

3.16 ABLK expresses the Relaxin-family receptor Lgr4

To date no cognate llp7 receptor is known. However, it is known that llp7 coevolved with the Relaxin-family receptor Leucine rich repeat containing G protein-coupled receptor 4 (Lgr4) across arthropod species (Gontijo and Garelli, 2018), which hinted that llp7 and Lgr4 may share a ligand-receptor relationship. Having identified ABLK neurons as a downstream partner for Dp7 neurons, whose activity depends on llp7 (Fig. 21C), I first investigated whether Lgr4 is expressed in ABLK neurons. To this end, I analyzed the expression of a Gal4 reporter incorporated in the endogenous Lgr4 mRNA (*Lgr4*^{T2A*Gal4*}). Lgr4 reporter signal was indeed detected in ABLK neurons (Fig. 24A) suggesting that Lgr4 is endogenously expressed. I next analyzed the localization of an ABLK expressed HA-tagged-Lgr4 relative to endogenous llp7 neuropeptide using anti-HA and anti-llp7 antibodies, respectively. I found that Lgr4 is localized along ABLK neuron projections close to llp7 puncta on the lateral dendritic branch of Dp7 neurons (Fig. 24B), possibly indicating that Dp7-derived llp7 neuropeptide acts through the Lgr4 receptor in ABLK neurons during light avoidance behavior.

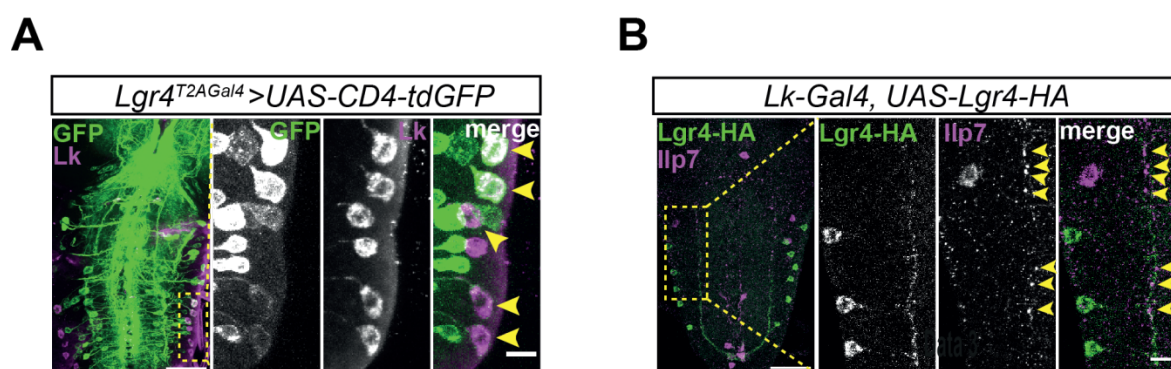


Figure 24: Lgr4 is expressed in ABLK neurons and is localized next to llp7 puncta. A. Endogenous Lgr4 reporter expression (*Lgr4*^{T2A*Gal4*}, UAS-*Cd4-tdGFP*) in ABLK neurons detected by anti-LK immunostaining.

3 Results

Overview and magnified lateral VNC region (boxed region) with ABLK neuron somata (GFP: green, LK: magenta). Scale bars = 50 μ m, 10 μ m for enlarged view. **B.** Lgr4-HA overexpression and localization in ABLK neurons (*LK-Gal4*, *UAS-Lgr4-HA*) with anti-Ilp7 immunostaining. Overview and magnified lateral VNC region (boxed region) showing ABLK somata and dendrites, with proximity of Lgr4 (green) and Ilp7 (magenta) puncta on the lateral arbor of Dp7 lateral arbor. Scale bars=50 μ m, 10 μ m.

3.17 Lgr4 receptor is required for light avoidance responses

To determine whether Lgr4 is physiologically required for light avoidance, I tested *Lgr4*^{T2AGal4} animals carrying the *T2A-Gal4* exon inserted after exon 2, which likely results in truncation of the endogenous Lgr4 mRNA and loss of Lgr4. *Lgr4*^{T2AGal4} animals showed significantly reduced light avoidance responses, which could be fully restored by expression of Lgr4 in its endogenous pattern (Fig. 25A).

I next wanted to find out whether ABLK neuron responses to UV light require Lgr4. I therefore imaged calcium responses of ABLK neurons using a confirmed *Lgr4* knockout allele (*Lgr4*^{ko}) (Deng et al., 2019). Similarly, to *ilp7*^{ko} (Fig. 21C), I detected a three-fold decrease in calcium responses towards UV light, which was rescued upon expression of Lgr4 only in Lk-positive neurons including ABLK (Fig. 25B, C). These data show that Lgr4 is required for UV-light responses and light avoidance behavior.

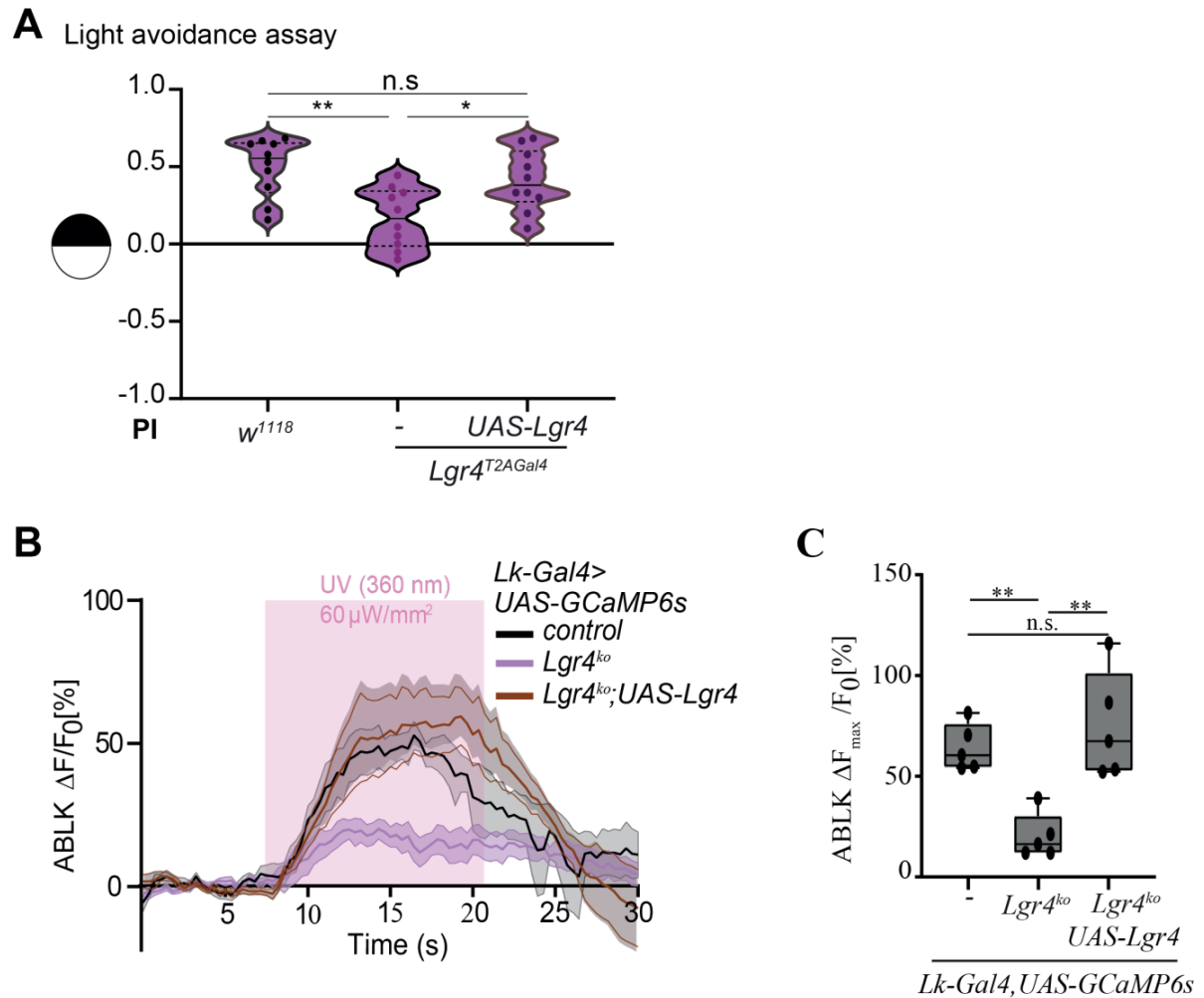


Figure 25: Lgr4 is needed for UV light responses of ABLK neuron and light avoidance behavior. **A.** *Lgr4^{T2AGal4}* animals showed reduced light avoidance, which was rescued by *UAS-Lgr4* expression (n=10 trials/genotype, *P<0.05, **P<0.01, one-way ANOVA with Tukey's post hoc test). **B.** GcaMP6s-expressing ABLK neuron responses to UV light in control and *Lgr4^{ko}* animals with and without *UAS-Lgr4* expression (*Lk-Gal4*>*GcaMP6s*, n=5 animals/genotype, mean \pm s.e.m.). **C.** Quantitative $\Delta F_{\text{max}}/F_0$ box plots of **B** (n=5, **P<0.01, one-way ANOVA, with Tukey's post-hoc test).

3.18 ABLK neurons are selectively required for light avoidance

Both, the light avoidance and mechanonociceptive circuits overlap at the sensory C4da and Dp7 neurons level. I therefore wanted to find out whether *Ilp7*-dependent output of Dp7 to ABLK neurons is specific for UV light.

3 Results

For this purpose, ABLK neuron responses to mechanonociceptive stimulation was analyzed and in sharp contrast to UV stimulation, mechanical stimulation did not trigger calcium signals in ABLK neurons (Fig. 26A). These results thus indicate that divergence of the mechanonociceptive and light avoidance circuits occurs downstream of Dp7 neurons through Ilp7-mediated action on ABLK neurons.

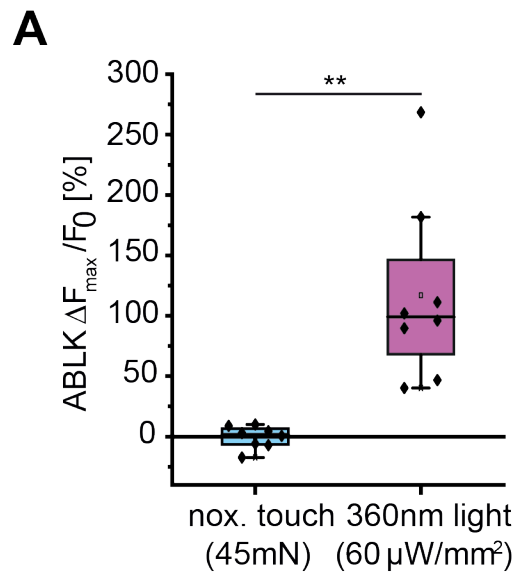


Figure 26: Divergence of mechanonociceptive and light avoidance circuits occurs at ABLK neurons level. A. Maximum ABLK neuron responses ($\% \Delta F_{\max}/F_0$) to noxious touch (45 millinewton (mN)) or UV light stimulations in semi-intact live larval preparations (n=8, unpaired t-test with Welch`s correction, $**P<0.01$, experiment performed by Chun Hu).

3 Results

3.19 Fructose foraging behavior in *Drosophila* larvae is modulated by Ilp7 and sNPF neuropeptides

The proximal axons of Dp7 neurons project to the SEZ, a site where gustatory neurons converges (Miroschnikow et al., 2018). Moreover, Dp7 neurons receive synaptic input from a subset of gustatory neurons the so called AN-bundle derived neurons (Fig. 11E and E'). Both sNPF and Ilp7 neuropeptides have some link with feeding functions in the larvae (Cognigni et al., 2011; Wu et al., 2003). Based on these observations, I speculated that Dp7 neurons and its neuropeptides sNPF and Ilp7 may be involved in foraging behavior in the larvae.

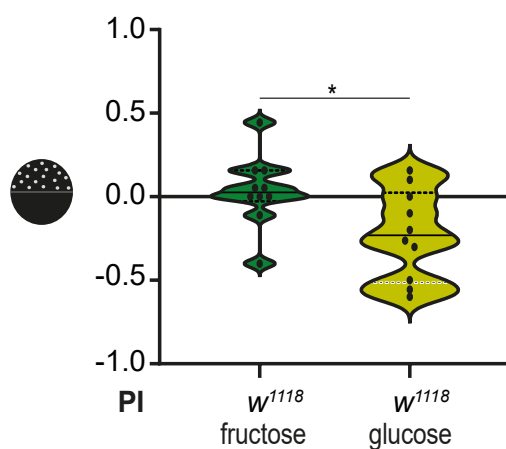
I thus tested whether Ilp7 and sNPF could be involved in foraging responses to sugars which are one of the major dietary constituents of *Drosophila* that forage on rotten fruits in the wild. To this end, I quantitatively assayed the preference for glucose and fructose in third instar foraging larvae in a two-choice assay that contained 2M sugar in 2% agar in one compartment versus 2% plain agar in the other compartment. In the larvae, fructose from the environment is sensed by Gr43a receptor expressing gustatory neurons (Mishra et al., 2013). Fructose is also known to induce a preference in L1 and L3 larvae when tested against agarose (Almeida-Carvalho et al., 2017; Mishra et al., 2013; Rohwedder et al., 2015). I used 2% agar instead of agarose as a substrate, where L3 larvae also had a preference for fructose (Fig. 27A). Preference for glucose was negative although it is the main sugar used by the adult fly (Fig. 27A).

sNPF has a known impact on larval gustatory behavior by boosting olfactory sensitivity and inducing food search behavior upon starvation (Root et al., 2011). I thus tested sNPF mutants in gustatory assays. sNPF mutant animals displayed decreased fructose preference (Fig. 27B) indicating that sNPF neuropeptide is required for gustatory preference for fructose in the larvae. Ilps are also known regulators of feeding (Zhan et al., 2016). In *Drosophila*, mutation of Ilps leads to diabetes-like phenotypes (Rulifson et al., 2002). To test for a possible function of Ilp7 in gustatory preference for fructose I analyzed the distribution of *ilp7^{ko}* larvae in the fructose preference assay. The data showed that loss of Ilp7 increased preference to fructose compared to wild type.

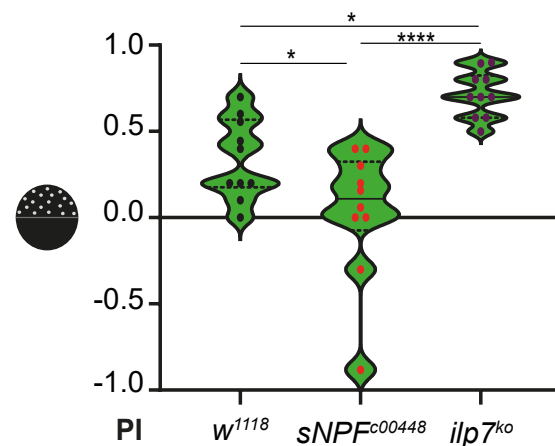
3 Results

Thus, it seems that the two neuropeptides sNPF and Ilp7 exert opposing forces on foraging behavior in the larva. sNPF likely promotes foraging while Ilp7 dampens foraging behavior (Fig. 27B). Unexpectedly, I also found that loss of Ilp7 not only increases preference for the attractive sugar fructose, but it also promotes foraging on the unattractive sugar glucose (Fig. 27C). It thus seems that Ilp7 has a broad effect for sugar foraging.

A Sugar preference



B Fructose preference assay



C Glucose preference

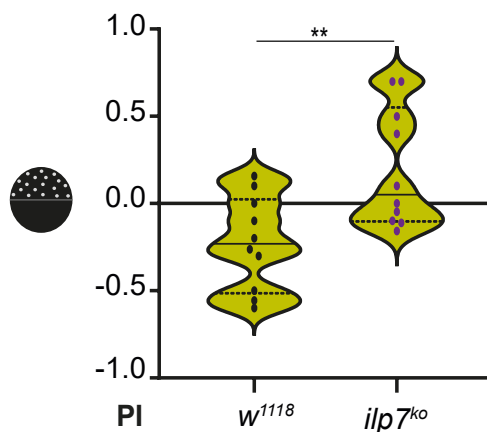


Figure 27: Sugar preference in the larva and its modulatory elements. A. Compared to glucose, larvae have a significantly higher performance index for fructose (n=10 trials, *P<0.05, unpaired t-test with Welch's correction). **B.** *Ilp7^{ko}* larvae showed an increase in fructose preference compared to the controls, while *sNPF* mutant animals showed reduced fructose preference (n=10 trials, *P<0.05, ****P<0.0001, one-way-ANOVA with Tukey's *post-hoc* test). **C.** *Ilp7^{ko}* animals also showed an increase in glucose preference (n=10 trials, **P<0.01, unpaired t-test with Welch's correction).

3 Results

3.20 Dp7 neurons and its Ilp7 neuropeptide limits foraging behavior in *Drosophila* larvae

Ilp7 neuropeptide is produced by eighteen neurons in the larval brain, which includes Dp7 neurons, two neurons in T3 (anteriorly from Dp7 neurons) with sparse SEZ projections, six lateral locally projecting neurons in the VNC and four pairs of neurons residing in the posterior part of the VNC (Miguel-Aliaga et al., 2008). The latter innervate the hindgut providing a brain-gut circuit which regulate appetite in the larvae through Ilp7 neuropeptide modulation (Cognigni et al., 2011).

To test whether Dp7 neurons specifically is involved in fructose preference, I made use of larvae where Dp7 neurons were silenced through the expression of Kir2.1 (*Dp7-LexA>LexAop-Kir2.1*) in the fructose preference assay. Dp7 silencing indeed resulted in an increased preference for fructose (Fig. 28A), like the phenotype seen in *ilp7^{ko}* animals (Fig. 27B). The fact that Dp7 neuron silencing significantly promotes foraging implies that Dp7 neurons, like Ilp7, negatively modulate foraging. To determine whether Ilp7 derived from Dp7 neurons is required for fructose preference in the larvae, I performed a rescue experiment, where Ilp7 neuropeptide was expressed in Dp7 neurons (*Dp7-Gal4>UAS-ilp7*) in an *ilp7^{ko}* background. Under these conditions, fructose preference was rescued to wildtype levels. Thus, Dp7 neuron derived Ilp7 is not only required, but is also sufficient to limit foraging responses to fructose in *Drosophila* larvae (Fig. 28B). The 3rd instar larvae eat voraciously during the foraging stage as they need to prepare for metamorphosis. Therefore, breaks in feeding could potentially be advantageous to control developmental progression on low quality or noxious food.

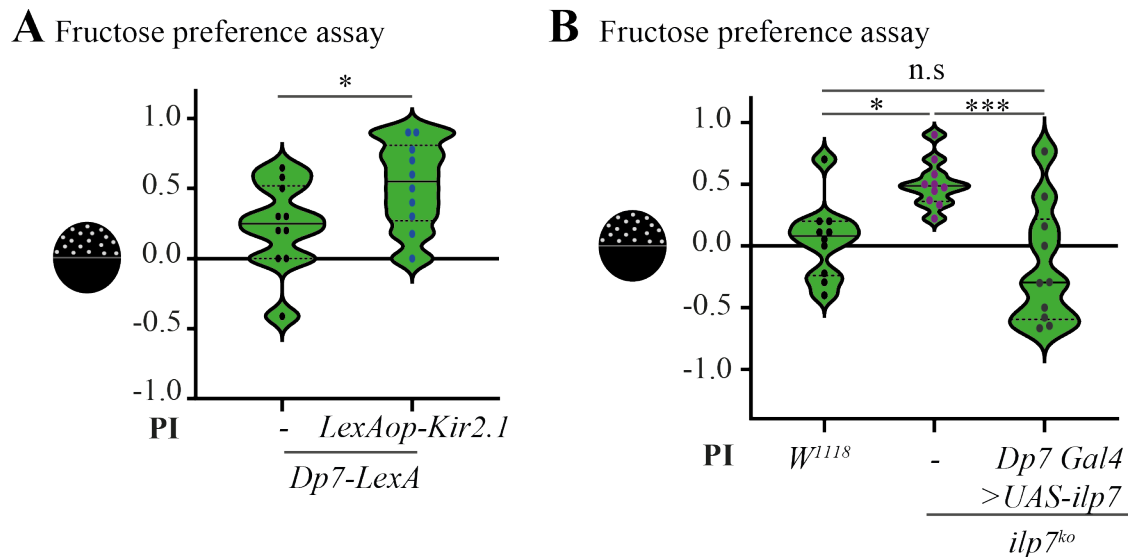


Figure 28: Dp7 neurons and its neuropeptide Ilp7 modulate fructose preference in *Drosophila* larvae. **A.** Larvae with silenced Dp7 neurons (*Dp7-LexA*>*LexAop-Kir 2.1*) had a higher preference for fructose (n=10 trials, *P<0.05, unpaired t-test with Welch's correction). **B.** Expression of Ilp7 (*UAS-Ilp7*) exclusively in Dp7 neurons (*Dp7-Gal4*) in an Ilp7 mutant (*ilp7^{ko}*) background restores foraging behavior to wild type levels (n=10 trials, *P<0.05, ***P<0.001, n.s., non-significant, one-way-ANOVA with Tukey's *post-hoc* test).

3.21 Candidate neurons from the Dp7 connectome that may be involved in foraging behaviors

The connectome serves as a crucial tool which can help in deducing potential partners of Dp7 neurons that may be involved in mediating foraging responses in the larvae. Analysis of the downstream connectome of Dp7 neurons hinted those two neuronal subsets, the IPCs and Hugin-PC (Fig. 29A and B, Appendix 1), may be involved in foraging responses to fructose. The IPCs are known for regulating appetite and sugar intake in flies, while Hugin-PC mediate avoidance to bitter tasting substances in the larvae (Hückesfeld et al., 2016; Kannan and Fridell, 2013). Sparse synaptic connection between Hugin-PC and Dp7 are found at the SEZ region, but most synapses are found in the PC (Fig. 29A'). Dp7 also synapse with the IPCs in the larval PC (Fig. 29B').

3 Results

To date the fructose-sensing circuit of Gr43a-positive gustatory neurons is unknown. Assuming that the AN-B2-derived neurons that weakly connect to Dp7 neurons may be the Gr43a positive neurons, I checked the downstream connectivity of the latter and mapped out two subsequent neuronal layers, consisting of the T2 neuron, which connects the SEZ to the thoracic segment 2, and the Pre-goro 3 neuron, a dorsally located neuron, which has descending projection along the midline of the larvae up to the A8 segment (Fig. 29C, D, E). Since the Pre-goro 3 neurons projects dorsally this could imply that they connect to premotor or motor neurons that may be involved in locomotor responses during larval foraging. Moreover, the AN-bundle derived neurons annotated individually as AN-B2- 1-3, the T2 neurons and the pre-Goro 3 neurons also make synapses at the SEZ region close to the axonal arbor of Dp7 neurons (Fig. 29D'). Thus, it may be likely that Dp7 neurons regulate the foraging circuit in the SEZ region via Ilp7 modulation, possibly on the mapped neurons of the gustatory foraging circuit (Fig. 29E).

3 Results

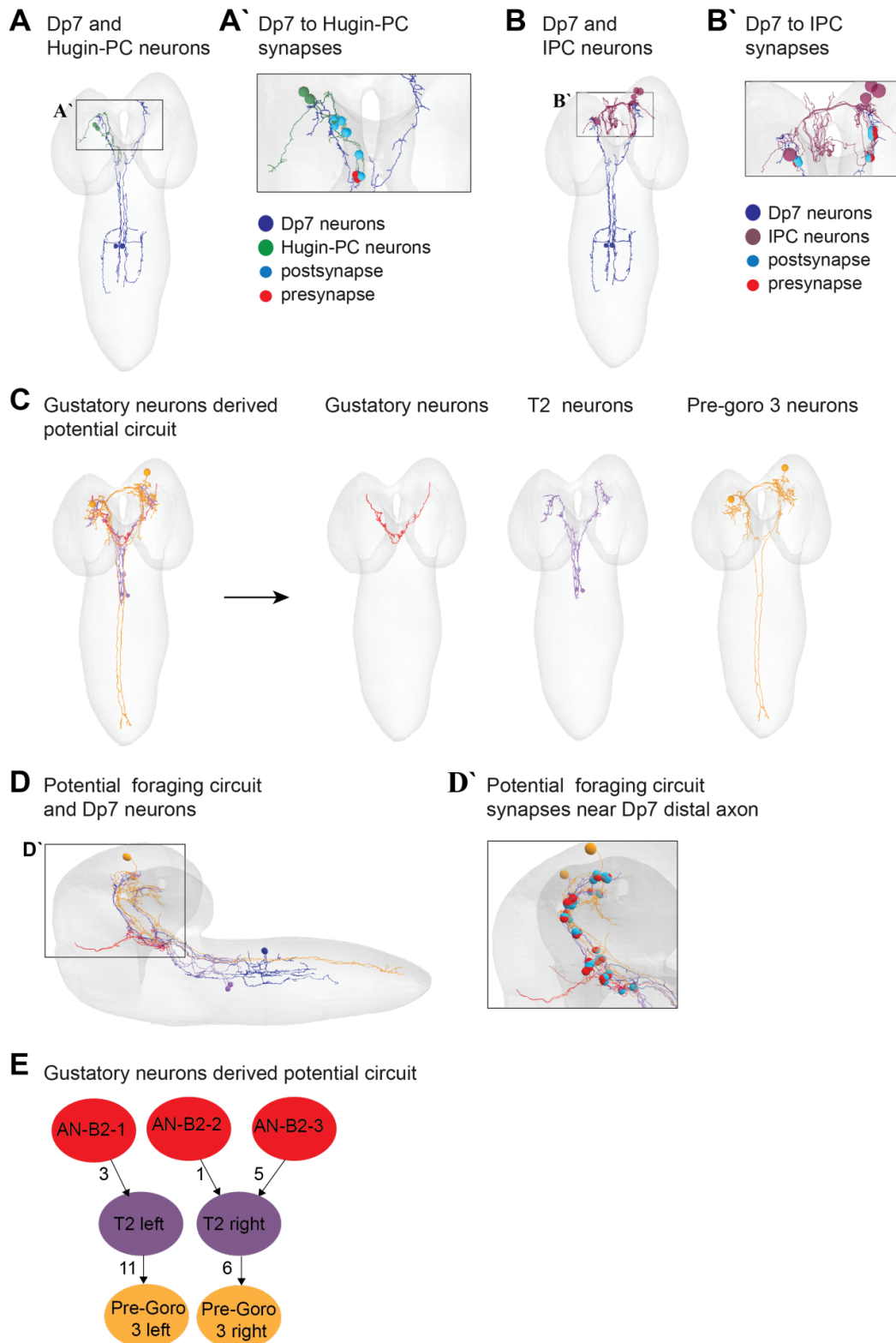


Figure 29: Potential circuit elements linked to Dp7 neurons. **A** and **A'**. Anatomical representation of EM-traced Dp7 neurons and Hugin-PC, which make most synapses in the PC region. **B** and **B'**. Anatomical representation of Dp7 neurons and IPCs, which also make synapses in the PC region.

3 Results

C. Anatomy of neurons which may make up the fructose sensing circuit. **D.** overlay of AN-B2 derived circuit elements with Dp7 neurons. **D.** The AN-B2-derived circuit elements make synapses with each other in the SEZ and PC in proximity with Dp7 distal axonal arbor. **E.** AN-B2 bundle-derived neurons synapse with T2 neurons, which subsequently synapse with Pre-goro 3 neurons. The numbers next to the arrows indicate the number of synapses, left and right refers to the neuronal position in the larvae.

3.22 *Drosophila* larvae integrate context and internal state to select for the most imminent behavior

Behavioral decisions often involve interactions and communication between several areas of the brain or even different organs (reviewed in (Leopold and Perrimon, 2007)). The initial information for the brain to decide about a behavior comes from perception of the sensory environment which is normally multisensory. This multisensory context and also the internal state of the animal are computed into behavioral decisions, which eventually leads to a behavioral action, the outcome of which may be memorised by the animal to aid future reencounters of the same events (Fig. 30A) (Anderson, 2016; Grunwald Kadow, 2019; Kim et al., 2017).

Light avoidance and foraging are innate behaviors, which are very different from each other. Since larvae can encounter both light and a food substrate at a given time point in its natural habitat, it is highly possible that the behavioral response might be hierarchically organized and depend on the environmental context and the larval feeding state. To quantitatively assay how context and internal state influence innate behavioral decisions, I designed a paradigm named context and state dependent assay. It integrates contextual variables, namely light paired with fructose versus darkness (Fig. 30B). Fed larvae with a low feeding drive, as well as starved larvae with a higher urge to feed, were subjected to the assay (Fig. 30B). Behavioral assays were done on 94-98h old larvae which were either fed or starved overnight. (Fig. 30C). Starvation is known to affect feeding responses indirectly by influencing innate odor preferences in flies (Root et al., 2011). Thus, to uncouple starvation from innate light avoidance and feeding behaviors, I performed light avoidance and fructose preference assays in wild type larvae, which were either fully fed on grape agar plates supplemented with yeast paste or starved overnight (Fig. 30 C, C', D and E).

3 Results

I found that the hunger state did not alter innate light avoidance or fructose preference in larvae (Fig. 30D and E).

I next performed the context and state-dependent assay on wild type animals. Interestingly, I found that while fed animals preferred darkness, starved larvae showed an increased preference for fructose in the presence of light (Fig. 30F). These data show that innate foraging behavior for fructose is prioritized over light avoidance behavior in starved but not fed larvae, which show normal light avoidance. This data thus brings to light a behavioral decision-making process, where the larva integrates its sensory context with its internal state to prioritize and select for the most demanding innate behavior at a given time point. This data also provides a platform for understanding the neural and molecular mechanisms underlying the decisive behavioral switch from light avoidance in the fed state to foraging in lit areas in starved state.

3 Results

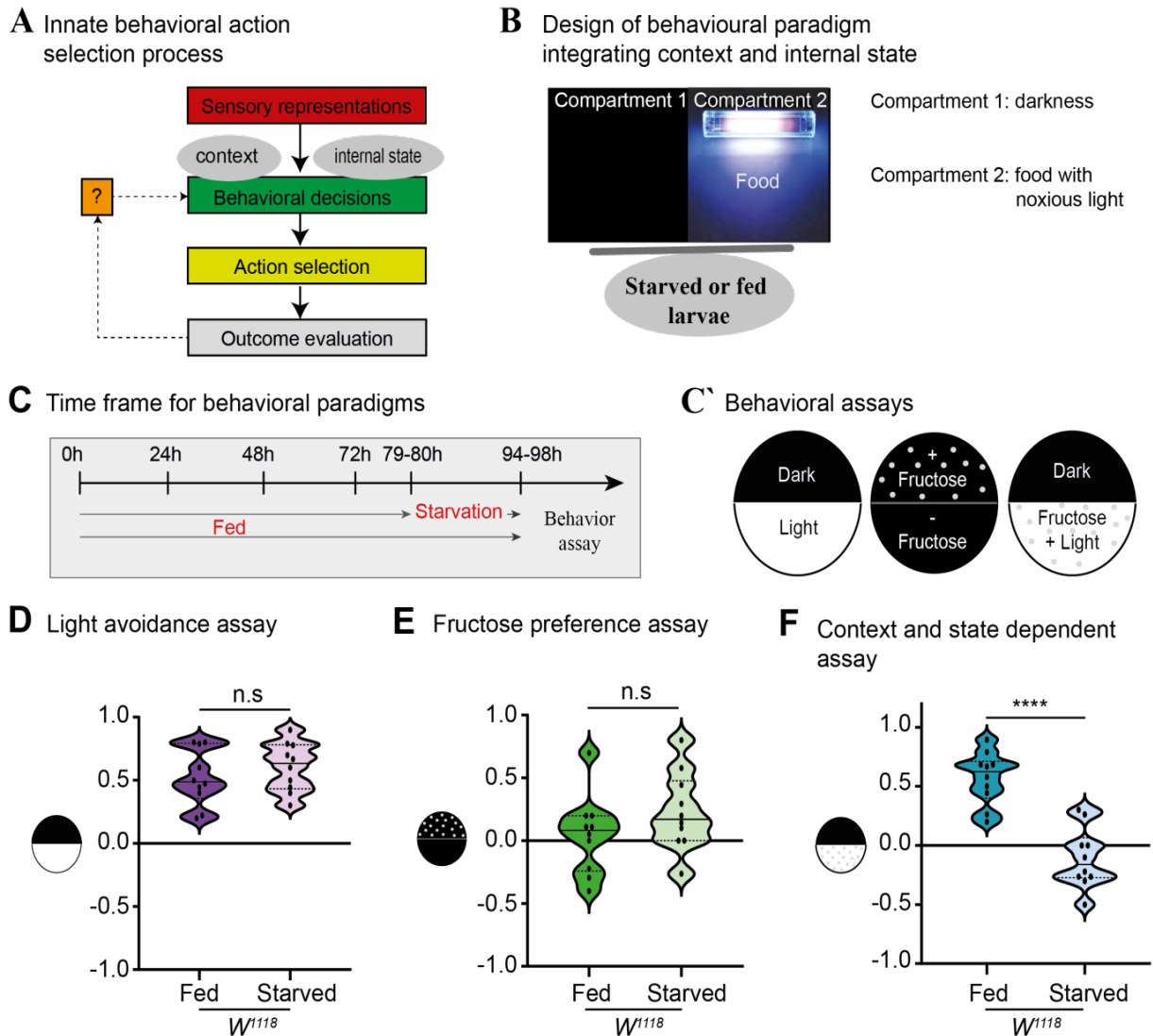


Figure 30: *Drosophila* larvae integrate context and hunger state to switch from avoidance of light to foraging for fructose under light exposure. A. Innate behavioral decisions integrate context and internal state. **B.** Design of a paradigm with darkness in compartment 1 and noxious light and fructose in compartment 2. Behavioral decisions for preference are made depending on the state of the larvae (fed or starved). **C.** Behavioral assays were performed on foraging mid-third instar larvae, which were fed or starved overnight. **C'.** Regular light avoidance and fructose preference assays were used as controls. For the context and feeding state paradigm, fructose was paired with white light in one compartment, while the other compartment consisted of plain agar in darkness. **D and E.** Starvation did not influence either light avoidance or fructose preference responses in wild type larvae (n=10 trials, n.s., non-significant, unpaired t-test with Welch's correction. positive value: preference for darkness and fructose in **D** and **E** respectively). **F.** Fed larvae avoided light although it was presented with fructose, but when starved, the preference of larvae shifted towards the fructose side despite the aversive light cue.

3 Results

(n=10 trials, ****P<0.0001, unpaired t-test with Welch's correction, positive value: preference for darkness, negative value: preference for paired light and fructose).

3.23 *Drosophila* larvae adaptively tune down light avoidance when starved to forage on fructose

Adaptive behavior is widespread across the animal kingdom to promote survival (Branco and Redgrave, 2020; Padilla et al., 2016; Siju et al., 2021). Thus, larvae might as well exert adaptable light tolerance when they are starved and when fructose is present, which might account for the behavioral switch from preference of darkness in the fed state to preference for fructose and light in starved animals (Fig. 30F).

To explore this possibility quantitatively, I assayed fed and starved larvae in a two-choice assay for their preference for fructose in darkness versus fructose and light (Fig. 31A). I did not find significant difference between fed and starved larvae in the tolerance assay (Fig. 31A). However, as starved larvae did not display a clear preference for either compartment in the tolerance assay, a heatmap was generated to show the average distribution of the fed and starved larvae over the time frame of 10 to 15 mins. I found that fed larvae were preferentially distributed on the dark side with fructose indicating that they can still sense light as being noxious (Fig. 31B). Interestingly, starved larvae had a more even distribution across the two compartments suggesting that they tolerate light to forage and to possibly subsequently feed to satisfy their demand for food (Fig. 31C).

It may be useful to perform other statistical interpretations to validate the point that starved larvae tolerate light in the presence of fructose. For example, speed and turning behavior may be worth quantifying as I observed that in contrast to uni-modal assays with light, where starved larvae moved faster (data not quantified), the speed of the larvae appeared to be reduced in the tolerance assay. Moreover, the larvae did not attempt to cross the light and dark boundary in the middle of the petri dish, suggesting that starved larvae might forage wherever they find a food source, indicating local feeding independent of the light conditions. Altogether, my data tends to indicate that starved larvae adaptively tune down avoidance behavior to forage for food.

3 Results

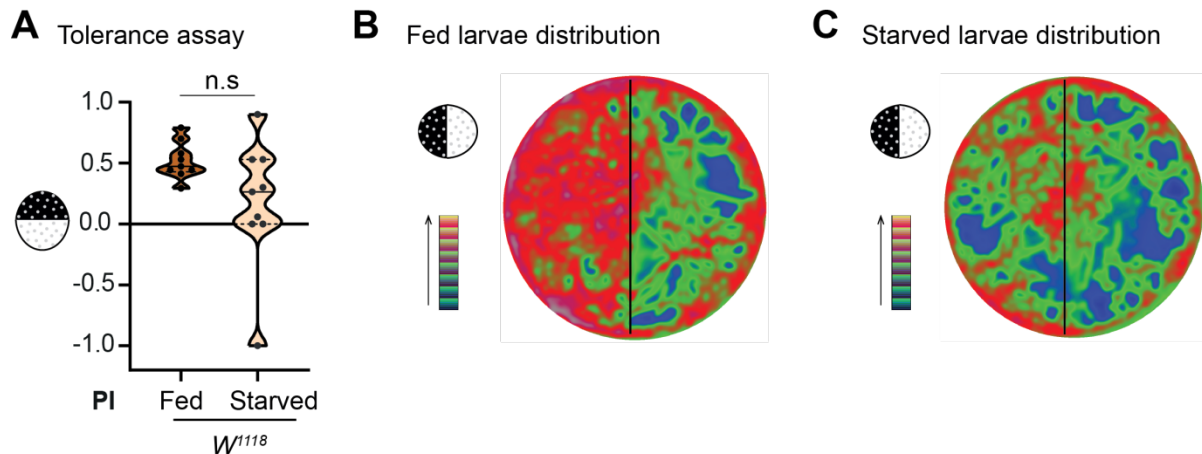


Figure 31: Adaptability of light avoidance on fructose under starvation. **A.** The tolerance assay consisted of one compartment with darkness and fructose and another compartment with light and fructose. Fed w^{1118} larvae showed normal light avoidance on fructose, while starved larvae showed a more random distribution (n.s: not significant, unpaired t-test with Welch's correction, $n=9$ trials, positive values: preference for fructose with dark, negative values: preference for fructose with light). **B.** Heatmap showing the distribution of fed larvae from 10 to 15 mins, with most larvae distributed on the dark side. **C.** Heatmap showing that starved larva appears more evenly distributed from 10 to 15 mins (heatmap was made as an average of all the 9 trials).

3.24 Dp7 neurons mediate a context and internal state-dependent behavioral switch

I next explored the neural substrate where hunger, noxious light and the foraging circuits may intersect and interact. Peptidergic hub neurons have been known for their role in integrating and regulating information from several sensory modalities (Macosko et al., 2009). Dp7 neurons positively regulate light avoidance and negatively regulate foraging (Fig. 9A, 28A). Thus, Dp7 neurons might be such a hub, which in addition might also receive input from an internal feeding state sensor with the ability to switch the hierarchy of these two innate behaviors (Fig. 32A). Light avoidance responses decreased in starved larvae in which Dp7 neurons were silenced (Fig. 32B), like the fed state (Fig. 9A). However, when compared with wild type data the distribution for the control appears to be slightly shifted to higher values, which may be due to the genetic background (Figs. 32B, 30D). Nonetheless, my data shows that independent of internal state, Dp7 neuron silencing seems to decrease light avoidance responses in the larvae.

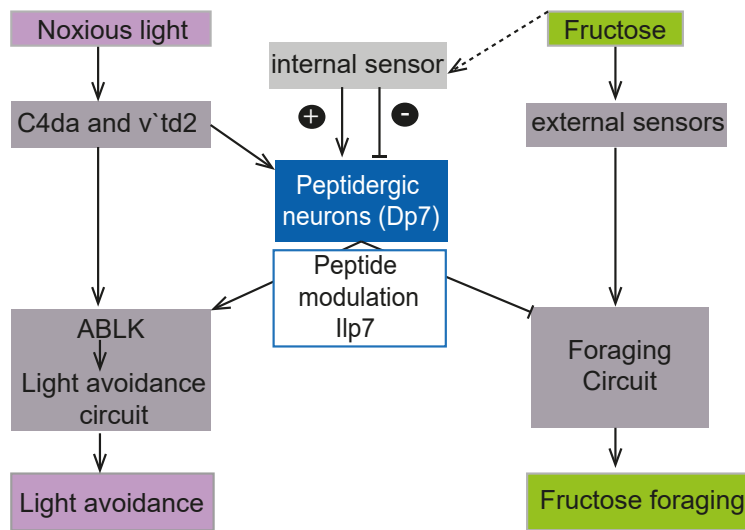
3 Results

Fructose preference responses in starved larvae with silenced Dp7 neurons (*Dp7-LexA>LexAop-Kir2.1*) appears to be unaffected (Fig. 32C). However, compared to wild type data set (Fig. 30E) the controls appear to be shifted towards a higher preference for fructose as well. This might be due to genetic background and to be fully conclusive the experiments need to be repeated with additional controls.

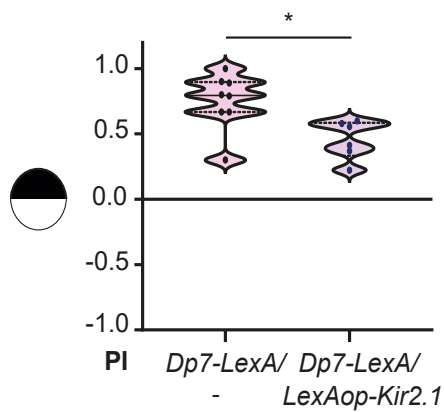
In the context and state-dependent assay, silencing of Dp7 neurons (*Dp7-LexA>LexAop-Kir2.1*) in both fed and starved states mimicked the phenotypes for starved control larvae (Figs. 32D, E, 30F)). As a result, Kir2.1-mediated silencing of Dp7 neurons resulted in no significant differences of larval preference compared to controls in the starved state, as all genotypes showed an increased for foraging for fructose in the presence of light (Fig. 32E). The data thus shows that Dp7 neurons likely modulate the behavioral switch from light avoidance to light tolerance in the presence of fructose in a hunger state-dependent manner.

3 Results

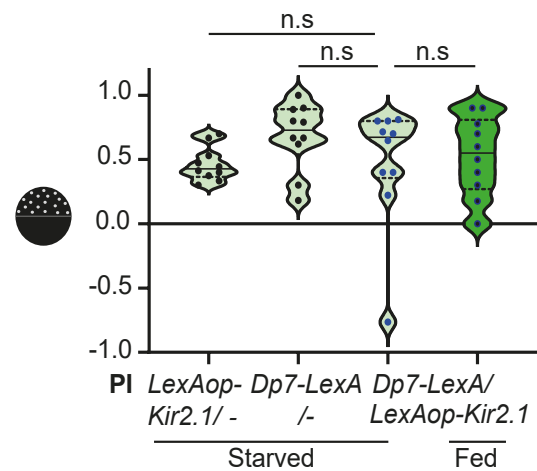
A Framework for neural representation of context and internal state mediated behavioral switch



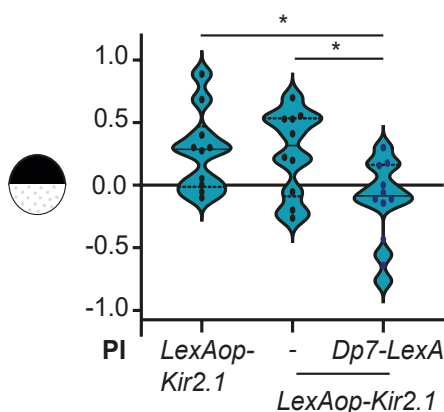
B Light avoidance assay - starved state



C Fructose preference assay - starved state



D Context and state dependent assay - fed state



E Context and state dependent assay - starved state

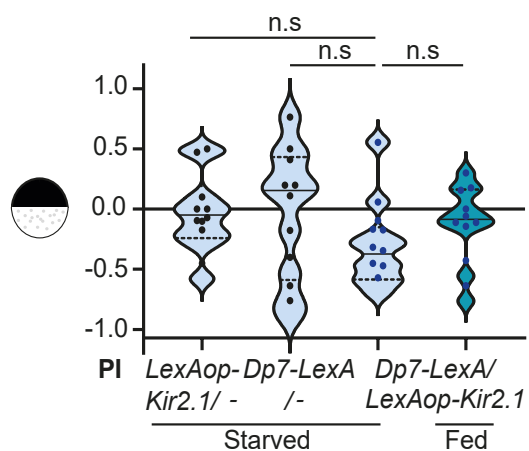


Figure 32: Modulatory Dp7 neurons mediate the behavioral switch from light avoidance to light tolerance in presence of fructose and hunger drive.

3 Results

A. Schematic framework showing modulatory Dp7 neurons that might receive inputs from internal sensors and may flexibly promote or inhibit the light avoidance and foraging circuits, respectively and depending on the feeding state. **B.** Light avoidance behavior is reduced in starved larvae where Dp7 neurons were silenced (*Dp7-LexA>LexAop-Kir2.1*, n=8,6 trials for fed and starved states respectively, *P<0.05 unpaired t-test with Welch's correction) **C.** No change in preference for fructose is detected upon silencing of Dp7 neurons (*Dp7-LexA>LexAop-Kir2.1*) in starved and fed larvae (fed Dp7 silenced larvae set similar as in Fig. 28A, n=10 trials, n.s. non-significant, one way ANOVA with Turkey's post hoc test). **D.** Fed larvae whose Dp7 neurons were silenced by expression of Kir2.1 (*Dp7-LexA>LexAop-Kir2.1*) shifted their distribution towards the fructose side with light as compared to the controls, which were distributed mostly in the dark (*Dp7-LexA>LexAop-Kir2.1*, n=10 trials, *P<0.05, one way ANOVA with Turkey's post hoc test). **E.** The distribution of fed or starved larvae, in which Dp7 neurons were silenced (*Dp7-LexA>LexAop-Kir2.1*), was not significantly different from starved controls (fed Dp7 silenced larvae data set same as in **D**, n=10 trials, n.s. non-significant, one way ANOVA with Turkey's post hoc test).

3.25 *Ilp7* regulates context and internal state-dependent innate behavior

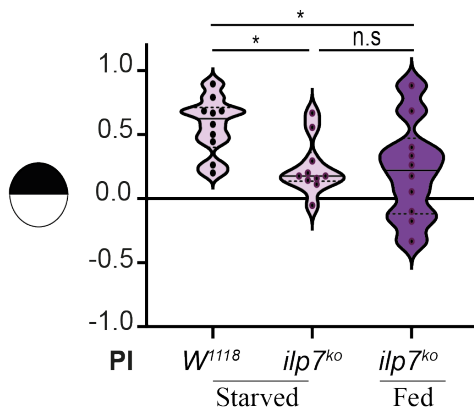
I next assayed the function of *Ilp7* and sNPF in the context and state-dependent assay. *Ilp7^{ko}* animals, whether fed or starved, showed a decrease in light avoidance indicating that *Ilp7* is an innate component of the light avoidance circuit (Fig. 9B, Fig. 33A). Fructose preference of starved *ilp7^{ko}* animals was not significantly different from controls, but qualitatively appeared similarly shifted as for fed *ilp7^{ko}* larvae (Fig. 33B). Thus, it seems that starvation does not affect Dp7 and *Ilp7* neuropeptide functions in unisensory context of fructose. Using my context and state dependent assay, I found that *ilp7^{ko}* larvae showed tolerance to light with fructose in the fed state, which is consistent with *Ilp7* being a mediator of the behavioral switch (Fig. 33C). Nonetheless, *Ilp7* also being a component of the innate light avoidance circuit limits clear conclusions about its role in switching from light avoidance to tolerance with fructose.

To validate that *Ilp7* derived from Dp7 neurons mediates this behavioral switch, *Ilp7* (*UAS-Ilp7*) was expressed only in Dp7 neurons (*Dp7-Gal4*) in *ilp7^{ko}* larvae and assayed in the context and state dependent assay.

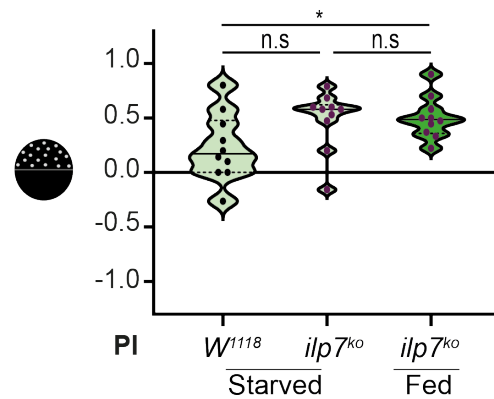
3 Results

The data showed that expressing *Ilp7* in Dp7 neurons rescued the behavior for preference of darkness over light and fructose (Fig 33D).

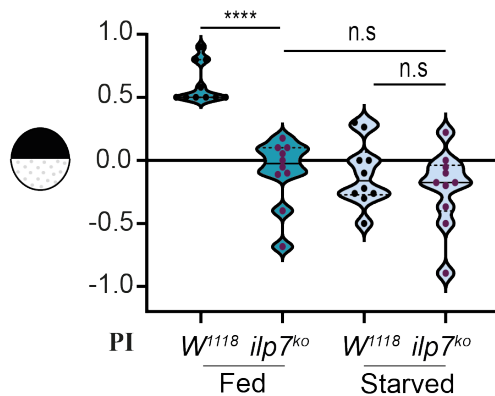
A Light avoidance assay - starved state



B Fructose preference assay - starved state



C Context and state dependent assay - fed and starved state



D Context and state dependent assay - fed state

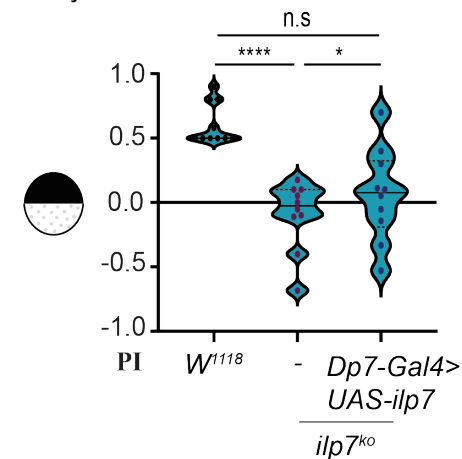


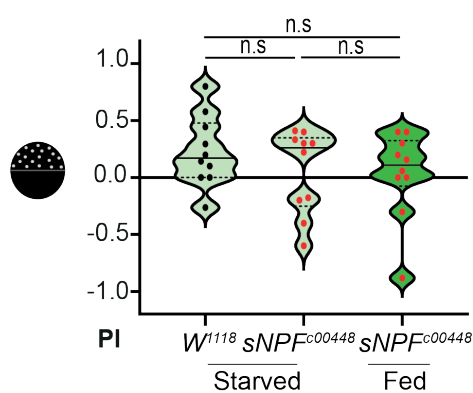
Figure 33: *Ilp7* peptide derived from Dp7 neurons is involved in context and state-dependent behavior. **A.** Light avoidance response is dampened in *ilp7^{ko}* in the starved and fed state (* $P < 0.05$, $n = 10$ trials, n.s., non-significant, one-way ANOVA with Turkey post hoc test, $n = 10$) **B.** No change in fructose preference was detected in starved *Ilp7^{ko}* compared to controls. However, fed *ilp7^{ko}* animals showed stronger fructose preference compared to starved controls ($n = 10$ trials, * $P < 0.05$, n.s., non-significant, one-way ANOVA with Turkey post hoc test) **C.** *Ilp7^{ko}* animals showed an increased preference for fructose with light, no significant difference was observed between fed and starved *ilp7^{ko}* animals (**** $P < 0.0001$, n.s., non-significant, one-way ANOVA with Turkey post hoc test, $n = 10$ trials). **D.** Expression of *Ilp7* in Dp7 neurons in fed *Ilp7^{ko}* larvae rescued dark preference (*w¹¹¹⁸* data set as in **C**, * $P < 0.05$, **** $P < 0.0001$, n.s., non-significant, one-way ANOVA with Turkey post hoc test, $n = 10$).

3 Results

3.26 sNPF neuropeptide modulates integration of light and fructose

Light and food commonly occur in the wild, thus integration of the two variables with a high feeding drive might already be established in larvae. While *sNPF* mutant animals showed a decrease in their preference for fructose in the fed state compared to wild type fed larvae (Fig. 27B), starvation did not further affect fructose preference of *sNPF* mutant larvae (Fig. 34A). *sNPF* mutant showed similar distribution in fed and starved states in the fructose preference assay (Fig. 34A) which may imply that in unisensory context of fructose, internal state does not influence the action of *sNPF* neuropeptide in fructose foraging behavior. When fructose is combined with light in the context and state-dependent assay, fed and starved *sNPF* mutant larvae displayed a similarly reduced preference for darkness (Fig. 34B). In unisensory context of light, *sNPF* is not required for light avoidance behavior (Fig. 9B) and *sNPF* mutants showed a slight reduction in fructose foraging behavior (Fig. 27B). However, in the multisensory context of light and fructose, fed *sNPF* mutants completely avoided the fructose side with light (Fig. 34B) suggesting that *sNPF* may aid in integration of light and fructose inputs to promote adaptive behavior to noxious light. The regulatory role of *sNPF* thus appears to be state dependent in the multisensory context of fructose and light and may be aiding in adaptive responses to noxious light in the multisensory context.

A Fructose preference assay
- starved state



B Context and state dependent assay
- fed and starved state

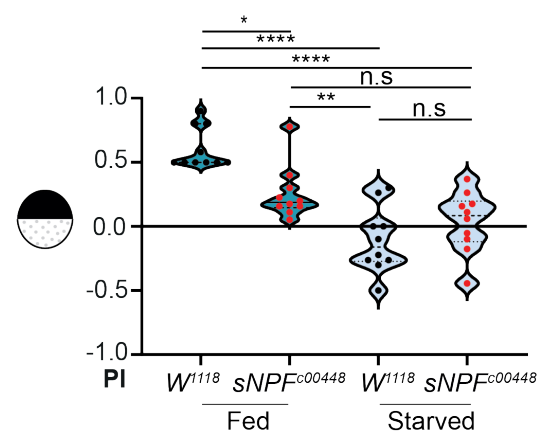


Figure 34: sNPF promotes integration of light and fructose to enable state dependent responses.

3 Results

A. No change in fructose preference was detected in starved and fed *sNPF* mutant animals (n=10 trials, n.s., non-significant, one-way ANOVA with Turkey post hoc test). **B.** *sNPF* mutant larvae displayed a reduced preference for darkness in the fed and starved state (w^{1118} : data set as in **Fig. 33C**, n.s. nonsignificant, * $P < 0.05$, ** $P < 0.01$, **** $P < 0.0001$, n.s., non-significant, one-way ANOVA with Turkey post hoc test, n=10).

3.27 Potential circuit elements linked to integration of contextual sensory input

The *Drosophila* mushroom body, which is the learning and memory center, also expresses sNPF (Nässel et al., 2008). In the larvae, sNPF mediates odor reward memory stabilization by a feedback mechanism from the mushroom body Kenyon cells to presynaptic partners, the dopaminergic primary protocerebral anterior medial cluster (pPAM) neurons (Lyutova et al., 2018). As sNPF seems to play a role in integration of light and fructose in a state dependent manner (Fig. 34B), this integration by sNPF may be happening at the level of the MB. Further experiments are required to test if sNPF derived from Dp7 neurons is involved in integrating light and fructose during the context and state-dependent behavior. If Dp7 neurons derived sNPF are involved in integration of multisensory light and fructose (Fig. 34B), the Bamas neurons may be worth investigating (Fig. 35A). The Bamas neurons receives strong inputs from Dp7 neurons in the SEZ region (Fig. 35B, B'). Analysis of the Bamas connectome revealed that it receives extensive inputs from the gustatory neurons also in the SEZ region and moreover it connects to the dopaminergic neurons (MBE1c) which connects to DANs in the mushroom body (Fig. 35C, C'). Circuit analysis revealed that Bamas neurons receive extensive inputs from both the gustatory neurons and Dp7 neurons and it also make strong connection to the dopaminergic neurons (Fig. 35D). Thus, Bamas neurons may be integrating gustatory inputs from the gustatory neurons and light inputs via Dp7 neurons and pass the information to the mushroom body via the MBE1c neurons. One may thus speculate possible that the Bamas neurons and its downstream neuron path to the mushroom body may be possible targets of Dp7 derived sNPF neuropeptide in promoting adaptive responses to noxious light in the larvae under multisensory context and under altered internal state.

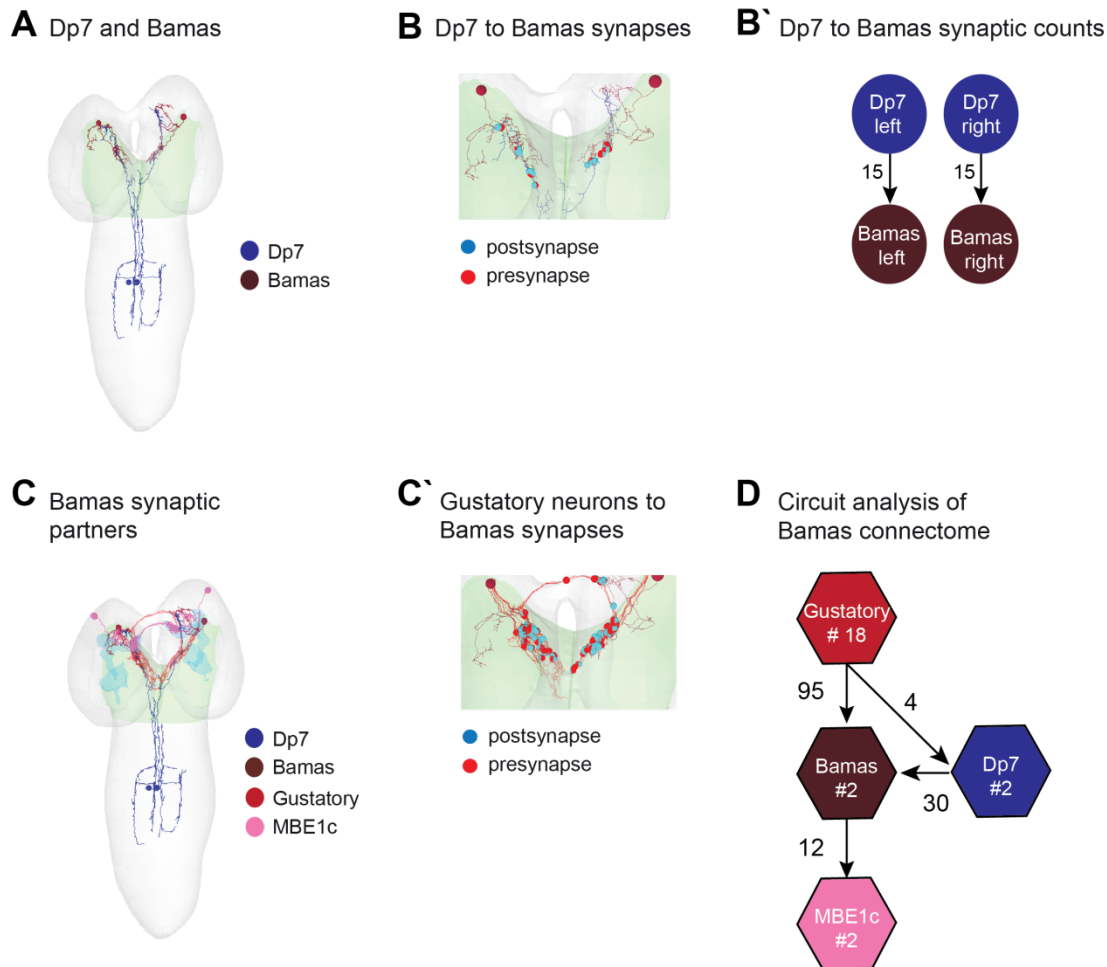


Figure 35: Bamas neurons possibly integrate noxious light and gustatory inputs. **A.** EM reconstruction of Bamas and Dp7 neurons. **B.** Dp7 makes synapses with Bamas neurons mostly in the SEZ region (green region). **B'.** Dp7 neurons show high connectivity to Bamas neurons with 15 synapses ipsilaterally connecting Dp7 and Bamas in each hemisphere. **C.** EM reconstruction of Bamas neurons and its neuronal partners the gustatory neurons, Dp7 neuron and the dopaminergic neuron (MBE1c) which sends its projection to the mushroom body (blue region). **C'.** Bamas neurons also receive gustatory neurons inputs in the SEZ region. **D.** Circuit analysis of Bamas neurons showing that it receives strong inputs from gustatory neurons as well as Dp7 neurons and it makes strong connection to the MBE1c neurons. Dp7 make weak synaptic connection with the gustatory neurons. The hexagon shows a group of neurons, # indicates number of neurons inside the hexagon, arrows indicate synaptic connection between 2 neurons and the number next to arrow indicates the number of synapses).

4. DISCUSSION

4.1 Network computation relies on modality- and circuit-specific neuromodulation to generate discrete escape behaviors

One of the key functions of the nervous system is to rapidly detect, process and generate appropriate escape behaviors in response to environmental threats (Dubin and Patapoutian, 2010; Tracey, 2017). *Drosophila melanogaster* larvae show very different contextual escape behaviors. While noxious light triggers a stop and turn avoidance response (Xiang et al., 2010), exposure to noxious touch elicits a corkscrew like rolling behavior (Tracey et al., 2003). Larvae detect nociceptive stimuli including high intensity UV and blue light (Xiang et al., 2010), heat (Zhong et al., 2012) and harsh touch (Tracey et al., 2003) by means of specialized multimodal nociceptors, the C4da neurons. How, when and where convergence and divergence in these nociceptive pathways occurs was so far not well understood.

By combining EM reconstruction, light microscopic connectivity analysis, behavioral assays, and functional imaging, I uncovered novel circuit elements from the sensory to the 3rd order level making up the somatosensory noxious light-sensing circuit (Fig. 36). Within this circuit, I identified the critical *Ilp7*-producing *Dp7* neuron, which not only serves as an integration hub for somatosensory modalities, but also as a processing node, which codes for next level responses. Using noxious light or mechanonociceptive stimuli together with genetic perturbation of neuropeptide signaling or neuronal function, I mapped converging and diverging circuit elements required for both or only a specific modality, respectively. With the help of an *in vivo* reporter for *Ilp7* release, I showed that light induced acute peptide release from these modulatory neurons. Moreover, I found that modality-specific activation of downstream *ABLK* neurons expressing the cognate receptor for *Ilp7*, *LGR4*, is required for light avoidance.

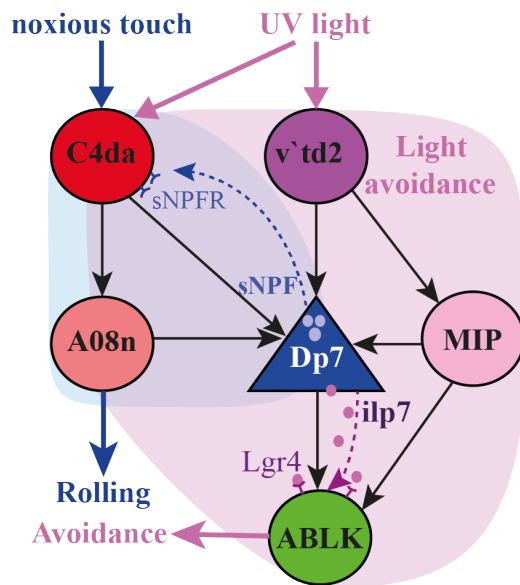


Figure 36: Schematic showing convergence of mechano and light avoidance circuit onto Dp7 neurons which are facilitating rolling and light avoidance behaviors by discrete peptide actions on specific circuit components.

4.1.1 Sensory neurons coding for different nociceptive modalities converge on peptidergic Dp7 hub neurons

The presence of extraocular light-sensing neurons has been reported in several animals including sensory neurons in *C.elegans* (Edwards et al., 2008), the hypothalamus of birds (Halford et al., 2009) and retinal ganglion cells in mammals (Hattar, 2002). Similarly, C4da neurons in *Drosophila* are also extraocular neurons capable of sensing noxious light through the Gr28b_c receptor to elicit avoidance behaviors in the larvae (Xiang et al., 2010). C4da neurons are particularly well suited to act in light avoidance behavior. Their dendrites tile the whole body wall of the larvae, thus noxious light in any part of the larvae can be detected and elicit an escape response (Xiang et al., 2010). In addition to the C4da neurons, larvae also have an eyelike structure termed the Bolwig's organ, which is mostly involved in detection of dim visible light, although it can also detect noxious light (Hassan et al., 2005).

4 Discussion

There is evidence for a hormonal relay system between Bolwig's organ and the extra-ocular C4da neurons via PTTH neurons (Yamanaka et al., 2013), but whether the circuits from the two regions converge at some point in the brain is not clear. As Dp7 axon projections are near the PTTH neurons (Master thesis work, Alisa Gruschka, Soba lab), they may connect the two circuits, either via peptide signaling or intermediate neurons, which remains to be investigated.

Interestingly, I identified another putative extra-ocular light-sensing neuron in larvae, ν td2, which is capable of encoding noxious light (Fig. 15B), likely also through the Gr28b_c receptor based on reporter expression (Qian et al., 2018). Combinatorial coding is a common feature of the olfactory and the gustatory system where combinations of different neurons and receptors can encode for different odors and taste, respectively (Chen et al., 2019; Malnic et al., 1999). Combinations of sound-sensitive neurons also exist in the auditory system where the combination of different frequencies codes for different sounds (Kandel et al., 2000). Similarly, the somatosensory system in the larvae might also rely on combinatorial coding by activation of different combinations of sensory neurons to drive contextual events to distinct behavioral action. While the combined action of C4da, C3da and C2da neurons encodes noxious touch (Hu et al., 2017), C4da and ν td2 neurons combinatorial action may code for noxious light.

4.1.2 Dp7 neuron derived *Ilp7* and the *Lgr4* receptor are involved in light avoidance behavior in the larvae.

Drosophila melanogaster encodes 8 insulin-like peptide genes, *Ilp1-8* (Grönke et al., 2010). Based on their structure, processing and receptor binding affinity, the Insulin superfamily includes insulin-like growth factors (IGFs), insulin and relaxin-family peptides (reviewed in (Gontijo and Garelli, 2018)). IGFs are quite easy to differentiate structurally, as they consist of the A-B and C peptide units. However, insulin and relaxin are more challenging to distinguish structurally, as both consist of the A and B chains. In *Drosophila*, *Ilp6* is the only IGF member. The other *Ilps* are believed to be either from the insulin or relaxin family ((Grönke et al., 2010), reviewed in (Gontijo and Garelli, 2018)).

4 Discussion

Ilp1-6 support different functional roles in development, lifespan and metabolism (Min et al., 2008; Oh et al., 2019; Zhan et al., 2016). Ilp7 is produced by 18 neurons in the larval brain (Miguel-Aliaga et al., 2008). The eight posterior Ilp7 cells are derived from dMP2 lineage cells, which survive apoptosis through Ilp7 peptide expression following their role as axonal scaffolding neurons (Miguel-Aliaga et al., 2008). In this study, I found that Dp7 neurons are likely derived from another lineage, the pCC-derived cells, which are also pioneering neurons required for axonal scaffolding (Jacobs and Goodman, 1989). The distinct anatomy and lineage of Dp7 and the posterior Dp7 neurons is consistent with their functional diversification. The eight posterior Ilp7 neurons are involved in the growth of trachea (Linneweber et al., 2014). The two most posterior Ilp7 expressing neurons which also expresses the neuropeptide Pigment dispersing factor (Pdf) are involved in larval defecation (Zhang et al., 2014). Based on the ligand-receptor function of Ilp7- insulin receptor (IR) in tracheal growth initiation (Linneweber et al., 2014), it appears that Ilp7 is derived from the insulin family. Phylogenetic analysis on the other hand suggested that Ilp7 coevolved with the type C relaxin-like G-protein-coupled receptor Lgr4 in various arthropod families suggesting possible functional conservation (Gontijo and Garelli, 2018). In line with this, I found in this study that Dp7-derived Ilp7 (Fig. 9C) as well as the relaxin-family GPCR Lgr4 (Fig. 25) are involved in larval avoidance responses towards noxious light. This suggests that for nociception, Ilp7 may be acting in a relaxin-like manner in the larvae, while for tracheal growth it acts more in an insulin-like manner. As Ilp7 neuropeptide shares the highest sequence homology of all Ilps to non-insect species (Grönke et al., 2010), other species possibly also share the functional relevance of Ilp7 in regard to nociception.

4.1.3 Dp7 neurons gate the generation of modality-specific behaviors through distinct neuropeptide actions

Specific innate behaviors are the result of elaborate and system-level computation by the underlying networks in response to contextual signals. To understand a behavior, knowledge of how the underlying neuronal constituents are wired together is very important (Bargmann and Marder, 2013; Kandel et al., 2000).

4 Discussion

Using EM data, I deduced seven predominant motifs from the sensory neurons to the Dp7 network (Fig. 17D). I showed that the feedforward motif from v`td2 to Dp7 to ABLK neurons is functionally required for light avoidance behavior (Figs. 15A, B, 16A, B, 21). Based on the connectome analyses (Fig. 13A, B), I also hypothesized that C4da to A08n to Dp7 neuron may be functionally involved in light avoidance, as is the case in mechanonociception (Hu et al., 2017). However, this circuit seems to be dispensable for light avoidance behavior (Fig. 14) despite the strong synaptic connections (Fig. 13A, B). It is possible that another 2-hop connection from C4da to Dp7 neurons is involved, or that a parallel circuit exists, which at some point converges with the v`td2-Dp7 circuit. Thus, while connectome data can display neurons which are wired together it may not necessarily predict specific functions. Indeed, based on the connectome alone, it is difficult to predict function given the large number of potential possibilities for a signal to flow (Bargmann, 2012; Bargmann and Marder, 2013). Studies on EM reconstruction in *Drosophila* have indeed shown that the sensory networks spreads out extensively with several neurons being added to each subsequent hierarchical level (Miroshnikow et al., 2018; Ohshima et al., 2015; Schneider-Mizell et al., 2016). Similarly, Dp7 neurons receive input from several converging sensory neurons, but at the same time provide outputs to 60 potential downstream neurons, making the possibilities to track where a sensory cue may pass through very challenging (Appendix 1).

Neuromodulatory neurons typically have more widespread projections in the brain, which probably relates to their functional diversity (Mao and Davis, 2009). Anatomically, Dp7 neurons span nearly all the key processing units of the larvae including the VNC, the SEZ, and the endocrine center. Such an anatomy might hint towards functional diversification of the neuron. It might also suggest that different context or internal state possibly select for a specific set of functional synapses among the wide range of anatomically specified possibilities to regulate modality or state-specific behaviors. Since a sensory input can take different pathways through the connectome, peptidergic actions can help information arriving at converging nodes to be segregated to distinct circuits. Thus, while the connectome is analogous to a “roadmap” with various routes that a signal might take, neuropeptides can act as traffic signals which guide specific inputs to correct pathways (Bargmann, 2012; Bargmann and Marder, 2013).

4 Discussion

Across species, escape behaviors are under the extensive control of neuromodulatory elements. Mice for example display alternative escape behaviors through interplay of competitive and mutually inhibitory circuits of corticotrophin-releasing factor (CCT) and somatostatin-positive neurons (SST) in the central amygdala. Even though the CCT circuit has been proposed to mediate conditioned flight, and the SST circuit to mediate passive freezing the exact mechanisms by which SST and CCT operate on the circuits is not clear (Fadok et al., 2017).

Here, I showed that Dp7-derived Ilp7 is required for mediating light avoidance behavior by acting in a feedforward manner on downstream neurons in the light avoidance circuit (Fig. 21C). A former study has shown that Dp7 neuron feedback action on mechanosensory neurons via sNPF, but not Ilp7 neuropeptide (Hu et al., 2017), is required for the generation of nocifensive rolling responses to noxious mechanical touch. Thus, while the Dp7 network has potential for eliciting both rolling and avoidance, sensory input-specific peptidergic action of Dp7 neurons generates discrete escape behaviors by creating divergent networks.

Interestingly, the C4da to Basin circuit, which is independent of Dp7 neurons, has also been proposed to be involved in rolling behavior in the larvae. The C4da-Dp7 circuit recruits facilitating action via sNPF signaling to enhance rolling towards mechanical touch (Hu et al., 2017). Conversely, the C4da-Basin circuit however integrates vibrational from the chordotonal neurons to promote rolling behavior (Ohyama et al., 2015). Thus, it seems that parallel circuits might operate in generating rolling behavior. Whether these parallel circuits converge at higher order levels is so far unresolved. It may be possible that the context determines which of the parallel circuits is activated. For example, light and harsh touch actions may activate the C4da to Dp7 circuit, while vibration and harsh touch may drive the C4da to Basin circuit, which however needs further investigation.

4 Discussion

4.1.4 Modality-specific circuits converge on distinct domains of Dp7 neurons

Hub neurons have the potential to be involved in the computation of several behaviors (Macosko et al., 2009). This implies that the hub neuron selectively passes on context-specific information to activate only a subset of its downstream neurons, while others are kept latent at a given time. It might also mean that the downstream neurons may not be sufficiently activated to elicit a behavioral response like the A08n neurons in light avoidance behavior (Fig. 14A). Two possible scenarios can account for context-driven selective circuit activation by the hub neuron. Firstly, neurons may be differentially activated depending on which sensory neurons they receive inputs from. For example, the spinoparabrachial G-protein coupled receptor 83 (Gpr83) neurons receive input from both low- and high-threshold primary mechanosensory neurons. However, depending on the intensity of the stimulus, the valence associated with the activity of Gpr83 neurons can be either positive or negative such that either appetitive gentle touch or aversive pain response is elicited in rodents (Choi et al., 2020). Secondly, specific domains within the hub neuron may be locally activated such that regional activity is triggered. Discrete functional domains have been described for the *Drosophila* mushroom body Kenyon cells, which display compartmentalized activity for encoding of context-specific aversive and appetitive functions by dopamine modulation (Cohn et al., 2015).

Here, I showed that inputs from UV-light receptive $v^{\text{td}2}$ neurons and ABLK neuron outputs converge on the lateral dendritic domain of Dp7 neurons, which also coincide with peptide release sites (Figs. 18A, B, 19C). Conversely, C4da and A08n neurons, which are involved in mechanonociception, provide input on the medial dendritic region of the Dp7 neurons (Fig. 18C). These data suggest that modality-specific compartmentalization of sensory inputs and outputs on Dp7 neurons might further increase the efficiency of network computation by providing proximity of synaptic domains with peptide release within the light avoidance circuit. Thus, domain-specific circuit actions may be a mechanism to generate context-specific behaviors.

4 Discussion

4.1.5 Ilp7 mediated co-transmission occurs during light avoidance behavior

Neurons normally possess a small molecule neurotransmitter, which functions through ionotropic receptor activation, and neuropeptides which act through GPCRs. In our case, Dp7 neurons possess at least three known signaling molecules, the small excitatory neurotransmitter acetylcholine (data not shown) and the neuropeptides sNPF and Ilp7. Co-transmission of signaling molecules is a phenomenon which is common in many species where it can promote behavioral states (reviewed in (Nusbaum et al., 2018)). I show here that Dp7 neuron activity is required for light avoidance behavior, as silencing of Dp7 neurons abolished ABLK UV-light induced responses (Fig. 21A, B). In the absence of Ilp7, only partial activity is seen in ABLK neurons, which probably occurs through the action of the small molecule neurotransmitter (Fig. 21C, D). This residual activity in ABLK neurons was however not sufficient to elicit a behavioral escape response towards noxious light suggesting that co-transmission from the hub neuron is fundamental for light avoidance behavior to occur. Converging co-transmission also occurs in other circuits in *Drosophila*. NPF and Corazonin are cotransmitted by a set of neurons which act on the IPCs expressing sNPF and Corazonin receptor (CrzR) to regulate stress metabolism and resistance (Kapan et al., 2012).

My data shows that sNPF is not required for light avoidance behavior and localizes differently from Ilp7 neuropeptide in Dp7 neurons (Hu et al., 2017), thus suggesting it is not a co-transmitter for this behavior. However, since the noxious light and mechanical circuits overlap at the Dp7 neuron level, one can speculate that co-release of the different signaling molecules, acetylcholine, Ilp7 and sNPF may all occur following bimodal stimulation of the larvae with noxious light and touch. Such release might also increase the net likelihood for the strongest escape behavior, namely rolling, to occur.

4.1.6 Ilp7 neuropeptide is acutely released upon light exposure

Peptide release can occur either following neuronal activity (Persoon et al., 2018) close to synaptic sites or independent of neuronal activity at non-synaptic sites through release of intracellular calcium stores (Leng and Ludwig, 2008).

4 Discussion

When release occurs close to synaptic sites, the phenomenon is described as co-release. Through serial EM images reconstruction Schlegel and colleagues identified peptide release from the Hugin neurons in *Drosophila* (Schlegel et al., 2016). I also detected peptide release sites along the lateral dendritic compartment of Dp7 neurons (Fig. 19B, C) immediately following input sites from v`td2 neurons, suggesting that synaptic activity might also trigger peptidergic co-release in this case.

Neuropeptides released from neurons can have either slow or fast kinetics (van den Pol, 2012). To some extent, peptide kinetics often correlates with physiological functions that they regulate. Slow acting modulators are well known for acting on targets that are considerable distances away from the sites where they are released. For example, in stress-induced analgesia, opioids released from the brainstem act on opioid receptors on primary nociceptive neurons, which are located considerable distances away, to attenuate their excitatory capabilities (Fields, 2004). As a result of this paracrine signaling mode of neuropeptides and the associated difficulty in predicting output sites, in vivo studies investigating the mode of peptide release on top of a functional physical connectome are largely lacking. In *Drosophila*, in vivo peptide release was demonstrated at the neuromuscular junction (NMJ) (Ding et al., 2019) and Octopamine release from motor neurons was shown to occur independently of extracellular calcium (Shakiryanova et al., 2006). In mice, Substance P was shown to be released from primary afferent nociceptors upon high stimulus pain responses (Cao et al., 1998; Mantyh et al., 1995).

Taking advantage of the fact that Dp7 neurons are anatomically aligned with ABLK neurons (Fig. 19A) and that I observed peptide release events in the serial EM volume in the domain of Dp7 neurons where light inputs and outputs converges (Fig. 19C), I investigated Ilp7 neuropeptide release dynamics in vivo. My data show that Ilp7 neuropeptide is released in a fast and acute manner upon UV light stimulation (Fig. 23A-D).

Putative peptide release was recorded also at the lateral dendritic compartment of Dp7 neurons, where input and output synapses from v`td2 and ABLK neurons converge.

4 Discussion

As ABLK neurons express the putative Ilp7 receptor Lgr4 which is localized adjacent to Ilp7 puncta on Dp7 neurons (Fig. 24B), I speculate that the released Ilp7 peptide acts on a fast time scale to mediate noxious light responses. This suggests that context-dependent acute release of Ilp7 and proximity to Lgr4 directly aid the fast decoding of light avoidance responses. Fast peptide actions from the intrinsic Dp7 neuromodulator may confer an advantage to circuits like innate nociceptive systems, which require fast processing to generate modality-specific escape behavior.

4.1.7 Ilp7-Lgr4 signaling mediating escape behaviors might be a conserved across species

Lgr4 and the recently characterized Lgr3, which signals via Ilp8, are homologous to the human Relaxin-family receptors (RXFP) 1/2 (Bathgate et al., 2013; Garelli et al., 2015; Gontijo and Garelli, 2018; Vallejo et al., 2015). Relaxin has a conserved role in escape behaviors, but their role in circuit function is poorly understood. Relaxin-3 has been shown to be involved in escape behaviors where it mediates inhibition of oxytocin neurons in the hypothalamus (Kania et al., 2017; Knobloch et al., 2012). Here, I show that the RXFP1/2 orthologue Lgr4 (reviewed in (Gontijo and Garelli, 2018)), which may be acting via Ilp7, is involved in light avoidance responses and behavior in the *Drosophila* larvae (Fig. 25). Given the high degree of similarity of circuit elements and conservation of GPCR signaling in *Drosophila* and in mammals (reviewed in (Gontijo and Garelli, 2018)), relaxin-type signaling analogous to Ilp7-Lgr4 may also be relevant for circuit computations in higher animals.

4 Discussion

4.2 Neuropeptidergic control of fructose foraging behavior in *Drosophila melanogaster* larvae

All animals exhibit innate feeding behaviors. Nonetheless, the regulatory mechanisms of feeding and its neural networks are still incompletely understood. Using behavioral assays and EM reconstruction, I showed that Dp7 neurons are a critical component of the fructose foraging circuit, and they act as a break on the foraging circuit to limit foraging behavior (Fig. 28A).

In addition, I also found that Dp7-derived Ilp7 (Fig. 28B) also acts similarly to Dp7 neurons in limiting fructose foraging in the larvae. Conversely to Ilp7, sNPF function (Fig. 27B) is required to promote fructose foraging behavior in the larvae. I also showed that Dp7 neurons are linked to several feeding related neurons in the SEZ and in the PC regions of the larva (Fig. 29). The SEZ and the PC regions are involved in feeding decisions and in the control of feeding behaviors, respectively (Hückesfeld et al., 2016; Miroshnikow et al., 2020; Rulifson, 2002), and may thus represent sites for Dp7, where its peptide Ilp7 is modulating foraging and probably also feeding decisions.

4.2.1 Dp7 neurons limit fructose-foraging behavior in the larvae

Sweetness is a taste modality which is associated with a sense of pleasantness and is an appealing food source. I show here that fructose, a sweet sensing compound is attractive to the *Drosophila* larvae (Fig. 27A) as in (Almeida-Carvalho et al., 2017). Several brain regions in *Drosophila melanogaster* have been associated with feeding regulation including distinct subsets of neurons residing in the SEZ, the PC and the MB (Hückesfeld et al., 2016; Lewis et al., 2015; Miroshnikow et al., 2020). Fructose is sensed by the Gr43a expressing neurons that send its axonal projection to the SEZ (Mishra et al., 2013). Distinct taste modalities also select for distinct neural activation in the SEZ suggesting modality-specific circuits for integration of feeding decisions (Harris et al., 2015). In flies, specific dopaminergic neurons in the PAM cluster of the mushroom body were shown to respond to sucrose stimulation and to modulate taste-odor associative reward (Liu et al., 2012). In the larva, Hugin-expressing neurons in the PC control food aversion towards bitter caffeine substance (Hückesfeld et al., 2016).

4 Discussion

Here, I identified an involvement of Dp7 neurons, whose somata reside in the VNC region of the larvae, in fructose foraging responses in the larvae. Silencing of Dp7 neurons in the larvae caused an increase in fructose preference suggesting that Dp7 neuron function limits foraging towards fructose (Fig. 28A). Limiting foraging behavior is interesting as it indicates that even in the almost constantly feeding larva there is still a need for the larvae to balance food intake. This may be because aside from foraging the larvae also need to engage in other locomotive actions, which include sleeping (Szuperak et al., 2018) or escape from noxious stimuli (reviewed in (Im and Galko, 2012)) or predators (Hwang et al., 2007). Hence, neurons like Dp7 may serve as a break onto the feeding circuit allowing the larvae to commit to other actions. Similarly, in mammals, feeding thresholds are maintained by neuronal subsets in the hypothalamus, which plays a particular role in preventing excessive food intake. Specifically, the mechanisms involve global insulin and leptin signals which activate the anorexigenic POMC neurons, thus inhibiting the activity of the orexigenic NPY and AgRP neurons, ultimately leading to suppression of feeding behaviors (reviewed in (Baskin et al., 1988; Cowley et al., 2001; Schwartz et al., 2000; Sternson, 2013)). As the appetitive value of fructose is conserved in both humans and flies (Yarmolinsky et al., 2009) there might be conservation in the architecture of neural networks and the neuromodulatory mechanisms regulating it.

4.2.2 Dp7-derived Ilp7 neuropeptide limits fructose foraging behavior in the larva

Feeding is a complex behavior and under extensive neuromodulatory control, both in simple as well as higher order organism (Murphy and Bloom, 2006; Pool and Scott, 2014). In flies, at least 12 different neuropeptides control feeding behaviors (reviewed in (Pool and Scott, 2014)). Although relatively distant in the phylogenetic tree, flies and mammals share several peptide orthologues that regulate feeding behaviors, probably due to its pivotal role in sustaining vital metabolic actions. Insulin-like peptides have a well-documented role in maintaining sugar homeostasis in both mammals and flies (reviewed in (Fernandez and Torres-Alemán, 2012; Pool and Scott, 2014)).

4 Discussion

The IPCs, which are in the PI region of the larval PC, have an analogous role to the mammalian pancreatic beta cells. Genetic ablation of IPCs producing *Ilp2* resulted in significantly higher levels of blood sugar in the hemolymph of the larvae, which was rescued by ectopic expression of *Ilp2*, linking *Ilp2* deficiency to a diabetic type phenotype (Rulifson, 2002). *Ilp2* was further shown to act on the insulin receptor expressed in AKH cells.

While the IPCs derived *Ilp2* directly influences sugar metabolism, I show here that Dp7-derived *Ilp7* neuropeptide limits fructose foraging behavior in the larvae (Fig. 28B). Dp7 neurons send their axons to the PI region, where they make synaptic and maybe peptidergic connections to IPCs (Fig. 29B). A pair of glucose-sensing neurons was shown to promote the release of *Ilp2* from the IPCs when sugar levels in the haemolymph were high (Oh et al., 2019). Thus, similarly to the glucose sensing neurons which exerts some control over the activation of the IPCs in flies in regulating glucose homeostasis, it may also be possible that Dp7 may also function upstream of the IPCs to suppress consummatory feeding behaviors.

Insulin is produced by the pancreatic beta cells in mammals to systemically regulate sugar metabolism in various organs including the brain, which expresses the insulin receptor at high levels (Fernandez and Torres-Alemán, 2012; Prentki et al., 2013; Rorsman and Braun, 2013). IPCs have also been detected in dissociated brain cultures of fetal rodents suggesting that insulin can also be produced by neurons in mammals (Clarke et al., 1986). Whether *Ilp7* also has a hormonal role in maintaining sugar homeostasis in *Drosophila* remains to be examined. If this possibility does exist it may be through Dp7 innervation of the posterior *Ilp7* neurons (Miguel-Aliaga et al., 2008) which may subsequently secrete *Ilp7* into the gut to eventually get into the systemic circulation.

Flies and mammals share several peptides orthologues that regulate feeding behaviors. For example, both leptin and its fly analogue unpaired 1 are involved in suppression of feeding. In flies, knockdown of unpaired 1 resulted in increased attraction to food cues, increased food intake and weight. This effect occurs through the inhibitory function of *upd1* on the Domeless receptor in the orexigenic NPF neurons (Beshel et al., 2017).

4 Discussion

Similarly, in mice, leptin acting through the Leptin receptor hyperpolarizes NPY neurons that in turn disinhibit the anorexigenic POMC neurons (Cowley et al., 2001). To date, the analogue of Ilp7 is not known in vertebrates although several Ilps are also found in vertebrates (reviewed in (Nässel and Broeck, 2016; Wu and Brown, 2006)). As feeding is a behavior which is consistent across species it may be that an analogous peptide to Ilp7 can potentially regulate fructose feeding behaviors in higher order animal.

4.2.3 Dp7 neurons connect to several feeding-related neurons

Through EM mapping of the Dp7 connectome I identified that several synaptic partners have closely knit associations with feeding behavior in the larvae. Dp7 receives input from a subset of gustatory neurons from the AN-bundle (Fig. 29D). Gustatory AN-derived neurons play a role in feeding responses in the larvae including being involved in pharyngeal pumping responses (Schoofs et al., 2014).

While the connectivity from Dp7 to AN-bundle derived neuron is weak (Fig. 11E), it may still be possible that Dp7-derived Ilp7 neuropeptide, which is involved in limiting foraging, acts on the AN neuron or their downstream circuit to prevent food consumption. Dp7 neurons also connect to three subsets of Hugin neuropeptide-expressing neurons, Hugin-VNC, Hugin-RG and Hugin-PC (Appendix 1), which are involved in selection of motor output for feeding aversion (Schoofs et al., 2014). Hugin-PC has a known role in feeding aversion to unpleasant bitter caffeine substances (Hückesfeld et al., 2016). Ilp7 mutant larvae exhibited increased foraging responses not only to fructose, but also to glucose (Fig. 27C), suggesting that Ilp7 might be a general suppressive signal for foraging. In line with this, it is possible that Dp7 neurons may negatively regulate foraging signals through Hugin-PC neurons, which may eventually limit foraging.

4 Discussion

4.2.4 Dp7 neurons and Ilp7 possibly regulate local feeding networks in the SEZ region

In mammals, the hypothalamus is the region of the brain, which integrates both top-down and bottom up information to regulate a broad spectrum of behaviors, including feeding, mostly by peptidergic modulation (Morton et al., 2006; Williams et al., 2001). In *Drosophila*, the SEZ is the integration and decision making center for several systems including feeding, visual, nociceptive, olfactory and anemotaxis (Berck et al., 2016; Hückesfeld et al., 2016; Inagaki et al., 2015; Jovanic et al., 2019; Larderet et al., 2017; Miroshnikow et al., 2020; Tastekin et al., 2015). As a result, the SEZ in *Drosophila* has been compared to the mammalian hypothalamus especially in regard to generating feeding decision (Miroshnikow et al., 2020). Interestingly, Dp7 neurons receive inputs from gustatory neurons within the SEZ region. Thus, it may be possible that the receiving partners of Dp7 and Ilp7 neuropeptide might reside in the SEZ region itself to limit foraging.

It would thus be very interesting to map the site of action of Ilp7 on the fructose foraging circuit, which is itself unresolved downstream of the AN-bundle-derived gustatory neuron. In contrast to light avoidance, where I found that Lgr4 acts as the cognate receptor for Ilp7 to induce light avoidance behavior, Lgr4 does not appear to play a role in fructose foraging behavior (data not shown). An alternate receptor for Ilp7 in modulating fructose foraging is the IR which is the main receptor for most of the *Drosophila* Ilps (reviewed in (Nässel and Broeck, 2016)). In fact, both Ilp7 and IR have been shown to share a functional role in promoting tracheal growth in response to nutrition in *Drosophila* (Linneweber et al., 2014) suggesting a functional link between Ilp7 and IR. As IR has a wide expression and influences various functions including growth and developmental progression (reviewed in (Wu and Brown, 2006)), cell type specific and temporal silencing of IR may be a most appropriate way to test for the function of the receptor in fructose foraging behavior. To this end it would be interesting to identify IR-expressing candidate neurons, where Ilp7 may act on. Genetic mapping to report Ilp7 receptor action in vivo can possibly be a way to identify Ilp7-targeted downstream neuron. One approach might be by generating a Tango map.

4 Discussion

TANGO mapping was successfully applied to report increased Dopamine signaling in gustatory neurons during starvation in flies (Inagaki et al., 2012). Similarly, a Tango map for Ilp7-IR can be generated following the methods as in (Barnea et al., 2008). The Ilp7-IR Tango mapping can be directed to the Gr43a fructose sensing neurons in the larvae (Mishra et al., 2013) or their potential downstream connected partners (Fig. 29E) to probe whether Dp7 and the selected neuronal partner function via Ilp7-IR.

4.2.5 sNPF neuropeptide promotes fructose foraging behavior in the larvae

sNPF and the Ilp2/3 peptides share a common physiological role in modulating growth and metabolism in the larvae. sNPF-producing cells and the neighboring IPCs express the sNPF receptor (sNPFR). sNPFR activation in IPCs triggers ERK-regulated transcription of Ilp2 and Ilp3 (Lee et al., 2008). Several other neurons including a pair of glucose sensing neurons as well as Taotie neurons can control IPCs function (Oh et al., 2019; Zhan et al., 2016).

In the foraging assays, I found that sNPF is required for fructose preference (Fig. 27B), similarly to a study which identified sNPF expressing neurons in the brain lobes that promote foraging behaviors on glucose (Wu et al., 2003). This suggests that sNPF has a general role for promoting exploratory behavior towards appetitive sugars in the larvae. Overexpression of sNPF in IPCs led to a decrease of carbohydrates in the hemolymph and sNPF exerts a regulatory function of Ilp2 and 3 expressions to regulate body size (Lee et al., 2004). In my assay, I also observed that Ilp7 and sNPF seem to exert opposing effects on foraging. While Ilp7 seems to inhibit foraging, sNPF on the other hand has more of a facilitating role on foraging (Fig. 27B). However, further experiments are required to confirm the functional role of sNPF on foraging and to identify the neuronal substrates. Nonetheless, it is tempting to speculate that sNPF may be exerting modulatory control on Ilp7 production or function to control foraging behaviors.

4 Discussion

4.3 Context and state-dependent adaptation of innate behavior

The physical world is multi-sensory, which animals perceive using different sensory systems. Therefore, daily life behavioral decisions most likely rely on integration of multisensory stimuli occurring simultaneously in time and space, which requires selective filtering of significant events (Ghosh et al., 2017; Stein and Stanford, 2008). Additionally, the internal state of the organisms is also integrated into decision making processes to produce meaningful behaviors, which promote survival and fitness (Grunwald Kadow, 2019).

However, it is unclear how the brain can integrate a multisensory context with internal state to achieve plasticity in innate behaviors. To address this question, I designed a behavioral paradigm where the animals had to make a behavioral choice based on their internal state and integrated context (Fig. 30B). The assay consisted of an arena with 2 compartments, one containing nutritive and appetitive fructose in light and another containing plain agar (2%) in darkness. Using this paradigm, I showed that larvae avoid light despite the presence of fructose in the fed state, but this behavior is switched to foraging on fructose in the presence of light in starved animals (Fig. 30F). This switch is the result of the larvae tolerating light (Fig. 31) in a multisensory context with fructose, presumably due to the hunger drive of starved animals outweighing the need for light avoidance. This behavioral switch occurs through the action of Dp7 neurons and its neuropeptide Ilp7 (Figs. 32D, E, 33C, D), which positively regulate the light avoidance circuit and negatively affect the fructose foraging circuit. The multisensory context and internal state are thus likely integrated on Dp7 neurons, which malleably modulate circuit actions through peptidergic control to select for either light avoidance or fructose foraging behavior in the presence of light.

4.3.1 Internal state does not influence uni-sensory light avoidance or foraging behaviors

Behavioral decisions in response to a uni-sensory context are often state dependent allowing the animal to attune its current sensory experience to its physiological needs (Grunwald Kadow, 2019; Murakami et al., 2016; Root et al., 2011).

4 Discussion

Drosophila responses to the aversive odors menthol and geranyl acetate were reduced in starved states compared to fed states. These odors are sensed by distinct subsets of olfactory neurons which connect to the multiglomerular projection neurons (mPN). Upon starvation, serotonergic inputs activate an inhibitory neuron that blocks the activity of the mPN resulting in altered responses towards aversive olfactory odors (Vogt et al., 2020). Starvation also enhances olfactory sensitivity to food odors in flies. A global insulin signal is integrated in starved animals which increases the presynaptic activity of Or42b olfactory receptor neurons via sNPF signaling. Starvation ultimately leads to upregulation of the sNPF1 in the Or42b olfactory receptor neurons, which promotes food-odor driven foraging behaviors (Root et al., 2011). Rodents also display state-dependent changes towards odors (Murakami et al., 2016). Through a combination of electroencephalogram (EEG) to monitor sleep state and electrophysiology to monitor neuronal activity in the olfactory bulb neurons, Murakami and colleagues showed that the olfactory bulb neurons elicit robust spiking in awake but not in sleeping animals (Murakami et al., 2016).

Surprisingly, my results showed that internal state did not influence either innate light avoidance or fructose foraging behavior (Fig. 30D, E). Thus, while the hunger-state affects uni-sensory action selection to olfactory cues in *Drosophila* (Root et al., 2011; Vogt et al., 2020), it likely cannot be generalized to the gustatory cue fructose and noxious light in the larvae. Dp7 and Ilp7 neuropeptide function in light avoidance was unchanged in both sated and starved animals, indicating that internal state does not influence Dp7 and Ilp7 function in innate light avoidance behavior. (Figs. 9A, B, C, 32B, 33A). In the fed state, silencing of Dp7 neurons caused an increase in fructose foraging behavior in the larvae, but starved larvae with Dp7 neuron silencing did not show an increase in fructose foraging behavior (Figs. 28A, 32C). As the distribution of the controls for the starved larvae with Dp7 neuron silencing were slightly higher than wild type data (Figs. 32C, 30E), it is possible that significant differences can be reached if the starved controls distribution would be like for starved wild type larvae. This discrepancy in the distribution of the starved controls for Kir2.1-induced Dp7 neuron silencing (Fig. 32C) may be due to the genetic background and to be fully conclusive the experiments need to be repeated.

4 Discussion

4.3.2 A behavioral paradigm integrating contextual cues with the larval internal state

Multisensory integration of sensory modalities is an effective mechanism that endows the brain with increased speed, precision and accuracy for the generation of a behavioral outcome to particular sensory stimuli (reviewed in (Van Atteveldt et al., 2014; Murray et al., 2016; Shams et al., 2011)). Simultaneous integration of visual and auditory cues for example elicits a super-additive response in neurons in the superior colliculus of cats, while presentation of the unimodal cues elicits additive responses (Alvarado et al., 2007). Multisensory contexts with similar valences are moreover beneficial for information processing and retrieval of previous formed associative memory (Murray et al., 2005). Yet behavioral decisions are not only made based on the absolute values of contextual alternatives, hence factors like internal state have to be considered in behavioral paradigms (Ennedy et al., 2014). Thus, for my behavioral paradigm I incorporated context and state dependency, similar to the “go – no-go” assay (Frederick et al., 2011), but associating the positive cue fructose with a “no-go” light arena vs. a “go” darkness arena. Fed and starved animal likely compute their behavior via a cost-value over value calculation, where they integrate the external context with their internal feeding state to produce a favourable behavioral outcome.

4.3.3 *Drosophila* larvae integrate contextual cues with internal state to generate innate adaptive behaviors

Using my context and state-dependent assay, I found that when light and fructose are presented to fed larvae over darkness, the animals preferred light avoidance over foraging behavior (Fig. 30F). Starved larvae in contrast to fed larvae switched their behavior to foraging on fructose at the expense of light avoidance (Fig. 30F). Analogously to my data, but done in the context of inflammatory pain, a study in mice showed that in the hunger state the perception of inflammatory pain in animals is diminished to prioritize feeding. The behavioral response of reduced inflammatory pain under hunger state occurs through the action of AgRP neuron-derived NPY onto hindbrain neurons expressing NPY receptor (Alhadeff et al., 2018).

4 Discussion

Another study in mice showed that in a multisensory context of two appetitive stimuli, an attractive food odor and an attractive pheromone, fasted mice preferred the food odor over the pheromone. In contrast, fed mice displayed a similar preference for either of the attractive cue. The selection for the attractive food odor in fasted mice occurred through activation of the AgrP neurons and NPY action on thalamic NPYR5 expressing neurons (Horio and Liberles, 2021). My data and the related mouse studies (Alhadeff et al., 2018; Horio and Liberles, 2021) seem to suggest that hunger state does indeed favor a behavioral response towards feeding, independent of whether it has to be prioritized over another attractive or an aversive stimulus. Thus, in a multisensory context and under food deprivation, foraging and feeding are promoted to neutralize the hunger drive while responses towards both pleasant and unpleasant stimuli are suppressed. My data reflects this point as I found that starved animals prioritize foraging in a noxious light compartment rather than being in a dark environment (Fig. 30F).

In other words, the larvae adapt to the noxious light, which I showed with a tolerance assay, where starved animals were evenly distributed on a fructose with or without light (Fig. 31C). Similarly, to my results, but in the context of olfaction, when both the appetitive odor vinegar and the repulsive odor carbon dioxide were presented to flies, starved but not fed flies dampened their aversive response to CO₂. This response was mediated through the action of the PAM dopaminergic neurons which provide inhibitory inputs onto the MBON responsible for driving aversion responses towards CO₂ (Bräcker et al., 2013; Lewis et al., 2015). It thus seems that in a multisensory context with conflicting sensory signals, the internal state can alter aversive behaviors to promote foraging and feeding to return the hunger drive of the animal to its set point.

Collectively my data suggest that the selection of approach vs. avoidance in a context of conflicting sensory signals favours the equation rule of plus (indicating a positive stimulus) and minus (indicating a negative stimulus) is equal to minus (indicating avoidance towards the negative stimulus) in case of an unaltered internal state (Figure 37). This gives rise to the selection of light avoidance, which presents an advantage to a fed animal.

4 Discussion

However, upon starvation, foraging behavior prevails over escape from light, together with adaptation to light to satisfy the increased hunger drive of the animal (Fig. 37).

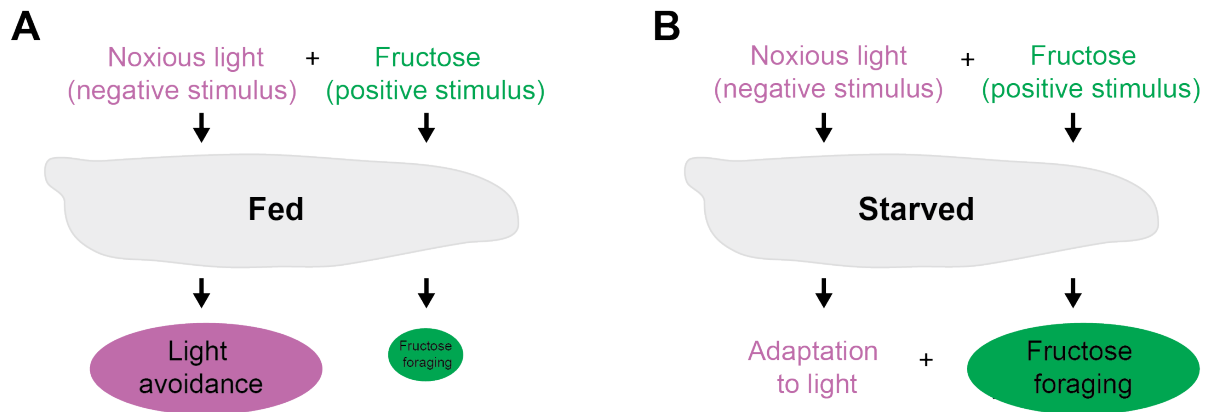


Figure 37: The larvae integrate contextual cues and internal state to decide for an appropriate behavioral response. A. Contextual noxious light and fructose which are aversive and attractive stimuli respectively are integrated in fed larvae to favor for light avoidance over foraging behavior. **B.** In the starved state, the larvae switch to fructose foraging and adaptation to noxious light behavior.

4.3.4 Dp7 neurons mediate a context and state-dependent behavioral switch

The behavioral switch from light avoidance in the fed state to foraging under light in the starved state suggests that the circuits underlying innate light avoidance and foraging may intersect at some point, probably on a hub neuron which can gate distinct innate or adaptive behavioral responses. Across organisms, hubs of convergence for multiple sensory modalities can be found, like the mushroom body in *Drosophila*, the RMG neuron in *C.elegans* (Macosko et al., 2009), and the basolateral amygdala complex (BLA) as well as the thalamus in rodents (Namburi et al., 2015; Salay et al., 2018). These hubs form computational units, which use activity and peptidergic mechanisms to generate different behavioral responses towards similar or distinct modalities. The MB in *Drosophila* is a large hub dedicated mostly to the formation of associative olfactory memories (Bräcker et al., 2013; Eschbach et al., 2020; Krashes et al., 2010; Lewis et al., 2015).

4 Discussion

It contains approximately 2000 Kenyon cells where inputs from diverse modalities including those from olfactory and gustatory circuits converge, the MB input neurons (MBIN) which provide teaching signals, and the MBON which encode valence and guide learned behavioral outcomes (reviewed in (Heisenberg, 2003; Thum and Gerber, 2019)). In addition, the MB also contains the peptidergic Dopamine (DANs) and Octopamine (OANs) releasing neurons which receives inputs from Kenyon cells and outputs onto both the Kenyon cells and the MBON (Eichler et al., 2017). The cells of the mushroom body thus function together as a hub to specific contextual signals to guide learned behaviors.

Mice respond to visual threats in the form of dark and rapidly expanding looming stimuli from above by freezing or escape. Depending on the arousal mode of the animal this behavior can be adapted to a lower saliency tail rattling behavior. The adaptive behavior exhibited by the mice were shown to be under the control of hub neurons in the ventral midline thalamus (vMT), which integrates the arousal state as well as sensory inputs from the superior colliculus and the hindbrain. Optogenetic activation of the vMT to the medial prefrontal cortex (mPFC) pathway promoted rattling behavior while activation of the vMT to the BLA pathway increased freezing behavior (Salay et al., 2018). The BLA, a region for emotional processing also functions as a hub in rodents. Distinct populations of neurons in the BLA undergo synaptic plasticity in response to stimuli of positive or negative valence that lead to encoding of either rewarding or fearful memories, respectively (Namburi et al., 2015).

In contrast to the above-mentioned hubs consisting of a population of neurons, I show here that only one pair of Dp7 neurons integrate and mediate context and state-dependent behavioral plasticity. Fed larvae where Dp7 neurons were silenced showed a switch from light avoidance to foraging behavior despite light exposure (Fig. 32D), a phenotype mimicking wild type starved larvae (Fig. 30F). No significant differences from controls were seen in starved Dp7 silenced larvae (Fig. 32E). It thus seems that Dp7 neurons activity is tuned by the context and internal state of the animal. Fed larvae which are exposed to light and fructose probably have increased Dp7 activity, which drives the light avoidance circuit, but also simultaneously inhibits the foraging circuit such that light avoidance is prioritized over foraging behavior.

4 Discussion

Conversely, under starvation, it is probable that activity of Dp7 neurons is dampened which would dampen of light avoidance behavior and promote fructose foraging behavior. The hub function of Dp7 neuron is structurally similar to the *npr-1* expressing RMG neuron in *C.elegans* that receives multiple sensory inputs and drives aggregation and acute octanol avoidance behavior (reviewed in (Bargmann, 2012; Macosko et al., 2009)). However, the RMG neuron controls behavior not only through chemical synapses and neuromodulation, but also through electrical synapses (reviewed in (Bargmann, 2012)) which is a common mechanisms in the worm (reviewed in (Jin et al., 2020)). In the case of Dp7 neurons, a behavioral outcome is unlikely to be elicited through electrical synapses, as no gap junction were detected between Dp7 neurons and its synaptic partners in the EM data set (data not shown). The generation of distinct innate behaviors by Dp7 neurons may thus be exclusively driven through chemical synapses and neuromodulation.

4.3.5 Neuromodulatory control of internal state-dependent innate behaviors

I showed that light avoidance, adaptation to light and fructose foraging behaviors can be plastically selected depending on the context and internal state. It therefore seems that the circuits underlying innate light avoidance and fructose foraging are non-static but rather dynamic and their output is adaptable to context and state. Neuropeptides are known to add plasticity to neuronal circuits to promote specific behavioral states. Moreover, neuropeptides also facilitate multisensory processing and are drivers of internal state-dependent behaviors (reviewed in (Bargmann, 2012; Destexhe and Marder, 2004; Ghosh et al., 2017; Sayin et al., 2018)). In *C.elegans* for example, the Neuropeptide receptor gene (*npr-1*) expressed in RMG neurons controls both aerotaxis and aggregation behavior. Aggregation requires low *npr-1* activity, while aerotaxis requires state-dependent high *npr-1* activity, which selectively silences the gap junction circuits while sparing the chemical circuits (Macosko et al., 2009).

Neuropeptides can also add plasticity to networks by remodeling of circuits configurations in a context-dependent manner.

4 Discussion

Such a role of neuropeptides was demonstrated in *C.elegans*, whereby during high salt stimulation the sensory ASE neuron releases insulin-like peptide 6 (INS6) in a transcription independent and acute manner that acts through the cognate receptor dauer diapause stage 2 (DAF-2) in olfactory neurons, which then function as interneurons. Conversely, under low salt configuration INS6 is not secreted, and the olfactory sensory neuron remains in its sensory configuration (Leinwand and Chalasani, 2013).

Here, I show that Dp7 neuron derived Ilp7 simultaneously tunes two innate circuits, namely for noxious light and fructose foraging, in an opposite manner. In fed larvae, Ilp7 modulation facilitates the light avoidance circuit, while simultaneously putting a break on the foraging circuit (Fig. 33C). This results in a preference for innate light avoidance behavior over foraging behavior in the fed larvae. The behavioral preference for fructose foraging over light avoidance was similar in both fed and starved larvae when Dp7 neurons were silenced (Fig. 33C) suggesting that Ilp7 may help in maintaining the fed larvae in a behavioral state which favors light avoidance over foraging behavior.

Moreover, it seems that Ilp7 modulation sets up a network configuration for the noxious light and the fructose sensing circuits to enable the animal to achieve behavioral plasticity under a multisensory context with altered feeding drives. In addition, I also obtained some interesting preliminary findings, which indicate that sNPF may also work together with the Ilp7 neuropeptide in mediating the context and state-dependent behavioral switch. In a multisensory context of light and fructose, where the larvae have equal potency to generate light avoidance or foraging behavior, Ilp7 neuropeptide is likely required to prioritize light avoidance behavior in fed animals, while sNPF potentially promotes foraging behavior in noxious light in starved animals. In the unisensory light context, sNPF mutants did not have a role in regulating light avoidance (Fig. 9B), while in the unisensory fructose context, sNPF regulates fructose foraging behavior in a positive manner (Fig. 27B). In the context and state-dependent assay, sNPF mutants displayed not only a reduced preference for fructose foraging, but more likely an aversive response to fructose and light (Fig. 34B).

4 Discussion

These data bring to light a new point that sensory inputs for light and fructose information are probably converging within the larval network. This association of light and fructose is highly probable as light and fructose coexist in the natural environment of *Drosophila melanogaster* and they can often be seen feeding on rotten fruits in bright tropical environments. Thus, during starvation and in the multisensory context, sNPF may exert a functional role in the light avoidance circuit by tuning down its action to facilitate fructose foraging behavior. However, for the sNPF data to be conclusive, additional mutants of sNPF and cell type-specific manipulation needs to be tested in the context and state-dependent assay.

Whether sNPF derived from Dp7 neurons triggers this behavior is still unclear. If Dp7-derived sNPF is involved, it may be mediating contextual plasticity by connecting to the memory centre for associative memory in the larvae, the MB. A possible neural pathway from Dp7 to the mushroom body is via the Bamas neurons, which is downstream of Dp7 and connects to dopaminergic neurons MBE1c providing input to the mushroom body (Fig. 35C, D). Furthermore, Bamas neurons also receive inputs from the gustatory neurons (Fig. 35C, C', D), which also include the weakly connected gustatory neurons connections to Dp7 neurons. This implies that fructose or other gustatory information could be integrated in Bamas neurons via direct presynaptic inputs from the gustatory neurons and Dp7 neurons pass on light information to the Bamas neurons which could integrate both signals and pass it to the MBE1c which potentially then transmit the inputs to the MB DANs.

The Bamas pathway may be worth investigating in terms of which subset of DANs it connects to, which may be either the PAM cluster mediating appetitive memory formation or the protocerebral posterior lateral (PPL) cluster mediating aversive memory formation (reviewed in (Das et al., 2016)). Subsequently, the outputs of the DANs to the mushroom body output neurons may also be inspected which may shed more light into the circuits influencing fructose foraging and adaptation to light behavior in starved animals. I speculate that sNPF may be acting at any level from the Bamas neurons to the MBON to allow retrieval of an associative link between light and fructose in starved larvae.

4 Discussion

4.3.6 Neuronal and peptidergic framework for achieving innate behavioral plasticity

Dp7 and Ilp7 peptides play key roles in mediating the context and state-dependent behavioral switch from light avoidance in the fed state to foraging and adaptive behavior to light in the starved state. Dp7 neurons receive inputs from the light sensing and possibly also gustatory sensing neurons, relating to a potential bottom-up multisensory integration in this hub neuron (Fig. 38). In conjunction with receiving contextual multisensory inputs, Dp7 neurons possibly also receives input from an internal state sensor (Fig. 38).

This suggests that Dp7 may function as a context and state coincidence detector. Co-incidence detection is a quite well documented mechanism which facilitates neuronal activity upon simultaneously presented sensory inputs from different modalities (Chatzigeorgiou and Schafer, 2011). Co-incidence activity occurs in the rodent somatosensory cortex. Long term potentiation (LTP) produced in layer 2/3 of the somatosensory cortex was shown by electrophysiology and whole cell recording to be generated by coincident activity derived from rhythmic whisker stimulation as well as from synaptic activity from thalamic networks that convey inputs about contextual events (Gambino et al., 2014).

In my context and state-dependent assay, the activity from the fructose sensing neuron and v^{td2} and C4da light sensing neurons may coincide in Dp7 neurons, whose activity level might further be set in resonance with the internal state of the animal. Based on the involvement of Dp7 neurons and Ilp7 peptide in promoting light avoidance over foraging in the fed state, it is likely that the activity of Dp7 neurons is further promoted by an internal state sensor (Fig. 38). One may speculate that increase activity of Dp7 would result in increased Ilp7 peptide release which would facilitate light avoidance and dampen fructose foraging behavior, the observed phenotype in fed animals (Fig. 30F). Albeit it is likely that the inputs from the internal state sensor onto Dp7 may be excitatory, it may nonetheless also be inhibitory (Fig. 38). Different internal state sensors, like sensors of either nutritive sugars or starvation states may be converging onto Dp7 neurons. *Drosophila* larvae have a metabolic internal fructose sensor, the Gr43a positive neurons in the brain, which sense circulating nutritive fructose levels (Mishra et al., 2013).

4 Discussion

I did not find any connection either from the connectome of Dp7 neurons or from Syb-GRASP experiments between these cells (data not shown). Nonetheless, it is possible that an intermediate neuron may relate state information from the internal sensors, the Gr43a neurons to Dp7 neurons, whose identity remains to be defined. Adult flies have, in addition to the internal Gr43a neurons, another internal sensor consisting of DH44 neurons, which sense circulating glucose levels through a hexokinase receptor and release of DH44 neuropeptide (Dus et al., 2015). Our recent RNA sequencing data from Dp7 neurons (data not shown) indicates that they express the DH44 receptor (DH44R) suggesting Dp7 neurons are responsive to DH44 levels. Thus, it is possible that DH44 neurons are peptidergically controlling Dp7 neuron activity via DH44-DH44R action depending on the nutritive status of the larvae.

Top-down integration of internal state is a well-documented process, which has been proposed to modulate multisensory processing in vertebrates (reviewed in (Choi et al., 2018)). Thus, if DH44 acts on DH44R in Dp7 neurons during the context and state dependent behavior, this would correlate with a top-down control from the internal sensor to Dp7 neurons. It would also suggest that the top-down flow of information from the internal sensor to the Dp7 hub neurons helps the latter to decode integrated multisensory inputs to generate innate and adaptive behaviors.

During the starved state in the multisensory context, a possible hypothesis may be that the activity of Dp7 neurons and Ilp7 is dampened by a metabolic internal state sensor to dampen light avoidance and promote foraging behavior (Fig. 38). However, as the hunger state alone is not sufficient to inhibit light avoidance responses (Fig. 30D), the activity level of the foraging circuit in the presence of fructose and light could impinge on the activity status of Dp7 neurons to prevent Ilp7 peptide release and action on ABLK neurons. How the fructose foraging circuit impinges on the light avoidance circuit such that light avoidance behavior is dampened in the context of fructose in starved larva remains to be determined.

4 Discussion

The inhibition of Dp7 neurons in the starved animals may be global or local. Kir2.1 mediated silencing of Dp7 neurons totally blocked ABLK responses to UV light (Fig. 21A, B), thus global inhibition may potentially block the activity of the downstream ABLK neurons in the light avoidance circuit, which can possibly account for dampening of light avoidance behavior and preference of fructose foraging behavior. Local inhibition by the internal sensor may possibly happen in the SEZ region where the neurons involved in regulating feeding behavior resides. The inhibition in the SEZ region would potentially prevent Ilp7 peptide release at that site, thus enabling the fructose foraging circuit to be activated to promote fructose foraging behavior. As I already established imaging of Ilp7 peptide release from Dp7 neurons in response to light, the next step would be to monitor somatic Ilp7 release in response to a combination of light and fructose in starved and fed larvae. The hypothesis would thus be that in starved larvae, there will be retention of Ilp7 in Dp7 neurons as compared to fed animals if peptide release is globally affected. If Ilp7 peptide release is locally inhibited in the SEZ, it is possible that starved but not fed animals exposed to light and fructose will show reduced local Ilp7 release.

Collectively my data indicates that the activity of Dp7 neurons and its neuropeptide Ilp7 reorganizes circuit functions and confers some level of plasticity towards the execution of innate behaviors. Such a flexible network configuration inevitably confers an animal with the advantage to best cope with both, their changing internal state and their immediate external context.

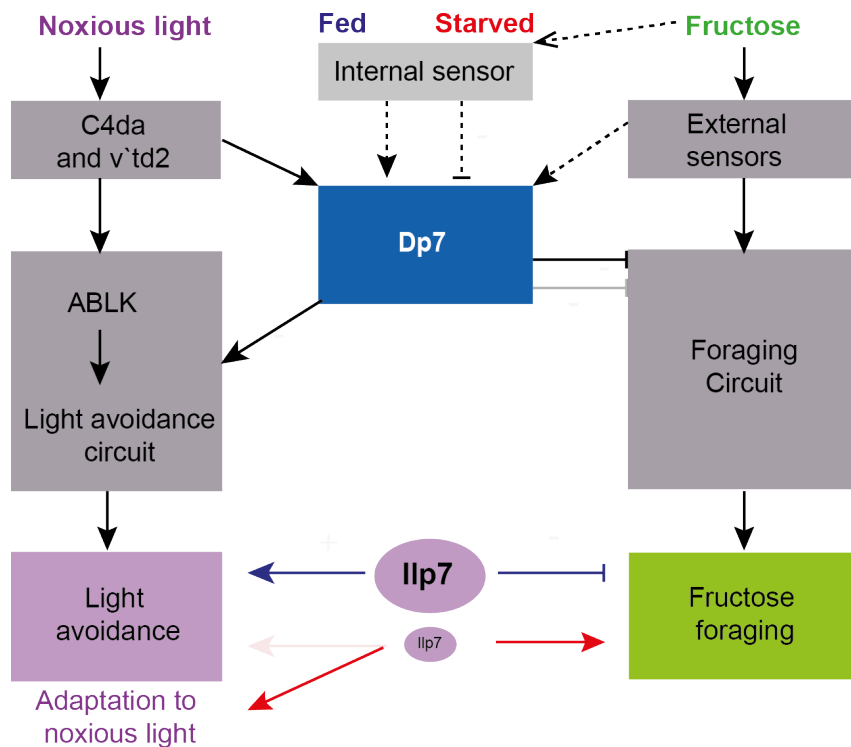


Figure 38: Neural framework for the context and state dependent behavioral switch In the fed state, Dp7 neurons receive noxious light inputs from C4da and v`td2 neurons. Activation of Dp7 neurons results in release of Ilp7 neuropeptide, which promotes light avoidance behavior (blue excitatory arrow) and suppresses foraging behavior (blue inhibitory arrow). Starved larvae show a preference for fructose foraging with adaptation to light behavior. This may be possible due to limited release of Ilp7 peptide which removes the break from the foraging circuit (subdued black inhibitory arrow), giving rise to fructose foraging behavior (red arrow). At the same time, reduced Ilp7 dampens light avoidance behavior (subdued red arrow) leading to adaptation to noxious light (red arrow). Black arrow indicates inputs in both fed and starved state. Dotted arrows indicate not yet tested hypothesized connections.

5 SUMMARY

Innate behaviors regulate a large degree of our daily actions including feeding and escaping from noxious stimuli. Except for reflex actions, innate behaviors are not always static and can be flexibly and adaptively tuned to the animal's current sensory context and internal state. Neuromodulators including neuropeptides are known to be key components involved in behavioral plasticity in animals. However, exactly where and how they act on innate circuits to regulate adaptive behaviors depending on context and internal state is not well understood. *Drosophila melanogaster* larvae have a relatively simple nervous system but exhibit an array of innate behaviors and express conserved neuromodulators. I show here that two innate behaviors, namely noxious light avoidance, and fructose foraging, are driven by the action of a pair of central nervous system neurons (Dp7) and Insulin-like peptide 7 (Ilp7). Interestingly, Dp7 neurons and its peptide Ilp7 promote noxious light avoidance, but limit foraging behavior. I reconstructed the Dp7 neuron network at the synaptic level and showed that they receive extensive somatosensory as well as gustatory input and connect to downstream neurons related to feeding functions. In addition, I identified a local region in Dp7 neurons where noxious light is processed, likely via acute release of Ilp7 acting via the Lgr4 receptor expressed in connected downstream neurons. The identified peptidergic feedforward circuit may aid fast processing of light avoidance behavior. Moreover, I found that in the multisensory context of noxious light and fructose, hunger drives the prioritization for fructose foraging and adaptively tunes down light avoidance behavior. Conversely, sated animals preferred light avoidance to foraging behavior. I could show that this behavioral switch depends on Dp7 neuron function and its neuropeptide Ilp7. In fed animals, Ilp7 action activates the light avoidance circuit, but puts a break on the fructose foraging circuit. In starved animals, reduced Dp7 neuron and Ilp7 function likely drives fructose foraging behavior. Dp7 neurons thus act as hub neurons that integrate the sensory context in a bottom-up manner to tune avoidance and foraging. Overall, the identified Dp7 network allows the larva to adaptively respond to its internal state and external environment, which is a key function of circuits regulating adaptive behavior in all animals.

5.1 ZUSAMMENFASSUNG

Angeborene Verhaltensweisen regulieren einen großen Teil unserer täglichen Handlungen, einschließlich der Nahrungsaufnahme und der Vermeidung von schädlichen Reizen. Mit Ausnahme von Reflexen sind angeborene Verhaltensweisen nicht immer statisch und können flexibel an den aktuellen sensorischen Kontext und den inneren Zustand des Tieres angepasst werden. Neuromodulatoren, einschließlich Neuropeptide, sind Schlüsselkomponenten, die an der Plastizität des Verhaltens bei Tieren beteiligt sind. Es ist jedoch nicht vollständig bekannt, wo und wie sie auf angeborene Schaltkreise einwirken, um adaptives Verhalten in Abhängigkeit von Kontext und internem Zustand zu regulieren. *Drosophila melanogaster*-Larven haben ein relativ einfaches Nervensystem, zeigen jedoch eine Reihe angeborener Verhaltensweisen und exprimieren konservierte Neuromodulatoren. Ich zeige hier, dass zwei angeborene Verhaltensweisen, nämlich Lichtvermeidung und Fructose-Nahrungssuche, durch die Wirkung eines Paares von Neuronen des Zentralnervensystems (Dp7) und Insulin-like Peptid 7 (Ilp7) gesteuert werden. Interessanterweise fördern Dp7-Neuronen und ihr Peptid Ilp7 die Vermeidung schädlichen Lichts, limitieren jedoch das Futtersuchverhalten. Durch Rekonstruieren des Dp7-Neuronennetzwerk auf synaptischer Ebene zeigte ich, dass die Neuronen umfangreiche somatosensorische sowie gustatorische Eingaben erhalten und sich mit nachgeschalteten Neuronen verbinden, die mit Fütterungsfunktionen zusammenhängen. Zusätzlich identifizierte ich eine lokale Region in Dp7-Neuronen, in der schädliches Licht verarbeitet wird, vermutlich durch akute Freisetzung von Ilp7, das über den Lgr4-Rezeptor wirkt, der in den verbundenen nachgeschalteten Neuronen exprimiert wird. Die identifizierte peptidergische Feedforward-Schaltung kann die schnelle Verarbeitung des Lichtvermeidungsverhaltens unterstützen. Darüber hinaus stellte ich fest, dass im multisensorischen Kontext von schädlichem Licht und Fructose Hunger die Priorisierung für Fructose-Nahrungssuche vorantreibt und Lichtvermeidungsverhalten adaptiv abschwächt. Umgekehrt bevorzugten gesättigte Tiere die Vermeidung von Licht gegenüber dem Futtersuchverhalten. Ich konnte zeigen, dass dieser Verhaltenswechsel von der Dp7-Neuronenfunktion und ihrem Neuropeptid Ilp7 abhängt.

5 Summary

Bei gefütterten Tieren aktiviert die Ilp7-Aktion den Lichtvermeidungskreislauf, unterbricht jedoch den Fruktose-Nahrungskreislauf. Bei ausgehungerten Tieren führt eine verminderte Dp7-Neuron- und Ilp7-Funktion wahrscheinlich zu einem Fruktose-Futtersuchverhalten. Dp7-Neuronen fungieren somit als Hub-Neuronen, die den sensorischen Kontext bottom-up integrieren, um Vermeidung und Nahrungssuche zu optimieren. Insgesamt ermöglicht das identifizierte Dp7-Netzwerk der Larve, adaptiv auf ihren internen Zustand und ihre externe Umgebung zu reagieren, welches eine Schlüsselfunktion von Schaltkreisen ist, die das adaptive Verhalten bei Tieren regulieren.

6 ABBREVIATIONS

Abbreviation	Full name
#	number
A4	abdominal segment 4
ABLK	abdominal leucokinin neurons
aCC	anterior commissural derived cells
AD	activation domain
AEL	after egg laying
AgRP	agouti related peptide
AKH	adipokinetic hormone
AN-B2	antennal nerve bundle derived
BLA	basolateral amygdala
<i>C.elegans</i>	<i>Caenorhabditis elegans</i>
C1da	class 1 dendritic arborization neurons
C2da	class 2 dendritic arborization neurons
C3da	class 3 dendritic arborization neurons
C4da	class 4 dendritic arborization neurons
C4da	class 4 dendritic arborization neurons
Cadps	calcium- dependent secretion activator
cAMP	cyclic adenosine monophosphate
CATMAID	Collaborative Annotation Toolkit for Massive Amount of Image Data
CCT	corticotrophin-releasing factor neurons
CGRP	calcitonin-gene related peptide
CO ₂	carbon dioxide
CrzR	corazonin receptor
CSK	Cholecystokinin
DAF-2	dauer diapause stage 2
DANs	dopaminergic neurons
DBD	DNA binding domain
DH44	diuretic hormone 44
DH44R	Dh44 receptor
DnB	Down and Back neurons
DO	dorsal organ
Dp7	dorsal pair insulin-like peptide 7
DSK	drosulphakinin
EEG	electroencephalogram
EH	eclosion hormone
EM	electron microscopy
ES	external sensory
ETH	ecdysis triggering hormone
<i>for</i>	<i>foraging</i> gene
GABA	gamma-aminobutyric acid
GcaMP	genetically encoded fluorescent calcium indicator
GFP	green fluorescent protein
GMC	ganglionic mother cell

6 Abbreviations

GPCRs	G-protein coupled receptors
Gpr83	G-protein coupled receptor 83
Gr	gustatory receptor
Gr28b _c	gustatory Receptor 28b _c
Gr43a	gustatory receptor 43a
HA	human influenza hemagglutinin
Ilp2	insulin like peptide 2
Ilp7	insulin like peptide 7
<i>Ilp7^{ko}</i>	<i>Ilp7</i> knockout
Ilps	insulin like peptides
INS6	insulin-like peptide 6 in <i>C.elegans</i>
IP3	inositoltriphosphate
IPCs	insulin producing cells
IR	insulin receptor
Irs	ionotropic receptors
ISN	intersegmental nerves neurons
Kir2.1	inward rectifier potassium channel 2
L1	first instar larvae
L2	second instar larvae
L3	third instar larvae
LDCVs	large dense core vesicles
LED	light emitting diode
Lgr3	leucine rich G protein coupled receptor 3
Lgr4	leucine rich G protein coupled receptor 4
LHLK	lateral horn LK neurons
LK	leucokinin neurons
LTP	long term potentiation
M	molar
MAPK	mitogen activated protein kinase
MB	mushroom body
MBIN	mushroom body input neurons
MBON	mushroom body output neurons
mN	millinewton
mPFC	medial prefrontal cortex
mPN	multiglomerular projection neurons
NMDA	N-Methyl-D-aspartic acid or N-Methyl-D-aspartate
NMJ	neuromuscular junction
<i>nompC</i>	<i>no mechanoreceptor potential channel</i>
NPRR	neuropeptide release reporter
NPRR ^{<i>Ilp7</i>}	neuropeptide release reporter for <i>Ilp7</i>
NPY	neuropeptide Y
NPYR1	neuropeptide Y receptor 1
OANs	octopaminergic neurons
PAM	protocerebral anterior medial cluster
PBS	phosphate buffer saline
PBST	PBS with 0.3% Triton x-100
PC	protocerebrum
pCC	posterior commissural cells

6 Abbreviations

PDF	pigment dispersing factor
PI	performance index
PI	pars intercerebralis
POMC	proopiomelanocortin
pPAM	primary protocerebral arterial medial cluster
<i>ppk</i>	<i>pickpocket</i>
PPL	protocerebral posterior lateral
PTTH	prothoracic hormone
recGFP	reconstituted GFP
RNAi	RNA interference
<i>rpk</i>	<i>ripped pocket</i>
RXFP	Relaxin-family receptors
s.e.m.	standard error of the mean
SCN9A	sodium Voltage-Gated Channel Alpha Subunit 9
SELK	sub-oesophageal zone LK neurons
SEZ	sub-oesophageal zone
sNPF	short neuropeptide F
sNPF _R	short neuropeptide F receptor
SST	somatostatin-positive neurons
ssTEM	serial section Transmission Electron Microscopy
Syb-GRASP	synaptobrevin- GFP reconstitution across synaptic partners
Syt α	synaptotagmin- α
T2A-Gal4	trojan Gal4
td	tracheal neurons
td SEZ	Tracheal neurons in sub-oesophageal zone
td VNC	Tracheal neurons in ventral nerve chord
td VNC MP	Tracheal neurons with projection in the VNC and towards the midline
Tk	tachykinin
TO	tarsal organ
<i>Trp</i>	transient receptor potential
<i>tsh</i>	<i>Tshirt</i> enhancer
UAS	upstream activator sequence
UV	ultraviolet
vMT	ventral midline thalamus
VNC	ventral nerve chord
<i>w</i>	white mutant background
<i>y, w</i>	yellow white mutant background
ZT	Zeitgeber

7 APPENDIX

Appendix 1: Reconstructed synaptic partners of Dp7 neurons

A

Dp7 presynaptic partners

Presynaptic neuron	skeleton ID	synapses Dp7_L	synapses Dp7_R
v td2	891237		18
v td2	3915835	21	
v td2	4061049		14
v td2	5638694		16
v td2	7012280	15	
v td2	12178825		14
v td2	16303262	4	
v td2	16911458	15	
v td2	19017854	17	
v td2	19037563		14
v td2	19120772	15	
C2da	3827179		3
C3da	110633	4	
C3da	2777891		4
C3da	7792781	4	
C3da	16307065	4	
C3da	17237088	3	
C4da	18303100	5	1
v td1	10852875		2
A08n	1927577	1	16
A08n	14899172	19	
MIP	7340664		4
MIP	11291634		3
MIP	11434579		6
MIP	13985838		3
MIP	19040382	3	1
TePh05	2558717		6
TePh05	18981220	18	
	2585319	8	
	2123393	3	
	3629633	3	
	4249897	3	
	6988490	3	
	13674287	3	
	19157404	3	
	2697511		7
	9428865		4
	11512247		4
	4179669		4
	2513992		4
	327601		3
	12617501		2

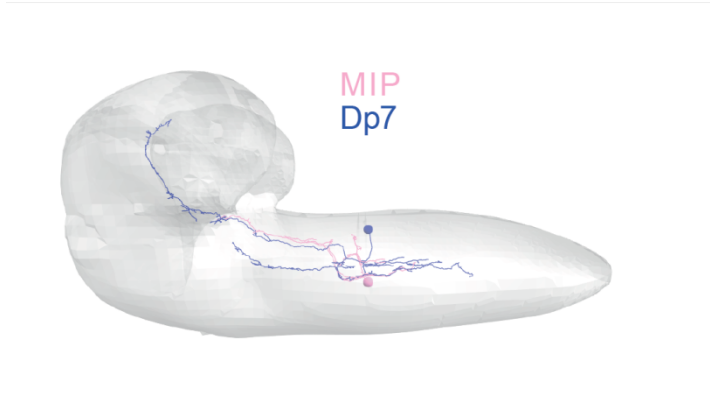
B

Dp7 postsynaptic connectome

Postsynaptic neuron	skeleton ID	synapses Dp7_L	synapses Dp7_R
ABLK	429906	4	
ABLK	3985549	3	
ABLK	10844198	3	
ABLK	19037553		3
ABLK	19166763	5	
Hugin-VNC	6795358	2	5
Hugin-VNC	2613540	4	4
Hugin-VNC	3594705	10	
Hugin-RG	5601924	1	3
Hugin-RG	2138427	7	2
Hugin-RG	5038703	1	2
Hugin-PC	9805520	3	
Bamas	17176866		15
Bamas	17176882	15	
Atf6	3946364	3	
BC	3801211		4
DPLm1 contralatera 1 left	6011278		4
DPMm1	3595837		3
DPMpm1	3944626	9	
IPC 6	2357110		3
MIP to the brain	9503414	9	
SN motor neuron	4050398	3	
	5644800	13	5
	8008617	13	5
	3793760	11	
	9524538	10	
	16500055	8	
	6445994	5	
	7345403	5	
	17019327	5	
	18694063	3	5
	16018440	3	1
	3918937	3	
	3945394	3	
	6568902	3	
	14839446	3	
	17415439	3	
	6802553	2	5
	19912140	2	5
	5071140	1	6
	5349961	1	3
	9424902		8
	4411688		6
	11946903		6
	161195633		6
	8546775		5
	15732471		5
	6300434		4
	11278919		4
	3729504		3
	5532548		3
	5613777		3
	6597872		3
	7340664		3
	14162492		3
	15304721		3
	10768709		2
	5378683		2

Appendix 2: EM reconstructed MIP neurons

MIP neurons (in pink) overlaps with the dendritic lateral arbour of Dp7 neurons



8 REFERENCES

- Al-Anzi, B., Armand, E., Nagamei, P., Olszewski, M., Sapin, V., Waters, C., Zinn, K., Wyman, R.J., and Benzer, S. (2010). The leucokinin pathway and its neurons regulate meal size in *Drosophila*. *Curr. Biol.* 20, 969–978.
- Alhadeff, A.L., Su, Z., Hernandez, E., Klima, M.L., Phillips, S.Z., Holland, R.A., Guo, C., Hantman, A.W., De Jonghe, B.C., and Betley, J.N. (2018). A Neural Circuit for the Suppression of Pain by a Competing Need State. *Cell* 173, 140-152.e15.
- Almeida-Carvalho, M.J., Berh, D., Braun, A., Chen, Y., Eichler, K., Eschbach, C., Fritsch, P.M.J., Gerber, B., Hoyer, N., Jiang, X., et al. (2017). The Ol 1 mpiad: concordance of behavioural faculties of stage 1 and stage 3 *Drosophila* larvae. *J. Exp. Biol.* 220, 2452–2475.
- Alon, U. (2007). Network motifs: Theory and experimental approaches. *Nat. Rev. Genet.* 8, 450–461.
- Alvarado, J.C., Vaughan, J.W., Stanford, T.R., and Stein, B.E. (2007). Multisensory versus unisensory integration: Contrasting modes in the superior colliculus. *J. Neurophysiol.* 97, 3193–3205.
- Anderson, D.J. (2016). Circuit modules linking internal states and social behaviour in flies and mice. *Nat. Rev. Neurosci.* 17, 692–704.
- Apostolopoulou, A.A., Mazija, L., Wüst, A., and Thum, A.S. (2014). The neuronal and molecular basis of quinine-dependent bitter taste signaling in *Drosophila* larvae. *Front. Behav. Neurosci.* 8, 1–13.
- Apostolopoulou, A.A., Rist, A., and Thum, A.S. (2015). Taste processing in *Drosophila* larvae. 9, 1–9.
- Ben Arous, J., Laffont, S., and Chatenay, D. (2009). Molecular and sensory basis of a food related two-state behavior in *C. elegans*. *PLoS One* 4, 1–8.
- Atasoy, D., Betley, J.N., Su, H.H., and Sternson, S.M. (2012). Deconstruction of a neural circuit for hunger. *Nature* 488, 172–177.
- Van Atteveldt, N., Murray, M.M.M., Thut, G., Schroeder, C.E.E., van Atteveldt, N., Murray, M.M.M., Thut, G., and Schroeder, C.E.E. (2014). Multisensory Integration: Flexible Use of General Operations. *Neuron* 81, 1240–1253.
- Baines, R.A., Uhler, J.P., Thompson, A., Sweeney, S.T., and Bate, M. (2001). Altered Electrical Properties in *Drosophila* Neurons Developing without Synaptic Transmission. *J. Neurosci.* 21, 1523–1531.
- Bargmann, C.I. (2012). Beyond the connectome: How neuromodulators shape neural circuits. *BioEssays* 34, 458–465.
- Bargmann, C.I., and Marder, E. (2013). From the connectome to brain function. *Nat. Methods* 10, 483–490.
- Barik, A., Thompson, J.H., Seltzer, M., Ghitani, N., and Chesler, A.T. (2018). A Brainstem-Spinal Circuit Controlling Nocifensive Behavior. *Neuron* 100, 1491-1503.e3.
- Barnea, G., Strapps, W., Herrada, G., Berman, Y., Ong, J., Kloss, B., Axel, R., and

8 References

- Lee, K.J. (2008). The genetic design of signaling cascades to record receptor activation. *Proc. Natl. Acad. Sci.* *105*, 64–69.
- Basbaum, A.I., Bautista, D.M., Scherrer, G., and Julius, D. (2009). Review Cellular and Molecular Mechanisms of Pain. 267–284.
- Baskin, D.G., Wilcox, B.J., Figlewicz, D.P., and Dorsa, D.M. (1988). Insulin and insulin-like growth factors in the CNS. *Trends Neurosci.* *11*, 107–111.
- Bathgate, R.A.D., Halls, M.L., van der Westhuizen, E.T., Callander, G.E., Kocan, M., and Summers, R.J. (2013). Relaxin Family Peptides and Their Receptors. *Physiol. Rev.* *93*, 405–480.
- Bavelloni, A., Piazzini, M., Raffini, M., Faenza, I., and Blalock, W.L. (2015). Prohibitin 2: At a communications crossroads. *IUBMB Life* *67*, 239–254.
- Berck, M.E., Khandelwal, A., Claus, L., Hernandez-Nunez, L., Si, G., Tabone, C.J., Li, F., Truman, J.W., Fetter, R.D., Louis, M., et al. (2016). The wiring diagram of a glomerular olfactory system. *Elife* *5*, 1–21.
- Beshel, J., and Zhong, Y. (2013). Graded encoding of food odor value in the *Drosophila* brain. *J. Neurosci.* *33*, 15693–15704.
- Beshel, J., Dubnau, J., and Zhong, Y. (2017). A Leptin Analog Locally Produced in the Brain Acts via a Conserved Neural Circuit to Modulate Obesity-Linked Behaviors in *Drosophila*. *Cell Metab.* *25*, 208–217.
- Biswas, A., and Banik, S.K. (2018). Interplay of synergy and redundancy in diamond motif. *Chaos* *28*.
- Bodmer, R., and Jan, Y.N. (1987). Morphological differentiation of the embryonic peripheral neurons in *Drosophila*. *Roux's Arch. Dev. Biol.* *196*, 69–77.
- Bouckaert, R., and Bryant, D. (2014). A rough guide to SNAPP. 1–15.
- Bräcker, L.B., Siju, K.P., Arel, N., So, Y., Hang, M., Hein, I., Vasconcelos, M.L., and Grunwald Kadow, I.C. (2013). Essential role of the mushroom body in context-dependent CO₂ avoidance in *drosophila*. *Curr. Biol.* *23*, 1228–1234.
- Branco, T., and Redgrave, P. (2020). The Neural Basis of Escape Behavior in Vertebrates. *Annu. Rev. Neurosci.* *43*, 417–439.
- Brand, A.H., and Perrimon, N. (1993). Targeted gene expression as a means of altering cell fates and generating dominant phenotypes. *415*, 401–415.
- Breckenridge, L.J., and Almers, W. (1987). Currents through the fusion pore that forms during exocytosis of a secretory vesicle. *Nature* *328*, 814–817.
- Broadus, J., Skeath, J.B., Spana, E., Bossing, T., Technau, G.M., and Doe, C.Q. (1995). New neuroblast markers and the origin of the aCC/pCC neurons in the *Drosophila* CNS. *Mech. Dev.* *54*, 1–10.
- Burgos, A., Honjo, K., Ohyama, T., Qian, C.S., Shin, G.J., Gohl, D.M., Silies, M., Tracey, W.D., Zlatic, M., Cardona, A., et al. (2018). Nociceptive interneurons control modular motor pathways to promote escape behavior in *Drosophila*. *Elife* *7*, 1–28.
- Callaway, E.M., and Luo, L. (2015). Monosynaptic circuit tracing with glycoprotein-deleted rabies viruses. *J. Neurosci.* *35*, 8979–8985.
- Cao, Y.Q., Mantyh, P.W., Carlson, E.J., Gillespie, A.M., Epstein, C.J., and Basbaum,

8 References

- A.I. (1998). Primary afferent tachykinins are required to experience moderate to intense pain. *Nature* 392, 390–394.
- Carlsson, M.A., Enell, L.E., and Nässel, D.R. (2013). Distribution of short neuropeptide F and its receptor in neuronal circuits related to feeding in larval *Drosophila*. *Cell Tissue Res* 511–523.
- Chatzigeorgiou, M., and Schafer, W.R. (2011). Lateral Facilitation between Primary Mechanosensory Neurons Controls Nose Touch Perception in *C. elegans*. *Neuron* 70, 299–309.
- Chen, Y.C.D., Park, S.J., Joseph, R.M., Ja, W.W., and Dahanukar, A.A. (2019). Combinatorial Pharyngeal Taste Coding for Feeding Avoidance in Adult *Drosophila*. *Cell Rep.* 29, 961-973.e4.
- Cheng, L.E., Song, W., Looger, L.L., Jan, L.Y., and Jan, Y.N. (2010). The Role of the TRP Channel NompC in *Drosophila* Larval and Adult Locomotion. *Neuron* 67, 373–380.
- Choi, I., Lee, J.Y., and Lee, S.H. (2018). Bottom-up and top-down modulation of multisensory integration. *Curr. Opin. Neurobiol.* 52, 115–122.
- Choi, S., Hachisuka, J., Brett, M.A., Magee, A.R., Omori, Y., Iqbal, N., Zhang, D., DeLisle, M.M., Wolfson, R.L., Bai, L., et al. (2020). Parallel ascending spinal pathways for affective touch and pain. *Nature*.
- Chyb, S., and Gompel, N. (2013). Introduction. *Atlas Drosoph. Morphol.* xi–xviii.
- Clarke, D.W., Mudd, L., Boyd, F.T., Fields, M., and Raizada, M.K. (1986). Insulin Is Released from Rat Brain Neuronal Cells in Culture. *J. Neurochem.* 47, 831–836.
- Cognigni, P., Bailey, A.P., and Miguel-Aliaga, I. (2011). Enteric Neurons and Systemic Signals Couple Nutritional and Reproductive Status with Intestinal Homeostasis. *Cell Metab.* 13, 92–104.
- Cohn, R., Morante, I., and Ruta, V. (2015). Coordinated and Compartmentalized Neuromodulation Shapes Sensory Processing in *Drosophila*. *Cell* 163, 1742–1755.
- Cowley, M.A., Smart, J.L., Rubinstein, M., Cerdán, M.G., Diano, S., Horvath, T.L., Cone, R.D., and Low, M.J. (2001). Leptin activates anorexigenic POMC neurons through a neural network in the arcuate nucleus. *Nature* 411, 480–484.
- Cox, J.J., Reimann, F., Nicholas, A.K., Thornton, G., Roberts, E., Springell, K., Karbani, G., Jafri, H., Mannan, J., Raashid, Y., et al. (2006). An SCN9A channelopathy causes congenital inability to experience pain. *Nature* 444, 894–898.
- Craig, W. (1918). Appetites and Aversions As Constituents of Instincts. *Biol. Bull.* 34, 91–107.
- Dahanukar, A., Lei, Y.T., Kwon, J.Y., and Carlson, J.R. (2007). Two Gr Genes Underlie Sugar Reception in *Drosophila*. *Neuron* 56, 503–516.
- Dana, H., Sun, Y., Mohar, B., Hulse, B.K., Kerlin, A.M., Hasseman, J.P., Tsegaye, G., Tsang, A., Wong, A., Patel, R., et al. (2019). High-performance calcium sensors for imaging activity in neuronal populations and microcompartments. *Nat. Methods* 16, 649–657.
- Das, G., Lin, S., and Waddell, S. (2016). Remembering Components of Food in *Drosophila*. *Front. Integr. Neurosci.* 10, 1–8.

8 References

- Deng, B., Li, Q., Liu, X., Cao, Y., Li, B., Qian, Y., Xu, R., Mao, R., Zhou, E., Zhang, W., et al. (2019). Chemoconnectomics: Mapping Chemical Transmission in *Drosophila*. *Neuron* 101, 876–893.e4.
- Destexhe, A., and Marder, E. (2004). Circuit Computations. *Nature* 431, 789–795.
- Diao, F., and White, B.H. (2012). A novel approach for directing transgene expression in *Drosophila*: T2A-Gal4 in-frame fusion. *Genetics* 190, 1139–1144.
- Diegelmann, S., Klagges, B.R.E., Michels, B., Schleyer, M., and Gerber, B. (2013). Maggot learning and Synapsin function. *J. Exp. Biol.* 216, 939–951.
- Ding, K., Han, Y., Seid, T.W., Buser, C., Karigo, T., Zhang, S., Dickman, D.K., and Anderson, D.J. (2019). Imaging neuropeptide release at synapses with a genetically engineered reporter. *Elife* 8, 1–15.
- Du, E.J., Ahn, T.J., Wen, X., Seo, D.W., Na, D.L., Kwon, J.Y., Choi, M., Kim, H.W., Cho, H., and Kang, K.J. (2016). Nucleophile sensitivity of *Drosophila* TRPA1 underlies light-induced feeding deterrence. *Elife* 5, 1–26.
- Dubin, A.E., and Patapoutian, A. (2010). Nociceptors : the sensors of the pain pathway. *Rev. Ser.* 120.
- Dus, M., Lai, J.S.Y., Gunapala, K.M., Min, S., Tayler, T.D., Hergarden, A.C., Geraud, E., Joseph, C.M., and Suh, G.S.B. (2015). Nutrient Sensor in the Brain Directs the Action of the Brain-Gut Axis in *Drosophila*. *Neuron* 87, 139–151.
- Dus, M., Lai, J.S., Gunapala, K.M., Min, S., Tayler, T.D., Hergarden, A.C., Geraud, E., Joseph, C.M., and Suh, G.S.B. (2016). HHS Public Access. 87, 139–151.
- Edwards, S.L., Charlie, N.K., Milfort, M.C., Brown, B.S., Gravlin, C.N., Knecht, J.E., and Miller, K.G. (2008). A novel molecular solution for ultraviolet light detection in *Caenorhabditis elegans*. *PLoS Biol.* 6, 1715–1729.
- Eichler, K., Li, F., Litwin-Kumar, A., Park, Y., Andrade, I., Schneider-Mizell, C.M., Saumweber, T., Huser, A., Eschbach, C., Gerber, B., et al. (2017). The complete connectome of a learning and memory centre in an insect brain. *Nature* 548, 175–182.
- Ennedy, A.N.N.K., Sahina, K.E.A., Oopfer, E.R.I.C.H., Nagaki, H.I.I., Ung, Y.O.J., Ee, H.Y.L., Emedios, R.Y.A.N.R., and Nderson, D.A.J.A. (2014). Internal States and Behavioral Decision-Making : Toward an Integration of Emotion and Cognition. *LXXIX*.
- Eschbach, C., Fushiki, A., Winding, M., Schneider-Mizell, C.M., Shao, M., Arruda, R., Eichler, K., Valdes-Aleman, J., Ohshima, T., Thum, A.S., et al. (2020). Recurrent architecture for adaptive regulation of learning in the insect brain. *Nat. Neurosci.* 23, 544–555.
- Ewers, H. (2012). Nano Resolution Optical Imaging Through Localization Microscopy. *Cell. Imaging Tech. Neurosci. Beyond* 81–100.
- Fadok, J.P., Krabbe, S., Markovic, M., Courtin, J., Xu, C., Massi, L., Botta, P., Bylund, K., Müller, C., Kovacevic, A., et al. (2017). A competitive inhibitory circuit for selection of active and passive fear responses. *Nature* 542, 96–99.
- Farina, M., van de Bospoort, R., He, E., Persoon, C.M., van Weering, J.R.T., Broeke, J.H., Verhage, M., and Toonen, R.F. (2015). CAPS-1 promotes fusion competence of stationary dense-core vesicles in presynaptic terminals of mammalian neurons.

8 References

Elife 4, 1–22.

Fernandez, A.M., and Torres-Alemán, I. (2012). The many faces of insulin-like peptide signalling in the brain. *Nat. Rev. Neurosci.* 13, 225–239.

Fields, H. (2004). State-dependent opioid control of pain. *Nat. Rev. Neurosci.* 5, 565–575.

Filosa, A., Barker, A.J., Dal Maschio, M., and Baier, H. (2016). Feeding State Modulates Behavioral Choice and Processing of Prey Stimuli in the Zebrafish Tectum. *Neuron* 90, 596–608.

Fitzpatrick, M.J., Feder, E., Rowe, L., and Sokolowski, M.B. (2007). Maintaining a behaviour polymorphism by frequency-dependent selection on a single gene. *Nature* 447, 210–212.

Flavell, S.W., Pokala, N., Macosko, E.Z., Albrecht, D.R., Larsch, J., and Bargmann, C.I. (2013). Serotonin and the neuropeptide PDF initiate and extend opposing behavioral states in *C. Elegans*. *Cell* 154, 1023–1035.

Frederick, D.E., Rojas-Líbano, D., Scott, M., and Kay, L.M. (2011). Rat behavior in go/no-go and two-alternative choice odor discrimination: Differences and similarities. *Behav. Neurosci.* 125, 588–603.

Fushiki, A., Zwart, M.F., Kohsaka, H., Fetter, R.D., Cardona, A., and Nose, A. (2016). A circuit mechanism for the propagation of waves of muscle contraction in *Drosophila*. *Elife* 5, 1–23.

Gambino, F., Pagès, S., Kehayas, V., Baptista, D., Tatti, R., Carleton, A., and Holtmaat, A. (2014). Sensory-evoked LTP driven by dendritic plateau potentials in vivo. *Nature* 515, 116–119.

Garelli, A., Heredia, F., Casimiro, A.P., Macedo, A., Nunes, C., Garcez, M., Dias, A.R.M., Volonte, Y.A., Uhlmann, T., Caparros, E., et al. (2015). Dilp8 requires the neuronal relaxin receptor Lgr3 to couple growth to developmental timing. *Nat. Commun.* 6, 8732.

Gerhard, S., Andrade, I., Fetter, R.D., Cardona, A., and Schneider-Mizell, C.M. (2017). Conserved neural circuit structure across drosophila larval development revealed by comparative connectomics. *BioRxiv* 6.

Ghosh, D.D., Nitabach, M.N., Zhang, Y., and Harris, G. (2017). Multisensory integration in *C. elegans*. *Curr. Opin. Neurobiol.* 43, 110–118.

Ghysen, A., Dambly-Chaudière, C., Aceves, E., Jan, L.Y., and Jan, Y.N. (1986). Sensory neurons and peripheral pathways in *Drosophila* embryos. *Roux's Arch. Dev. Biol.* 195, 281–289.

Gigandet, X., Griffa, A., Kober, T., Daducci, A., Gilbert, G., Connelly, A., Hagmann, P., Meuli, R., Thiran, J.-P., and Krueger, G. (2013). A connectome-based comparison of diffusion MRI schemes. *PLoS One* 8, e75061.

Gong, Z., Liu, J., Guo, C., Zhou, Y., Teng, Y., and Liu, L. (2010). Two pairs of neurons in the central brain control *Drosophila* innate light preference. *Science* 330, 499–502.

Gontijo, A.M., and Garelli, A. (2018). The biology and evolution of the Dilp8-Lgr3 pathway: A relaxin-like pathway coupling tissue growth and developmental timing control. *Mech. Dev.* 154, 44–50.

8 References

- Gordon, M.D., and Scott, K. (2009). Motor control in a *Drosophila* taste circuit. *Neuron* 61, 373–384.
- Greene, J.S., Brown, M., Dobosiewicz, M., Ishida, I.G., Macosko, E.Z., Zhang, X., Butcher, R.A., Cline, D.J., McGrath, P.T., and Bargmann, C.I. (2016). Balancing selection shapes density-dependent foraging behaviour. *Nature* 539, 254–258.
- Grönke, S., Clarke, D.-F.F., Broughton, S., Andrews, T.D., and Partridge, L. (2010). Molecular Evolution and Functional Characterization of *Drosophila* Insulin-Like Peptides. *PLoS Genet.* 6, e1000857.
- Grueber, W.B., Jan, L.Y., and Jan, Y.N. (2002). Tiling of the *Drosophila* epidermis by multidendritic sensory neurons. *Development* 129, 2867–2878.
- Grueber, W.B., Ye, B., Yang, C., Younger, S., Borden, K., Jan, L.Y., and Jan, Y.-N.Y.-N. (2007). Projections of *Drosophila* multidendritic neurons in the central nervous system: links with peripheral dendrite morphology. *Development* 134, 55–64.
- Grunwald Kadow, I.C. (2019). State-dependent plasticity of innate behavior in fruit flies. *Curr. Opin. Neurobiol.* 54, 60–65.
- Gu, P., Gong, J., Shang, Y., Wang, F., Ruppell, K.T., Ma, Z., Sheehan, A.E., Freeman, M.R., and Xiang, Y. (2019). Polymodal Nociception in *Drosophila* Requires Alternative Splicing of TrpA1. *Curr. Biol.* 29, 3961-3973.e6.
- Halford, S., Pires, S.S., Turton, M., Zheng, L., González-Menéndez, I., Davies, W.L., Peirson, S.N., García-Fernández, J.M., Hankins, M.W., and Foster, R.G. (2009). VA Opsin-Based Photoreceptors in the Hypothalamus of Birds. *Curr. Biol.* 19, 1396–1402.
- de Haro, M., Al-Ramahi, I., Benito-Sipos, J., López-Arias, B., Dorado, B., Veenstra, J.A., and Herrero, P. (2010). Detailed analysis of leucokinin-expressing neurons and their candidate functions in the *Drosophila* nervous system. *Cell Tissue Res.* 339, 321–336.
- Harris, D.T., Kallman, B.R., Mullaney, B.C., and Scott, K. (2015). Representations of Taste Modality in the *Drosophila* Brain. *Neuron* 86, 1449–1460.
- Hassan, J., Iyengar, B., Scantlebury, N., Moncalvo, V.R., and Campos, A.R. (2005). Photic input pathways that mediate the *Drosophila* larval response to light and circadian rhythmicity are developmentally related but functionally distinct. *J. Comp. Neurol.* 481, 266–275.
- Hattar, S. (2002). Melanopsin-Containing Retinal Ganglion Cells: Architecture, Projections, and Intrinsic Photosensitivity. *Science* (80-.). 295, 1065–1070.
- Hauser, A.S., Attwood, M.M., Rask-Andersen, M., Schiöth, H.B., and Gloriam, D.E. (2017). Trends in GPCR drug discovery: New agents, targets and indications. *Nat. Rev. Drug Discov.* 16, 829–842.
- He, L., Wu, X.S., Mohan, R., and Wu, L.G. (2006). Two modes of fusion pore opening revealed by cell-attached recordings at a synapse. *Nature* 444, 102–105.
- Heisenberg, M. (2003). Mushroom body memoir: from maps to models. *Nat. Rev. Neurosci.* 4, 266–275.
- Helmstaedter, M., Briggman, K.L., Turaga, S.C., Jain, V., Seung, H.S., and Denk, W. (2013). Connectomic reconstruction of the inner plexiform layer in the mouse retina.

8 References

Nature 500, 168–174.

Hidalgo, A., and Brand, A.H. (1997). Targeted neuronal ablation: The role of pioneer neurons in guidance and fasciculation in the CNS of *Drosophila*. *Development* 124, 3253–3262.

Horio, N., and Liberles, S.D. (2021). Hunger enhances food-odor attraction through a neuropeptide Y spotlight. *Nature*.

Hu, C., Petersen, M., Hoyer, N., Spitzweck, B., Tenedini, F., Wang, D., Gruschka, A., Burchardt, L.S., Szpotowicz, E., Schweizer, M., et al. (2017). Sensory integration and neuromodulatory feedback facilitate *Drosophila* mechanonociceptive behavior. *Nat. Neurosci.* 1–14.

Hückesfeld, S., Peters, M., and Pankratz, M.J. (2016). Central relay of bitter taste to the protocerebrum by peptidergic interneurons in the *Drosophila* brain. *Nat. Commun.* 7, 12796.

Hwang, R.Y., Zhong, L., Xu, Y., Johnson, T., Zhang, F., Tracey, W.D., Deisseroth, K., and Tracey, W.D. (2007). Nociceptive neurons protect *Drosophila* larvae from parasitoid wasps. *Curr Biol* 17, 2105–2116.

Im, S.H., and Galko, M.J. (2012). Pokes, sunburn, and hot sauce: *Drosophila* as an emerging model for the biology of nociception. *Dev. Dyn.* 241, 16–26.

Inagaki, H.K., Ben-Tabou de-Leon, S., Wong, A.M., Jagadish, S., Ishimoto, H., Barnea, G., Kitamoto, T., Axel, R., and Anderson, D.J. (2012). Visualizing Neuromodulation In Vivo: TANGO-Mapping of Dopamine Signaling Reveals Appetite Control of Sugar Sensing. *Cell* 148, 583–595.

Inagaki, H.K., Panse, K., and Anderson, D.J. (2015). bitter taste sensitivity during starvation in *Drosophila*. 84, 806–820.

Ito, K., Urban, J., and Technau, G.M. (1995). Distribution, Classification, and Development of *Drosophila* Glial-Cells in the Late Embryonic and Early Larval Ventral Nerve Cord. *Roux's Arch Dev Biol* 204, 284–307.

Jacobs, J.R., and Goodman, C.S. (1989). Embryonic development of axon pathways in the *Drosophila* CNS. I. A glial scaffold appears before the first growth cones. *J. Neurosci.* 9, 2402–2411.

Jin, E.J., Park, S., Lyu, X., and Jin, Y. (2020). Gap junctions: Historical discoveries and new findings in the *Caenorhabditis elegans* nervous system. *Biol. Open* 9, 1–8.

Jourjine, N., Mullaney, B.C., Mann, K., and Scott, K. (2016). Coupled Sensing of Hunger and Thirst Signals Balances Sugar and Water Consumption. *Cell* 166, 855–866.

Jovanic, T., Schneider-Mizell, C.M., Shao, M., Masson, J.B., Denisov, G., Fetter, R.D., Menseh, B.D., Truman, J.W., Cardona, A., and Zlatic, M. (2016). Competitive Disinhibition Mediates Behavioral Choice and Sequences in *Drosophila*. *Cell* 167, 858-870.e19.

Jovanic, T., Winding, M., Cardona, A., Truman, J.W., Gershow, M., and Zlatic, M. (2019). Neural Substrates of *Drosophila* Larval Anemotaxis. *Curr. Biol.* 29, 554-566.e4.

Jung, L.J., and Scheller, R.H. (1991). Peptide processing and targeting in the neuronal secretory pathway. *Science* (80-.). 251, 1330–1335.

8 References

- Kandel, E.R., Schwartz, J.H., and Jessell, R.M. (2000). Principles of neural science.
- Kaneko, T., Macara, A.M., Li, R., Hu, Y., Iwasaki, K., Dunning, Z., Firestone, E., Horvatic, S., Guntur, A., Shafer, O.T., et al. (2017). Serotonergic Modulation Enables Pathway-Specific Plasticity in a Developing Sensory Circuit in *Drosophila*. *Neuron* 95, 623–638.e4.
- Kaneko, T., Macara, A.M., Li, R., Hu, Y., Iwasaki, K., Firestone, E., Horvatic, S., Guntur, A., Shafer, O.T., Yang, H., et al. (2018). HHS Public Access. 95, 623–638.
- Kania, A., Gugula, A., Grabowiecka, A., de Ávila, C., Blasiak, T., Rajfur, Z., Lewandowski, M.H., Hess, G., Timofeeva, E., Gundlach, A.L., et al. (2017). Inhibition of oxytocin and vasopressin neuron activity in rat hypothalamic paraventricular nucleus by relaxin-3-RXFP3 signalling. *J. Physiol.* 595, 3425–3447.
- Kannan, K., and Fridell, Y.C. (2013). Functional implications of *Drosophila* insulin-like peptides in metabolism, aging, and dietary restriction. 4, 1–8.
- Kapan, N., Lushchak, O. V., Luo, J., and Nessel, D.R. (2012). Identified peptidergic neurons in the *Drosophila* brain regulate insulin-producing cells, stress responses and metabolism by coexpressed short neuropeptide F and corazonin. *Cell. Mol. Life Sci.* 69, 4051–4066.
- Kaun, K.R., Riedl, C.A.L., Chakaborty-Chatterjee, M., Belay, A.T., Douglas, S.J., Gibbs, A.G., and Sokolowski, M.B. (2007). Natural variation in food acquisition mediated via a *Drosophila* cGMP-dependent protein kinase. *J. Exp. Biol.* 210, 3547–3558.
- Keene, A.C., and Sprecher, S.G. (2012). Seeing the light: Photobehavior in fruit fly larvae. *Trends Neurosci.* 35, 104–110.
- Keene, A.C., Duboué, E.R., McDonald, D.M., Dus, M., Suh, G.S.B., Waddell, S., and Blau, J. (2010). Clock and cycle limit starvation-induced sleep loss in *Drosophila*. *Curr. Biol.* 20, 1209–1215.
- Kelly, R.B. (1985). Pathways of protein secretion in eukaryotes. *Science* (80-). 230, 25–32.
- Kim, S.E., Coste, B., Chadha, A., Cook, B., and Patapoutian, A. (2012). The role of *Drosophila* Piezo in mechanical nociception. *Nature* 483, 209–212.
- Kim, S.M., Su, C.-Y., and Wang, J.W. (2017). Neuromodulation of Innate Behaviors in *Drosophila*.
- Knobloch, H.S., Charlet, A., Hoffmann, L.C., Eliava, M., Khrulev, S., Cetin, A.H., Osten, P., Schwarz, M.K., Seeburg, P.H., Stoop, R., et al. (2012). Evoked axonal oxytocin release in the central amygdala attenuates fear response. *Neuron* 73, 553–566.
- Ko, K.I., Root, C.M., Lindsay, S.A., Zaninovich, O.A., Shepherd, A.K., Wasserman, S.A., Kim, S.M., and Wang, J.W. (2015). Starvation promotes concerted modulation of appetitive olfactory behavior via parallel neuromodulatory circuits. *Elife* 4, 1–17.
- Krashes, M.J., Dasgupta, S., Vreede, A., White, B., Douglas, J., and Waddell, S. (2010). A neural circuit mechanism integrating motivational state with memory expression in *Drosophila*. *Cell* 139, 416–427.
- Krüger, E., Mena, W., Lahr, E.C., Johnson, E.C., and Ewer, J. (2015). Genetic analysis of Eclosion hormone action during *Drosophila* larval ecdysis. *Dev.* 142,

8 References

4279–4287.

- Kwon, J.Y., Dahanukar, A., Weiss, L.A., and Carlson, J.R. (2011). Molecular and cellular organization of the taste system in the *Drosophila* larva. *J. Neurosci.* *31*, 15300–15309.
- Landry, M., Aman, K., and Hokfelt, T. (1998). Galanin-R1 receptor in anterior and mid-hypothalamus: Distribution and regulation. *J. Comp. Neurol.* *399*, 321–340.
- Landry, M., Vila-Porcile, E., Hökfelt, T., and Calas, A. (2003). Differential routing of coexisting neuropeptides in vasopressin neurons. *Eur. J. Neurosci.* *17*, 579–589.
- Larderet, I., Fritsch, P.M.J., Gendre, N., Larisa Neagu-Maier, G., Fetter, R.D., Schneider-Mizell, C.M., Truman, J.W., Zlatic, M., Cardona, A., and Sprecher, S.G. (2017). Organization of the *drosophila* larval visual circuit. *Elife* *6*, 1–23.
- Lee, I., and Lee, C.H. (2013). Contextual behavior and neural circuits. *Front. Neural Circuits* *7*, 1–21.
- Lee, K.-S.S., Kwon, O.-Y.Y., Lee, J.H., Kwon, K., Min, K.-J.J., Jung, S.-A.A., Kim, A.-K.K., You, K.-H.H., Tatar, M., and Yu, K. (2008). *Drosophila* short neuropeptide F signalling regulates growth by ERK-mediated insulin signalling. *Nat. Cell Biol.* *10*, 468–475.
- Lee, K.S., You, K.H., Choo, J.K., Han, Y.M., and Yu, K. (2004). *Drosophila* short neuropeptide F regulates food intake and body size. *J. Biol. Chem.* *279*, 50781–50789.
- Lee, P., Zirin, J., Kanca, O., Lin, W., Schulze, K.L., Li-kroeger, D., Tao, R., Devereaux, C., Hu, Y., Chung, V., et al. (2018). A gene-specific T2A-GAL4 library for *Drosophila*. 1–24.
- Lee, T., Lee, A., Luo, L., Aceves-Pina, E.O., Quinn, W.G., Cepko, C.L., Austin, C.P., Yang, X., Alexiades, M., Ezzeddine, D., et al. (1999). Development of the *Drosophila* mushroom bodies: sequential generation of three distinct types of neurons from a neuroblast. *Development* *126*, 4065–4076.
- Leinwand, S.G., and Chalasani, S.H. (2013). Neuropeptide signaling remodels chemosensory circuit composition in *Caenorhabditis elegans*. *Nat. Neurosci.* *16*, 1461–1467.
- Leng, G., and Ludwig, M. (2008). Neurotransmitters and peptides: whispered secrets and public announcements. *J. Physiol.* *586*, 5625–5632.
- Leopold, P., and Perrimon, N. (2007). *Drosophila* and the genetics of the internal milieu. *Nature* *450*, 186–188.
- Lewis, L.P.C., Siju, K.P., Aso, Y., Friedrich, A.B., Bulteel, A.J.B., Rubin, G.M., and Grunwald Kadow, I.C. (2015). A Higher Brain Circuit for Immediate Integration of Conflicting Sensory Information in *Drosophila*. *Curr. Biol.* *25*, 2203–2214.
- Li, C., and Kim, K. (2008). Neuropeptides. *WormBook* 1–36.
- Li, L., Rutlin, M., Abraira, V.E., Cassidy, C., Kus, L., Gong, S., Jankowski, M.P., Luo, W., Heintz, N., Koerber, H.R., et al. (2011). The functional organization of cutaneous low-threshold mechanosensory neurons. *Cell* *147*, 1615–1627.
- Liman, E.R., Zhang, Y. V., and Montell, C. (2014). Peripheral coding of taste. *Neuron* *81*, 984–1000.

8 References

- Linneweber, G.A., Jacobson, J., Busch, K.E., Hudry, B., Christov, C.P., Dormann, D., Yuan, M., Otani, T., Knust, E., De Bono, M., et al. (2014). Neuronal control of metabolism through nutrient-dependent modulation of tracheal branching. *Cell* 156, 69–83.
- Liu, C.M., and Kanoski, S.E. (2018). Homeostatic and non-homeostatic controls of feeding behavior: Distinct vs. common neural systems. *Physiol. Behav.* 193, 223–231.
- Liu, C., Plaçais, P.Y., Yamagata, N., Pfeiffer, B.D., Aso, Y., Friedrich, A.B., Siwanowicz, I., Rubin, G.M., Preat, T., and Tanimoto, H. (2012). A subset of dopamine neurons signals reward for odor memory in *Drosophila*. *Nature* 488, 512–516.
- Lowell, B.B. (2019). New Neuroscience of Homeostasis and Drives for Food, Water, and Salt. *N. Engl. J. Med.* 380, 459–471.
- Luan, H., Peabody, N.C., Vinson, C.R.R., and White, B.H. (2006). Refined Spatial Manipulation of Neuronal Function by Combinatorial Restriction of Transgene Expression. *Neuron* 52, 425–436.
- Lumpkin, E.A., and Caterina, M.J. (2007). Mechanisms of sensory transduction in the skin. *Nature* 445, 858–865.
- Lyutova, R., Pfeuffer, M., Segebarth, D., Habenstein, J., Selcho, M., Wegener, C., Thum, A.S., and Pauls, D. (2018). Reward signaling in a recurrent circuit of dopaminergic neurons and Kenyon cells. *BioRxiv*.
- Macosko, E.Z., Pokala, N., Feinberg, E.H., Chalasani, S.H., Butcher, R.A., Clardy, J., and Bargmann, C.I. (2009). A hub-and-spoke circuit drives pheromone attraction and social behaviour in *C. elegans*. *Nature* 458, 1171–1175.
- Macpherson, L.J., Zaharieva, E.E., Kearney, P.J., Alpert, M.H., Lin, T.-Y.Y., Turan, Z., Lee, C.-H.H., and Gallio, M. (2015). Dynamic labelling of neural connections in multiple colours by trans-synaptic fluorescence complementation. *Nat. Commun.* 6, 1–9.
- Malnic, B., Hirono, J., Sato, T., Buck, L.B., and Hughes, H. (1999). [<Olfactory_Cell_article_Malnic.pdf>](#). 96, 713–723.
- Mantyh, P., DeMaster, E., Malhotra, A., Ghilardi, Rogers, S., Mantyh, C., Liu, H., Basbaum, A., Vigna, Maggio, J., et al. (1995). Receptor endocytosis and dendrite reshaping in spinal neurons after somatosensory stimulation. *Science* (80-.). 268, 1629–1632.
- Mao, Z., and Davis, R.L. (2009). Eight different types of dopaminergic neurons innervate the *Drosophila* mushroom body neuropil: Anatomical and physiological heterogeneity. *Front. Neural Circuits* 3, 1–17.
- Marder, E., and Thirumalai, V. (2002). Cellular, synaptic and network effects of neuromodulation. *Neural Networks* 15, 479–493.
- Mazzoni, E.O., Desplan, C., and Blau, J. (2005). Circadian pacemaker neurons transmit and modulate visual information to control a rapid behavioral response. *Neuron* 45, 293–300.
- McNabb, S.L., Baker, J.D., Agapite, J., Steller, H., Riddiford, L.M., and Truman, J.W. (1997). Disruption of a behavioral sequence by targeted death of peptidergic

8 References

- neurons in *Drosophila*. *Neuron* 19, 813–823.
- Melcher, C., and Pankratz, M.J. (2005). Candidate gustatory interneurons modulating feeding behavior in the *Drosophila* brain. *PLoS Biol.* 3, 1618–1629.
- Miguel-Aliaga, I., Thor, S., and Gould, A.P. (2008). Postmitotic specification of *Drosophila* insulinergic neurons from pioneer neurons. *PLoS Biol.* 6, 0538–0551.
- Milo, R., Shen-Orr, S., Itzkovitz, S., Kashtan, N., Chklovskii, D., and Alon, U. (2011). Network Motifs: Simple Building Blocks of Complex Networks. *Struct. Dyn. Networks* 9781400841, 217–220.
- Min, K.J., Yamamoto, R., Buch, S., Pankratz, M., and Tatar, M. (2008). *Drosophila* lifespan control by dietary restriction independent of insulin-like signaling. *Aging Cell* 7, 199–206.
- Miroschnikow, A., Schlegel, P., Schoofs, A., Hueckesfeld, S., Li, F., Schneider-Mizell, C.M., Fetter, R.D., Truman, J.W., Cardona, A., and Pankratz, M.J. (2018). Convergence of monosynaptic and polysynaptic sensory paths onto common motor outputs in a *Drosophila* feeding connectome. *Elife* 7, 1–25.
- Miroschnikow, A., Schlegel, P., and Pankratz, M.J. (2020). Making Feeding Decisions in the *Drosophila* Nervous System. *Curr. Biol.* 30, R831–R840.
- Mishra, D., Miyamoto, T., Rezenom, Y.H.H., Broussard, A., Yavuz, A., Slone, J., Russell, D.H.H., Amrein, H., Yavuz, A., Slone, J., et al. (2013). The Molecular Basis of Sugar Sensing in *Drosophila* Larvae. *Curr. Biol.* 23, 1466–1471.
- Mishra, D., Thorne, N., Miyamoto, C., Jagge, C., and Amrein, H. (2018). The taste of ribonucleosides: Novel macronutrients essential for larval growth are sensed by *Drosophila* gustatory receptor proteins. *PLoS Biol.* 16, 1–19.
- Miyamoto, T., Slone, J., Song, X., Amrein, H., Tetsuya Miyamoto, Jesse Slone¹, Xiangyu Song, and H.A., Miyamoto, T., Slone, J., Song, X., and Amrein, H. (2012). A Fructose Receptor Functions as a Nutrient Sensor in the *Drosophila* Brain. *Cell* 151, 1113–1125.
- Morton, G.J., Cummings, D.E., Baskin, D.G., Barsh, G.S., and Schwartz, M.W. (2006). Central nervous system control of food intake and body weight. *Nature* 443, 289–295.
- Murakami, K., Yurgel, M.E., Stahl, B.A., Masek, P., Mehta, A., Heidker, R., Bollinger, W., Gingras, R.M., Kim, Y.J., Ja, W.W., et al. (2016). Translin Is Required for Metabolic Regulation of Sleep. *Curr. Biol.* 26, 972–980.
- Murphy, K.G., and Bloom, S.R. (2006). Gut hormones and the regulation of energy homeostasis. *Nature* 444, 854–859.
- Murray, M.M., Foxe, J.J., and Wylie, G.R. (2005). The brain uses single-trial multisensory memories to discriminate without awareness. 27, 473–478.
- Murray, M.M., Lewkowicz, D.J., Amedi, A., and Wallace, M.T. (2016). Multisensory Processes : A Balancing Act across the Lifespan. *Trends Neurosci.* 39, 567–579.
- Nakazato, M., Murakami, N., Date, Y., Kojima, M., Matsuo, H., Kangawa, K., and Matsukura, S. (2001). A role for ghrelin in the central regulation of feeding. *Nature* 409, 194–198.
- Namburi, P., Beyeler, A., Yoroizu, S., Calhoun, G.G., Halbert, S.A., Wichmann, R.,

8 References

- Holden, S.S., Mertens, K.L., Anahtar, M., Felix-Ortiz, A.C., et al. (2015). A circuit mechanism for differentiating positive and negative associations. *Nature* 520, 675–678.
- Nässel, D.R. (2002). Neuropeptides in the nervous system of *Drosophila* and other insects: multiple roles as neuromodulators and neurohormones. *Prog. Neurobiol.* 68, 1–84.
- Nässel, D.R., and Broeck, J. Vanden (2016). Insulin/IGF signaling in *Drosophila* and other insects: Factors that regulate production, release and post-release action of the insulin-like peptides. *Cell. Mol. Life Sci.* 73, 271–290.
- Nässel, D.R., and Winther, Å.M.E. (2010). *Drosophila* neuropeptides in regulation of physiology and behavior. *Prog. Neurobiol.* 92, 42–104.
- Nässel, D.R., Enell, L.E., Santos, J.G., Wegener, C., and Johard, H.A.D. (2008). A large population of diverse neurons in the *Drosophila* central nervous system expresses short neuropeptide F, suggesting multiple distributed peptide functions. *BMC Neurosci.* 9, 90.
- Nässel, D.R., Pauls, D., and Huetteroth, W. (2019). Neuropeptides in modulation of *Drosophila* behavior : how to get a grip on their pleiotropic actions. 1–19.
- Nassif, C., Noveen, A., and Hartenstein, V. (2003). Early development of the *Drosophila* brain: III. The pattern of neuropile founder tracts during the larval period. *J. Comp. Neurol.* 455, 417–434.
- Nusbaum, M.P., Blitz, D.M., and Marder, E. (2018). Functional consequences of neuropeptide and small-moleculeco-transmission. 18, 389–403.
- Oh, Y., Lai, J.S.Y., Mills, H.J., Erdjument-Bromage, H., Giammarinaro, B., Saadipour, K., Wang, J.G., Abu, F., Neubert, T.A., and Suh, G.S.B. (2019). A glucose-sensing neuron pair regulates insulin and glucagon in *Drosophila*. *Nature* 574, 559–564.
- Ohyama, T., Schneider-mizell, C.M., Fetter, R.D., Aleman, J.V., Franconville, R., Rivera-alba, M., Mensh, B.D., Branson, K.M., Simpson, J.H., Truman, J.W., et al. (2015). A multilevel multimodal circuit enhances action selection in *Drosophila*. 31.
- Oishi, Y., and Lazarus, M. (2017). The control of sleep and wakefulness by mesolimbic dopamine systems. *Neurosci. Res.* 118, 66–73.
- Okusawa, S., Kohsaka, H., and Nose, A. (2014). Serotonin and Downstream Leucokinin Neurons Modulate Larval Turning Behavior in *Drosophila*. *J. Neurosci.* 34, 2544–2558.
- Padilla, S.L., Qiu, J., Soden, M.E., Sanz, E., Nestor, C.C., Barker, F.D., Quintana, A., Zweifel, L.S., Rønnekleiv, O.K., Kelly, M.J., et al. (2016). Agouti-related peptide neural circuits mediate adaptive behaviors in the starved state. *Nat. Neurosci.* 19, 734–741.
- Park, D., Li, P., Dani, A., and Taghert, P.H. (2014). Peptidergic Cell-Specific Synaptotagmins in *Drosophila*: Localization to Dense-Core Granules and Regulation by the bHLH Protein DIMMED. *J. Neurosci.* 34, 13195–13207.
- Persoon, C.M., Moro, A., Nassal, J.P., Farina, M., Broeke, J.H., Arora, S., Dominguez, N., Weering, J.R., Toonen, R.F., and Verhage, M. (2018). Pool size estimations for dense-core vesicles in mammalian CNS neurons. *EMBO J.* 37, 1–18.

8 References

- Pfeiffer, B.D., Ngo, T.T.B., Hibbard, K.L., Murphy, C., Jenett, A., Truman, J.W., and Rubin, G.M. (2010). Refinement of tools for targeted gene expression in *Drosophila*. *Genetics* 186, 735–755.
- van den Pol, A.N. (2012). Neuropeptide Transmission in Brain Circuits. *Neuron* 76, 98–115.
- Pool, A.H., and Scott, K. (2014). Feeding regulation in *Drosophila*. *Curr. Opin. Neurobiol.* 29, 57–63.
- Prentki, M., Matschinsky, F.M., and Madiraju, S.R.M. (2013). Metabolic signaling in fuel-induced insulin secretion. *Cell Metab.* 18, 162–185.
- Qian, C.S., Kaplow, M., Lee, J.K., and Grueber, W.B. (2018). Diversity of Internal Sensory Neuron Axon Projection Patterns Is Controlled by the POU-Domain Protein Pdm3 in *Drosophila* Larvae. *J. Neurosci.* 38, 2081–2093.
- Renden, R., Berwin, B., Davis, W., Ann, K., Chin, C.-T., Kreber, R., Ganetzky, B., Martin, T.F.J., and Broadie, K. (2001). *Drosophila* CAPS Is an Essential Gene that Regulates Dense-Core Vesicle Release and Synaptic Vesicle Fusion. *Neuron* 31, 421–437.
- Rist, A., and Thum, A.S. (2017). A map of sensilla and neurons in the taste system of *drosophila* larvae. *J. Comp. Neurol.*
- Robertson, J.L., Tsubouchi, A., and Tracey, W.D. (2013). Larval Defense against Attack from Parasitoid Wasps Requires Nociceptive Neurons. *PLoS One* 8, 1–9.
- Rohwedder, A., Selcho, M., Chassot, B.B., and Thum, A.S. (2015). Neuropeptide F neurons modulate sugar reward during associative olfactory learning of *Drosophila* larvae. *J. Comp. Neurol.* 523, 2637–2664.
- Root, C.M., Ko, K.I., Jafari, A., and Wang, J.W. (2011). Presynaptic facilitation by neuropeptide signaling mediates odor-driven food search. *Cell* 145, 133–144.
- Rorsman, P., and Braun, M. (2013). Regulation of insulin secretion in human pancreatic islets. *Annu. Rev. Physiol.* 75, 155–179.
- Rulifson, E.J. (2002). Ablation of Insulin-Producing Neurons in Flies: Growth and Diabetic Phenotypes. *Science* (80-.). 296, 1118–1120.
- Rulifson, E.J., Kim, S.K., and Nusse, R. (2002). Insulin-Producing Neurons in Flies : Growth and Diabetic Phenotypes. *Science* (80-.). 296, 1118–1120.
- Saalfeld, S., Cardona, A., Hartenstein, V., Tomancak, P., and Tomančák, P. (2009). CATMAID: Collaborative annotation toolkit for massive amounts of image data. *Bioinformatics* 25, 1984–1986.
- Salay, L.D., Ishiko, N., and Huberman, A.D. (2018). A midline thalamic circuit determines reactions to visual threat. *Nature* 557.
- Sandkühler, J. (2009). Models and mechanisms of hyperalgesia and allodynia. *Physiol. Rev.* 89, 707–758.
- Sawin-McCormack, E.P., Sokolowski, M.B., and Campos, A.R. (1995). Characterization and genetic analysis of *Drosophila melanogaster* photobehavior during larval development. *J. Neurogenet.* 10, 119–135.
- Sayin, S., Boehm, A.C., Kobler, J.M., De Backer, J.-F.F., and Grunwald Kadow, I.C. (2018). Internal state dependent odor processing and perception—The role of

8 References

- neuromodulation in the fly olfactory system. *Front. Cell. Neurosci.* 12, 1–17.
- Scheller, R.H., and Axel, R. (1984). How genes control an innate behavior. *Sci. Am.* 250, 54–62.
- Schlegel, P., Texada, M.J., Miroshnikow, A., Schoofs, A., Hückesfeld, S., Peters, M., Schneider-Mizell, C.M., Lacin, H., Li, F., Fetter, R.D., et al. (2016). Synaptic transmission parallels neuromodulation in a central food-intake circuit. *Elife* 5, 1–32.
- Schneider-Mizell, C.M., Gerhard, S., Longair, M., Kazimiers, T., Li, F., Zwart, M.F., Champion, A., Midgley, F.M., Fetter, R.D., Saalfeld, S., et al. (2016). Quantitative neuroanatomy for connectomics in *Drosophila*. *Elife* 5, 1–36.
- Schneider, J.E., Wise, J.D., Benton, N.A., Brozek, J.M., and Keen-Rhinehart, E. (2013). When do we eat? Ingestive behavior, survival, and reproductive success. *Horm. Behav.* 64, 702–728.
- Schoofs, A., Hückesfeld, S., Schlegel, P., Miroshnikow, A., Peters, M., Zeymer, M., Spieß, R., Chiang, A.-S., and Pankratz, M.J. (2014). Selection of Motor Programs for Suppressing Food Intake and Inducing Locomotion in the *Drosophila* Brain. *PLoS Biol.* 12, e1001893.
- Schwartz, M.W., Woods, S.C., Porte, D., Seeley, R.J., and Baskin, D.G. (2000). Central nervous system control of food intake. *Nature* 404, 661–671.
- Shakiryanova, D., Tully, A., and Levitan, E.S. (2006). Activity-dependent synaptic capture of transiting peptidergic vesicles. *Nat. Neurosci.* 9, 896–900.
- Shams, L., Wozny, D.R., Kim, R., Seitz, A., Jr, T.J.P., and Forest, W. (2011). Influences of multisensory experience on subsequent unisensory processing. 2, 1–9.
- Shang, Y., Donelson, N.C., Vecsey, C.G., Guo, F., Rosbash, M., and Griffith, L.C. (2013). Short Neuropeptide F Is a Sleep-Promoting Inhibitory Modulator. *Neuron* 80, 171–183.
- Shoval, O., and Alon, U. (2010). SnapShot: Network Motifs. *Cell* 143, 326–326.e1.
- Siju, K.P., De Backer, J.F., and Grunwald Kadow, I.C. (2021). Dopamine modulation of sensory processing and adaptive behavior in flies. *Cell Tissue Res.* 207–225.
- Smith, E., Lewin, G.. R., St.John Smith, E., and Lewin, G.. R. (2009). Nociceptors : a phylogenetic view International Association for the Study of Pain. *J Comp Physiol A* 1089–1106.
- Sokabe, T., Chen, H.-C., Luo, J., and Montell, C. (2016). A Switch in Thermal Preference in *Drosophila* Larvae Depends on Multiple Rhodopsins. *Cell Rep.* 17, 336–344.
- Somanathan, H., Saryan, P., and Balamurali, G.S. (2019). Foraging strategies and physiological adaptations in large carpenter bees. *J. Comp. Physiol. A Neuroethol. Sensory, Neural, Behav. Physiol.* 205, 387–398.
- Sossin, W.S., and Scheller, R.H. (1991). Biosynthesis and sorting of neuropeptides. *Curr. Opin. Neurobiol.* 1, 79–83.
- Sporns, O., and Kötter, R. (2004). Motifs in Brain Networks. *PLoS Biol.* 2.
- Sprecher, S.G., Cardona, A., and Hartenstein, V. (2011). The *Drosophila* larval visual system: High-resolution analysis of a simple visual neuropil. *Dev. Biol.* 358, 33–43.

8 References

- Stein, B.E., and Stanford, T.R. (2008). Multisensory integration: Current issues from the perspective of the single neuron. *Nat. Rev. Neurosci.* 9, 255–266.
- Sternson, S.M. (2013). Hypothalamic survival circuits: Blueprints for purposive behaviors. *Neuron* 77, 810–824.
- Stoeckel, L.E., Cox, J.E., Cook, E.W., and Weller, R.E. (2007). Motivational state modulates the hedonic value of food images differently in men and women. *Appetite* 48, 139–144.
- Szentirmai, E., and Krueger, J.M. (2006). Central administration of neuropeptide Y induces wakefulness in rats. *Am. J. Physiol. - Regul. Integr. Comp. Physiol.* 291.
- Szuperak, M., Churgin, M.A., Borja, A.J., and Raizen, D.M. (2018). A sleep state in *Drosophila* larvae required for neural stem cell proliferation. 1–19.
- Szüts, D., and Bienz, M. (2000). LexA chimeras reveal the function of *Drosophila* Fos as a context-dependent transcriptional activator. *Proc. Natl. Acad. Sci. U. S. A.* 97, 5351–5356.
- Taghert, P.H., and Nitabach, M.N. (2012). Peptide Neuromodulation in Invertebrate Model Systems. *Neuron* 76, 82–97.
- Talay, M., Richman, E.B., Snell, N.J., Hartmann, G.G., Fisher, J.D., Sorkaç, A., Santoyo, J.F., Chou-Freed, C., Nair, N., Johnson, M., et al. (2017). Transsynaptic Mapping of Second-Order Taste Neurons in Flies by trans-Tango. *Neuron* 96, 783–795.e4.
- Tastekin, I., Riedl, J., Schilling-Kurz, V., Gomez-Marin, A., Truman, J.W., and Louis, M. (2015). Role of the subesophageal zone in sensorimotor control of orientation in *drosophila* larva. *Curr. Biol.* 25, 1448–1460.
- Tenedini, F.M., Sáez González, M., Hu, C., Pedersen, L.H., Petruzzi, M.M., Spitzweck, B., Wang, D., Richter, M., Petersen, M., Szpotowicz, E., et al. (2019). Maintenance of cell type-specific connectivity and circuit function requires Tao kinase. *Nat. Commun.* 10.
- Terada, S.-I., Matsubara, D., Onodera, K., Matsuzaki, M., Uemura, T., and Usui, T. (2016). Neuronal processing of noxious thermal stimuli mediated by dendritic Ca(2+) influx in *Drosophila* somatosensory neurons. *Elife* 5, e12959.
- Thum, A.S., and Gerber, B. (2019). Connectomics and function of a memory network: the mushroom body of larval *Drosophila*. *Curr. Opin. Neurobiol.* 54, 146–154.
- Tobin, D.M., and Bargmann, C.I. (2004). Invertebrate nociception: Behaviors, neurons and molecules. *J. Neurobiol.* 61, 161–174.
- Tobin, D.M., Bargmann, C.I., and Elegans, I.N.C. (2004). Invertebrate Nociception : Behaviors , Neurons and Molecules ABSTRACT : MEDIATE MECHANICAL NOCICEPTION.
- Tracey, W.D. (2017). Nociception. *Curr. Biol.* 27, R129–R133.
- Tracey, W.D., Wilson, R.I., Laurent, G., and Benzer, S. (2003). painless , a *Drosophila* Gene Essential for Nociception. 113, 261–273.
- Tsubouchi, A., Yano, T., Yokoyama, T.K., Murtin, C., Otsuna, H., and Ito, K. (2017). Topological and modality-specific representation of somatosensory information in the

8 References

- fly brain. *Science* (80-). 358, 615–623.
- Umezaki, Y., Hayley, S.E., Chu, M.L., Seo, H.W., Shah, P., Hamada, F.N., Umezaki, Y., Hayley, S.E., Chu, M.L., Seo, H.W., et al. (2018). Feeding-State-Dependent Modulation of Temperature Preference Requires Insulin Signaling in *Drosophila* Warm-Sensing Neurons Report Feeding-State-Dependent Modulation of Temperature Preference Requires Insulin Signaling in *Drosophila* Warm-Sensing Neurons. *Curr. Biol.* 1–9.
- Vallejo, D.M., Juarez-Carreño, S., Bolivar, J., Morante, J., and Dominguez, M. (2015). A brain circuit that synchronizes growth and maturation revealed through Dilp8 binding to Lgr3. *Science* (80-). 350, aac6767.
- Venken, K.J.T., Simpson, J.H., and Bellen, H.J. (2011). Genetic manipulation of genes and cells in the nervous system of the fruit fly. *Neuron* 72, 202–230.
- Vogt, K., Zimmerman, D.M., Schlichting, M., Hernandez-Nunez, L., Qin, S., Malacon, K., Rosbash, M., Pehlevan, C., Cardona, A., and Samuel, A.D.T. (2020). Internal state configures olfactory behavior and early sensory processing in *Drosophila* larvae. *BioRxiv* 2–11.
- Wanner, A.A., Genoud, C., Masudi, T., Siksou, L., and Friedrich, R.W. (2016). Dense EM-based reconstruction of the interglomerular projectome in the zebrafish olfactory bulb. *Nat. Neurosci.* 19, 816–825.
- white J.G, southGate E, Thomson J.N, B. s (1986). The structure of the nervous system of the nematode *Caenorhabditis elegans*. *Philos. Trans. R. Soc. London. B, Biol. Sci.* 314, 1–340.
- Williams, G., Bing, C., Cai, X.J., Harrold, J. a, King, P.J., and Liu, X.H. (2001). The hypothalamus and the control of energy homeostasis. *Physiol. Behav.* 74, 683–701.
- Wong, M.Y., Cavolo, S.L., and Levitan, E.S. (2015). Synaptic neuropeptide release by dynamin-dependent partial release from circulating vesicles. *Mol. Biol. Cell* 26, 2466–2474.
- Woolf, C.J., and Ma, Q. (2007). Nociceptors-Noxious Stimulus Detectors. *Neuron* 55, 353–364.
- Wu, Q., and Brown, M.R. (2006). Signaling and function of insulin-like peptides in insects. *Annu. Rev. Entomol.* 51, 1–24.
- Wu, Q., Wen, T., Lee, G., Park, J.H., Cai, H.N., and Shen, P. (2003). Developmental control of foraging and social behavior by the *Drosophila* neuropeptide Y-like system. *Neuron* 39, 147–161.
- Wu, Q., Zhao, Z., and Shen, P. (2005). Regulation of aversion to noxious food by *Drosophila* neuropeptide Y- and insulin-like systems. *Nat. Neurosci.* 8, 1350–1355.
- Xiang, Y., Yuan, Q., Vogt, N., Looger, L.L., Jan, L.Y., and Jan, Y.N. (2010). Light-avoidance-mediating photoreceptors tile the *Drosophila* larval body wall. *Nature* 468, 921–926.
- Xiang, Y., Yuan, Q., Vogt, N., Looger, L.L., Jan, L.Y., and Nung, Y. (2011). Light-avoidance-mediating photoreceptors tile the *Drosophila* larval body wall. *Nature* 468, 921–926.
- Yam, M.F., Loh, Y.C., Tan, C.S., Adam, S.K., Manan, N.A., and Basir, R. (2018). General pathways of pain sensation and the major neurotransmitters involved in pain

8 References

regulation. *Int. J. Mol. Sci.* 19.

Yamanaka, N., Romero, N.M., Martin, F.A., Rewitz, K.F., Sun, M., O'Connor, M.B., and Léopold, P. (2013). Neuroendocrine Control of *Drosophila* Larval Light Preference. *Science* (80-). 341, 1113–1116.

Yan, Z., Zhang, W., He, Y., Gorczyca, D., Xiang, Y., Cheng, L.E., Meltzer, S., Jan, L.Y., and Jan, Y.N. (2013). *Drosophila* NOMPC is a mechanotransduction channel subunit for gentle-touch sensation. *Nature* 493, 221–225.

Yang, C. -h. C.-H., Belawat, P., Hafen, E., Jan, L.Y., and Jan, Y.-N.Y.-N. (2008). *Drosophila* egg-laying site selection as a system to study simple decision-making processes. *Science* 319, 1679–1683.

Yang, Y., Atasoy, D., and Sternson, S. (2011). Flip-flop memory circuit uses a synaptic AMPK-dependent positive feedback loop and is switched by hunger state. *Appetite* 57, S47.

Yarmolinsky, D.A., Zuker, C.S., and Ryba, N.J.P. (2009). Common Sense about Taste : From Mammals to Insects. 139, 234–244.

Zhan, Y.P., Liu, L., and Zhu, Y. (2016). Taotie neurons regulate appetite in *Drosophila*. *Nat. Commun.* 7, 13633.

Zhang, W., Yan, Z., Li, B., Jan, L.Y., and Jan, Y.N. (2014). Identification of motor neurons and a mechanosensitive sensory neuron in the defecation circuitry of *Drosophila* larvae. *Elife* 3, 1–18.

Zhong, L., Bellemer, A., Yan, H., Honjo, K., Robertson, J., Hwang, R.Y., Pitt, G.S., and Tracey, W.D. (2012). Article Thermosensory and Nonthermosensory Isoforms of *Drosophila melanogaster* TRPA1 Reveal Heat-Sensor Domains of a ThermoTRP Channel. 1–13.

Zimmerman, A., Bai, L., and Ginty, D.D. (2014). The gentle touch receptors of mammalian skin. *Science* 346, 950–954.

9 ACKNOWLEDGEMENTS

First and foremost, i would like to express my deepest gratitude to my PhD advisor Dr. Peter Soba for giving me the opportunity to do this PhD research. I really appreciate that you not only gave me ideas and options for my project, but you were also willing to listen to my ideas and guided me in achieving them. This really motivated me to dig deeper into scientific questions and to appreciate doing Science. I can say that your insightful knowledge, demanding and motivating mentorship has made me grow scientifically and personally to a level that i was not aware i could reach before. I am also very grateful to you for the support you provided to me at a human level when i was sick and during corona quarantine time. Thank you for everything!

I would like to thank my thesis committee members Prof. Oertner, Prof. Friese, Prof. Lohr for their time and effort in guiding me during my PhD. I especially appreciate our last meeting, the discussion, ideas, and feedback have been invaluable, and it has made me look at my project from a new angle and pushed me to write my PhD in a more interesting way. I am thankful to Dr. Albert Cardona for hosting me in his lab and for teaching me how to do neuronal reconstruction together with Laura Herren. I am grateful to all my colleagues in the Soba lab who have shared their knowledge with me and for their support. I thank Andrey Formozov for generating the heat maps for my tolerance assays, Fangmin Zhou for helping me in doing light avoidance behavior and Kathrin Sauter for doing the cloning.

Thank my dad Abboo Hassen Imambocus and mom, Bibi Affroze Imambocus for your unconditional selflessness, unwavering support and countless sacrifices that has opened many doors for me to grow and succeed. Thank you, siblings Fayeza, Parweza, Nooreza, Waeza, Salim, Urs, Sidick for your love and support. Finally, I could not have completed this dissertation without the support of my friends who helped me in writing the summary for my thesis in German, provided stimulating discussions as well as happy distractions to rest my mind outside of my research.

10 CURRICULUM VITAE

Bibi Nusreen Imambocus

Details

Address

Thiedeweg 21
Hamburg, 22047
Germany

Phone

004915212983863

Email

nusreenbib@icloud.com

Nationality

Mauritian

Languages

Creole



English



French



Urdu



German



Profile

PhD researcher in the lab of Dr. Peter Soba

Employment History

Post doc position, Limes institute, University of Bonn

Jan 2021 – Present Bonn, Germany

PhD position, ZMNH, UKE

Sep 2016 – Dec 2020 Hamburg, Germany

PhD student

Education

ZMNH, UKE, Enrolled in non medical PhD program

Sep 2016 – Present Hamburg, Germany

PhD thesis: Neuropeptergic control of innate and adaptive behaviors. Thesis advisor: Dr. Peter Soba

Thesis Committee members: Prof. Thomas Oertner, Prof. Manuel Frieze, Prof. Christian Lohr

University of Geneva, Master in Neuroscience

Sep 2013 – Sep 2015 Geneva, Switzerland

Master thesis: Neuronal VEGF regulates the migration of pyramidal neurons in the developing neocortex. Supervisor: Prof. J.Z Kiss

University of Mauritius, Bachelor of Science (Hons) in Biology

Aug 2005 – May 2008 Mauritius

11 PUBLICATION

Bibi Nusreen Imambocus, Annika Wittich, Federico Tenedini, Fangmin Zhou, Chun Hu, Kathrin Sauter, Ednilson Macarenhas Varela, Fabiana Herédia, Andreia P. Casimiro, André Macedo, Philipp Schlegel, Chung-Hui Yang, Irene Miguel-Aliaga, Michael J. Pankratz, Alisson M. Gontijo, Albert Cardona, Peter Soba. **Discrete escape responses are generated by neuropeptide-mediated circuit logic.** *bioRxiv*. DOI: <https://doi.org/10.1101/2020.09.22.307033>

12 AFFIDAVIT

Ich versichere ausdrücklich, dass ich die Arbeit selbständig und ohne fremde Hilfe verfasst, andere als die von mir angegebenen Quellen und Hilfsmittel nicht benutzt und die aus den benutzten Werken wörtlich oder inhaltlich entnommenen Stellen einzeln nach Ausgabe (Auflage und Jahr des Erscheinens), Band und Seite des benutzten Werkes kenntlich gemacht habe.

Ferner versichere ich, dass ich die Dissertation bisher nicht einem Fachvertreter an einer anderen Hochschule zur Überprüfung vorgelegt oder mich anderweitig um Zulassung zur Promotion beworben habe.

Ich erkläre mich einverstanden, dass meine Dissertation vom Dekanat der Medizinischen Fakultät mit einer gängigen Software zur Erkennung von Plagiaten überprüft werden kann.

Unterschrift:

Hamburg 17th May 2021 Bibi Nusreen Imambocus